Climate Risk and Vulnerability Assessment for Western Uzbekistan Water Supply

July 2017

Authors
Dr P. Droogers
Dr A.F. Lutz
Dr J.E. Hunink

Client
Asian Development Bank

FutureWater Report 171

FutureWater
Costerweg 1V
6702 AA Wageningen
The Netherlands

+31 (0)317 460050

info@futurewater.nl

www.futurewater.nl

Preface

Central Asia is an area highly vulnerable to climate change and expected to experience increased water stress in coming decades. Uzbekistan, and western Uzbekistan in particular, will be particularly affected as it is a downstream user of water from the Amu Darya, located in a very arid climate, and likely to face declining water supply in the coming decades.

A project has been proposed by the Asian Development Bank which intends to rehabilitate and expand water supply delivery in several districts in Karakalpakstan in the vicinity of Nukus and the Aral Sea. The project is expected to draw water from the Amu Darya, as well as explore alternative groundwater options. The river offtake may be negatively affected by changes in the level and pattern of river flow and precipitation driven by climate change. A primary risk is that there may not be sufficient reliable water availability at the proposed offtake points (or groundwater sources) for the target beneficiaries in future decades, thereby reducing the lifetime of the investment.

This Climate Risk and Vulnerability Assessment assesses expected future changes in climate over the lifetime of the project, and how these impact the local water resources and the project's target beneficiaries. Furthermore, climate change adaptation options required for a climate-proof design of the project are proposed. This assessment is linked to the formulation of a funding proposal to the Green Climate Fund, for co-financing of the climate-proofing component of the Water Supply project.

Dr A.F. Lutz
Dr P. Droogers
Wageningen, July 2017

Table of contents

Tables

Figures

Executive summary

This Climate Risk Vulnerability Assessment (CRVA) identifies the risks and vulnerabilities associated with future climate change for Asian Development Bank's proposed project to expand water supply in Western Uzbekistan in six districts of Karakalpakstan.

Climate change projections for the area show continuing increases in temperature, and variation in projections of future precipitation. For water supplied from the mountainous upstream areas, the hydrological projections show a steady decrease in flows, starting in the coming decades, accelerating towards the end of the century. These trends will already have effects at the project's horizon year in 2045. The people most vulnerable to climate change, living in the remote areas of Karakalpakstan, currently cannot rely on a sustainable source of water supply.

Taking into account the spread in the climate change scenarios, following measures are proposed for climate proofing of the proposed water supply project:

- Construct infrastructure to connect 160,000 (230,000 in 2045) people to the centralized water supply system taking water from the Amu Darya river. Thereby the use of groundwater and other unsafe water sources can be phased out, thus making the most vulnerable groups of the population in the Project area climate resilient. The costs of implementing this infrastructure are estimated at 35.8 million US$

- Implement programs aimed at changing operational protocols, generating awareness of climate change-induced risks, and implementation of long-term considerations, including climate change, in the development of strategies. The costs for implementing such programs is estimated at 4 million US$.

1.1 Background

Central Asia is an area highly vulnerable to climate change and expected to experience increased water stress in coming decades. The hydrological regimes of the two major rivers in the region, the Syr Darya and the Amu Darya, are complex and vulnerable to climate change. Water diversions to agricultural, industrial and domestic users have reduced flows in downstream regions, resulting in severe ecological damages, and water shortages. The administrative-institutional system is fragmented, with six independent countries sharing control, often with contradicting objectives.

The upstream states are mostly reliant on hydropower. In order to have enough hydropower generating capacity during winter, the upstream states save water during summer in the reservoirs. But this is the period when the downstream countries have the most pressing need for irrigation water. In the region, cotton is an important cash crop, and, at the same time, wheat is considered essential in order to meet national food security goals. Especially for Uzbekistan, considerations of self-sufficiency have become more important in recent times where food grain prices have increased considerably on the world market.

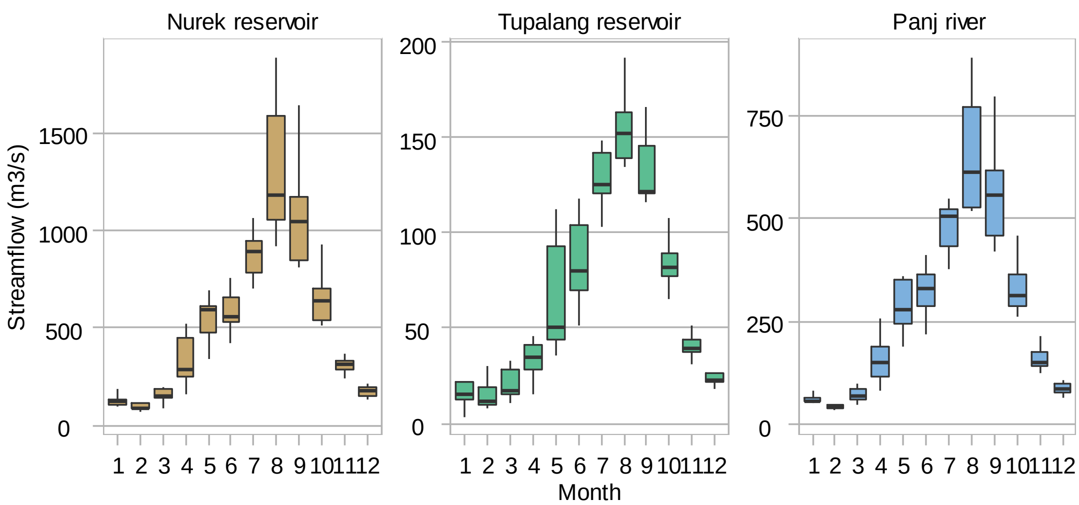

Figure 1.1. Monthly variability during the baseline period (2001-2010) of inflow in major reservoirs and rivers in the upstream reaches of the Amu Darya.

As a result, the water resources system is not managed collectively and cooperatively. A mixture of regional, national, and interstate institutions is responsible for allocation decisions. As a result, water and energy allocation among the various sectors and users is not efficient. It is thought that future water resources development in northern Afghanistan will further add fuel to the water and energy conflict in the region.

Future climate change poses additional challenges. The discharge in the Syr Darya and the Amu Darya rivers is driven to a large extent by snow and glacier melt, especially for the Amu Darya. The impact of a warming climate on these key hydrological processes is starting to be understood better (Bernauer and Siegfried, 2012; Chen et al., 2016, 2017; Lutz et al., 2014; Sorg et al., 2014) but no mitigation and adaptation strategies are in place. Whereas changes in precipitation levels are hard to predict for the future, there is a solid consensus that average global temperatures are rising. As a result, more precipitation will fall as rain in the upstream and the ice volume in the Tien Shan and Pamir mountain ranges will likely shrink in the long term. Furthermore, changes in sediment loads may pose additional problems.

Uzbekistan, and western Uzbekistan in particular, will be particularly affected as it is a downstream user of water from the Amu Darya, and thus is likely to face declining water supply due to glacial retreat in the long term and increased competition from upstream users. The area is characterized by a very arid climate, making is largely dependent on upstream water resources.

The proposed Asian Development Bank (ADB) project intends to rehabilitate and expand water supply delivery in multiple districts of Karakalpakstan, in the vicinity of Nukus and the Aral Sea. The project is expected to draw water from the Amu Darya, as well as explore alternative groundwater options. The river offtake may be negatively affected by changes in the level and pattern of river flow and precipitation driven by climate change. A primary risk is that there may not be sufficient reliable water availability at the proposed offtake points (or groundwater sources) for the target beneficiaries in future decades, thereby reducing the lifetime of the investment.

This Climate Risk and Vulnerability Assessment (CRVA) assesses expected future changes in climate over the lifetime of the project, and how these impact the local water resources and the project's target beneficiaries. Furthermore, climate change adaptation options required for a climate-proof design of the project are proposed. This assessment is linked to the formulation of a funding proposal to the Green Climate Fund (GCF), for co-financing of the climate-proofing component of the Water Supply project.

1.2 Climate-related risks

The water supply in the Republic of Karakalpakstan (RK) is already highly exposed to and impacted by a combination of human-driven factors and on-going long-term climate changes. River flow from the Amu Darya, the primary source of water supply for RK, is expected to decline in the long run due to receding glaciers in the upstream areas of Tajikistan and changes in rainfall, water consumption and evaporation. The project will draw water from the Amu Darya, whose level and flow is expected to be negatively affected in the coming decades by decline in glacial coverage in upstream areas and changing patterns of precipitation due to climate change. A primary risk to RK water supply and thus the project investments is that in future decades there may be insufficient reliable water availability at the proposed offtake points for the target beneficiaries, thereby reducing the lifetime of the investment.

Water users are already highly vulnerable to these effects, as much of its infrastructure has deteriorated and requires rehabilitation. Services are unreliable, leakage losses reportedly high, and raw water quality is a mounting concern. Relatively high per-capita system costs coupled with low affordability levels constrain investment and inhibit delivery. Some consumers only receive water supplies for two hours per day. Without the proposed intervention, and with continued deterioration of the water supply due to climate change, the population may be forced to relocate out of their communities in RK due to lack of water availability.

The Western Uzbekistan Water Supply System Development Project (WUWSSDP) aims at improving and expanding the water supply service in six districts in Karakalpakstan, namely: Amudarya, Beruni, Karauzak, Nukus, Kungrad and Muynak and to improve the financial, operational and water supply system management capacity of the Republic of Karakalpakstan Department for Operation of Interregional Water Supply Tuyamuyun – Nukus (DOIWS-TN), commonly referred to as TN.

Figure 1.2: The six districts in Karakalpakstan where the project will be implemented.

The horizon year of the Project is 2045. Based on the project's feasibility study a population of 388,000 living in 116 rural settlements and the six district centers will benefit of improved of new water service upon completion of the construction works in 2022. At the project horizon, this number is projected to be around 520,000. The physical works will mainly consist of the construction or rehabilitation of around 1250 km of water pipelines and of several pumping water distribution centers, the rehabilitation of the 2nd lift pumping station at the Tuyamuyun water treatment plant (WTP) and the extension of the treatment capacity of the existing WTP at Takiatash. It is recommended to consider also the construction of a new WTP in Mangit (Amudarya district). Based also on preliminary reviews the option of desalination plants will be considered only in cases of extreme necessity.

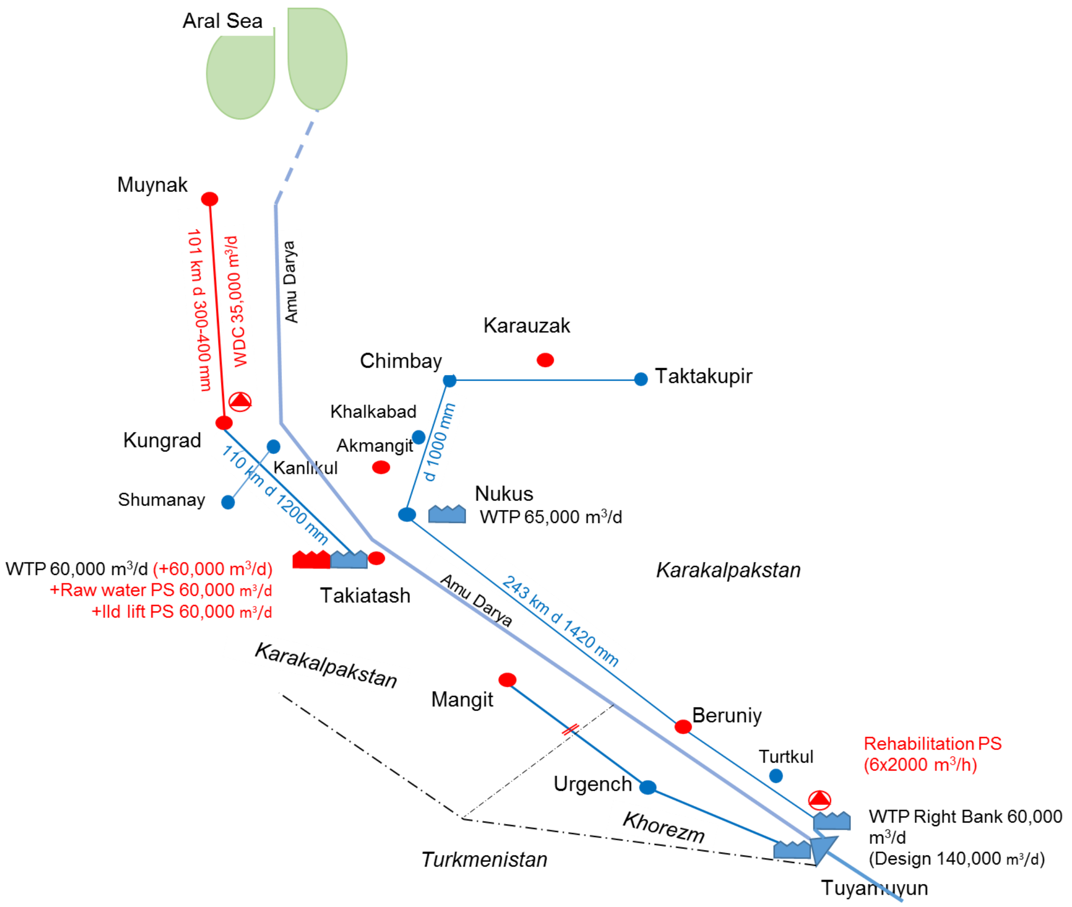

Figure 1.3. Layout of main Project's features

1.3 Objective

Due to the abovementioned risks, the project feasibility study will include a climate risk and vulnerability study, including a detailed hydrological study of the Amu Darya, to assess expected changes in the pattern and level of river flow over the lifetime of the project, as well as expected changes on groundwater recharge. The results of the assessment will inform project design including selection of (i) most vulnerable beneficiaries, (ii) offtake points, (iii) water storage and distribution options and the development of an integrated climate risk management system to ensure sustained climate resilience.

The CRVA will assess expected changes in the pattern and level of river flow over the lifetime of the project, as well as expected changes on groundwater recharge. The results of the assessment will inform project design including (i) selection of target beneficiaries, (ii) offtake points, (iii) water storage and distribution options, (iv) alternative sources, and (v) risk management and support a grant application to the Green Climate Fund (GCF) for co-financing.

1.4 Modelling approach

The work described here shows results of three components of the modelling study: (i) the climate scenario downscaling based on the latest IPCC reports and scenarios (ii) the upstream hydrological modelling, and (iii) the downstream river basin system modelling. The basin is divided in an upstream part and a downstream part (Figure 1.4, Figure 1.5). For the upstream part, a hydrological model called SPHY model (Terink et al., 2015b), was developed as part of the Asian Development Bank study *Water and Adaptation Interventions in Central and West Asia (TA7532)* (Immerzeel et al., 2012; Lutz et al., 2012). This model was further updated using the latest insights in high mountain hydrology as detailed in the methodological section. For the upstream part no major human infrastructure influences the hydrological regime. For the downstream part of both basins, a water allocation model was set up including all the main infrastructure, supplies and demands, using the Water Evaluation and Planning (WEAP) tool, also further detailed below.

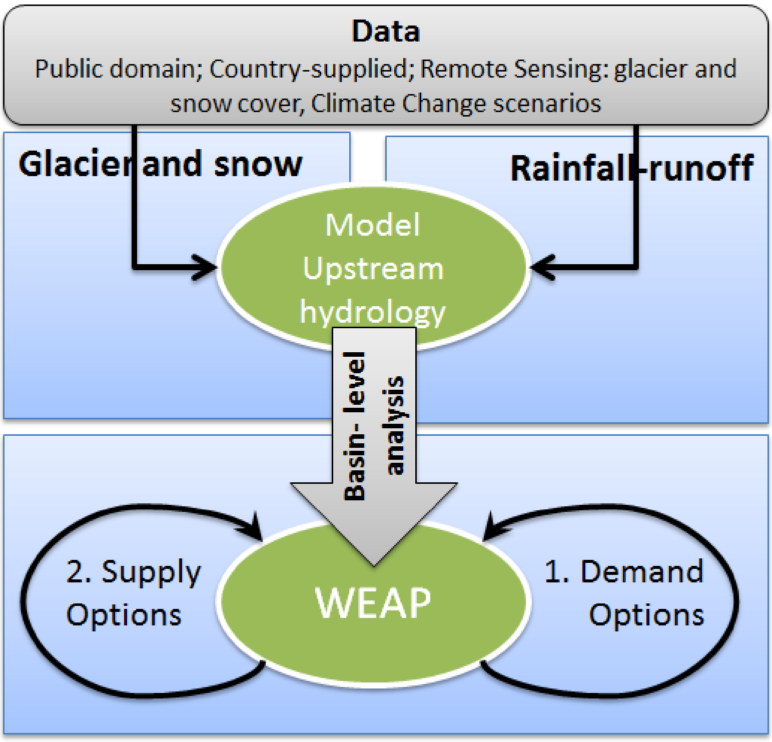

Figure 1.4: Schematic representation of the coupled modelling approach.

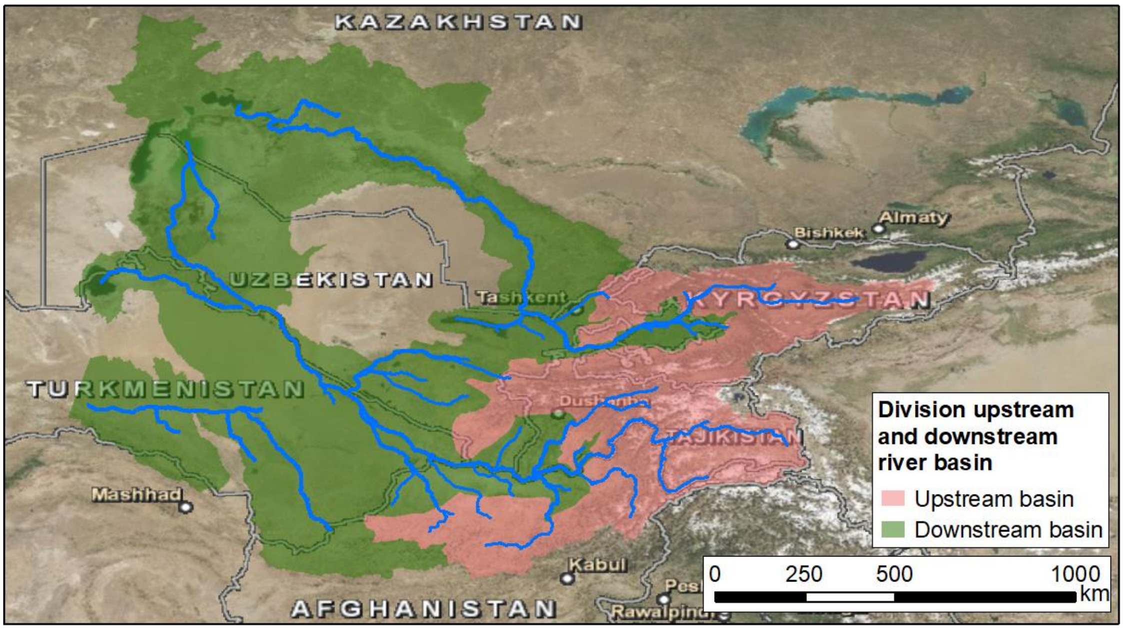

Figure 1.5: Geographic representation of the coupled modelling approach.

1.5 Climate scenarios

Scientific literature on projected climatic changes in Central Asia is sparse. A study analyzing a large range of projections from CMIP3 (Meehl et al., 2007), which was the basis for IPCC AR4 and CMIP5 (Taylor et al., 2012), which was the basis for IPCC AR5, indicates a large spread in the projections for the Central Asian mountain ranges (Lutz et al., 2013). The more recent CMIP5 scenarios not only project a larger increase in air temperature compared to CMIP3, but also a larger uncertainty in future precipitation.

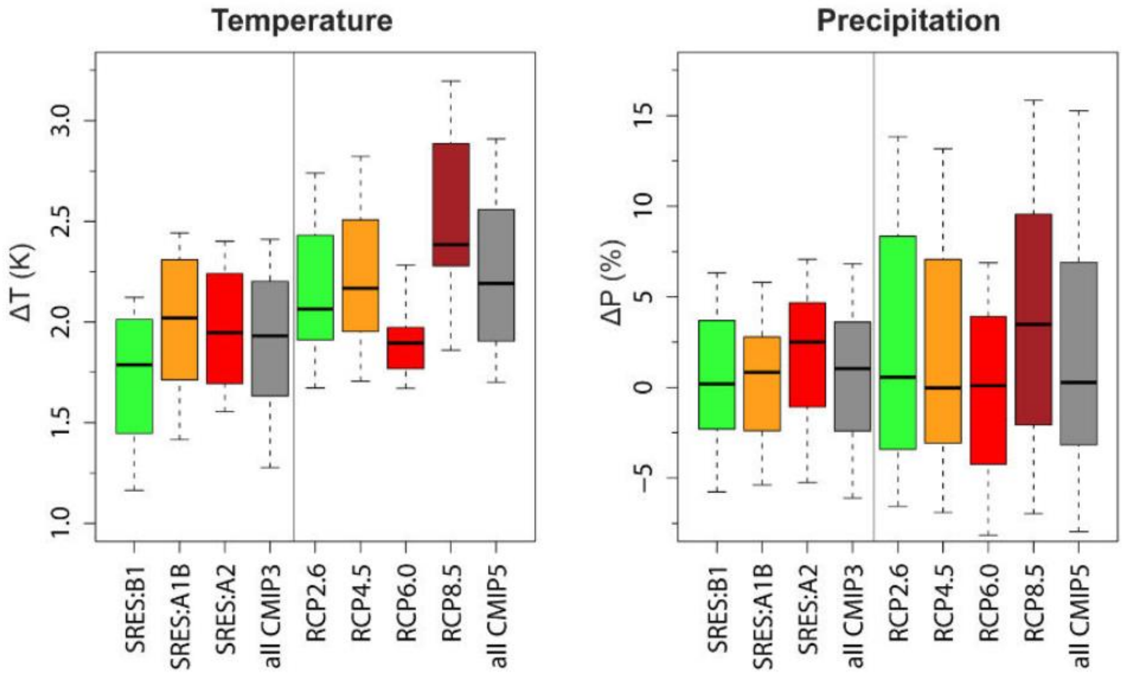

Figure 1.6: Projected changes in climate for the Central Asian mountain ranges according to CMIP3 and CMIP5 between 1961–1990 and 2021–2050 (Lutz et al., 2013)**.**

Figure 2.4 shows the range of projections in temperature and precipitation change in the upstream parts of the Amu Darya and Syr Darya river basins according to all AR5 GCM runs for RCP4.5 and RCP8.5. From the figure the large uncertainty in future climate over Central Asia is evident. The likely increase in temperature during a period of 100 years ranges from +2.5 °C to +7.5 °C, whereas the likely change in precipitation ranges from -20% to +20%. These values represent the region-averaged changes. The spatial variability in the climate change signal is large. At the local scale, the uncertainties may be even larger.

Given the large spread in the projections, for climate change impact studies it is essential to include an ensemble of climate models in the analysis, representing a wide range of possible futures (Lutz et al., 2016). In this study, four marker scenarios are selected, reflecting this strategy. The four marker scenarios represent an arid, hot/dry, central, warm/wet future, as further explained in the following chapter.

2 Climate Change Impacts

2.1 Regional climate

The deserts and semi-deserts of Central Asia have a continental climate. Summers are hot, cloudless and dry, and winters are moist and relatively warm in the south and cold with severe frosts in the north (Lioubimtseva et al., 2005). In the north of the semi-desert zone the winters are very cold. Precipitation in the northern deserts is associated mainly with the prevailing westerlies and has a distinct maximum in spring–summer as the influence of the Siberian high diminishes and convective activity becomes stronger. In the southern part of the region winters are milder. Precipitation in this subregion has a maximum in spring, which is associated with the northward migration of the Iranian branch of the Polar front (Lioubimtseva et al., 2005). Most frequently rain is brought by depressions which develop over the Eastern Mediterranean, migrate north-eastwards, and regenerate over the Caspian Sea. Westerly cyclones of the temperate zone change their trajectories in summer over the Aral Sea from a west–east to a north–south direction and approach the zone affected by the Indian monsoon.

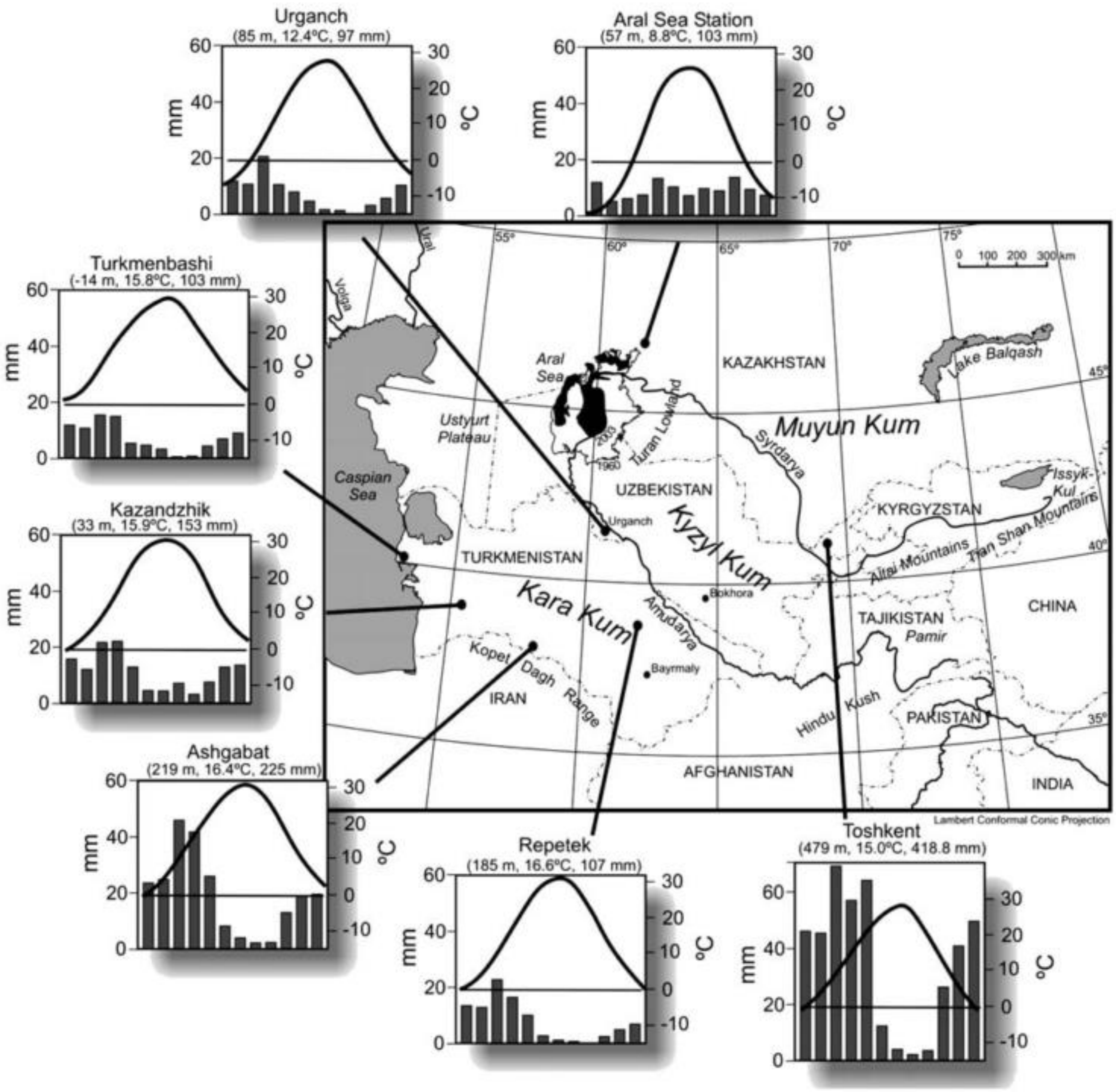

Figure 2.1: Regional climate as represented by different meteorological stations in Central Asia (Lioubimtseva et al., 2005)

By far most precipitation falls in the upstream mountainous parts of the Amu Darya and Syr Darya river basins, located in the Tien Shan and Pamir mountain ranges (Figure 2.2). Combined with the very arid downstream climate, this makes the downstream parts, where also the project area is located, very dependent on water coming from the mountains. Therefore, the future water availability in the project area depends to a large extent on future climate change in the Pamir mountain ranges, where the Amu Darya has its headwaters. This implies that climate change impacts for the complete Amu Darya basin should be considered in this CRVA study.

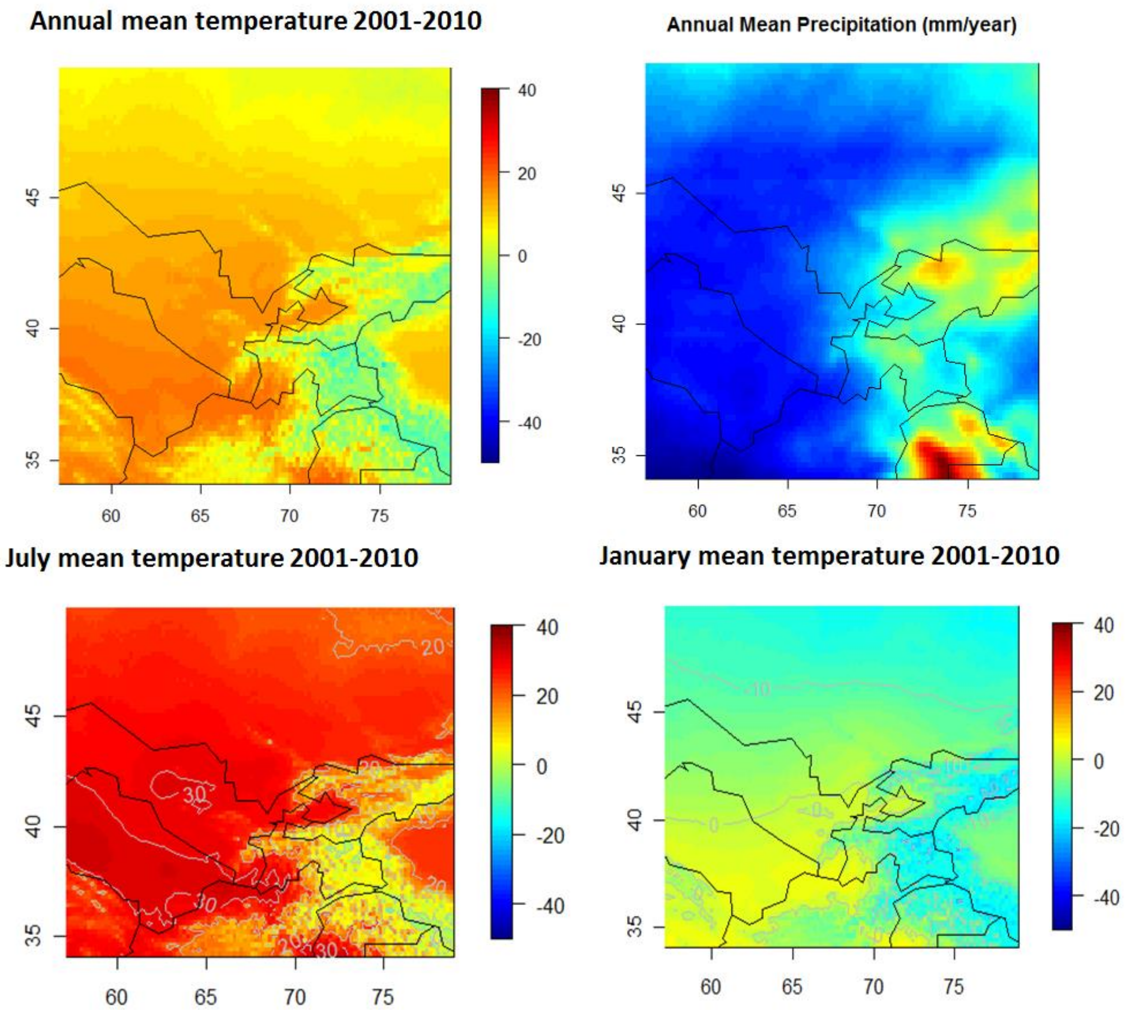

Figure 2.2: Annual mean precipitation during 2001-2010 (mm/year) based on satellite-based rainfall products PERSIANN and TRMM (2006, 2007) (upper right). Annual, July and January mean (2001-2010) temperatures (°C) based on measurements made at observing stations interpolated to 0.2°*0.2° grid using Kriging-intepolation method (ADB, 2012b).

2.2 Observed climate change

Meteorological data series available since the end of the 19th century show a steady increase of annual and winter temperatures in the Central Asian region. Analysis of aggregated temperature data downloaded from the Climate Research Unit (CRU) dataset (Harris et al., 2013) and a study of individual meteorological stations across the region (Lioubimtseva et al.,

2005) indicate a steady significant warming trend in the Central Asian region (Lioubimtseva and Henebry, 2009) (Figure 2.3).

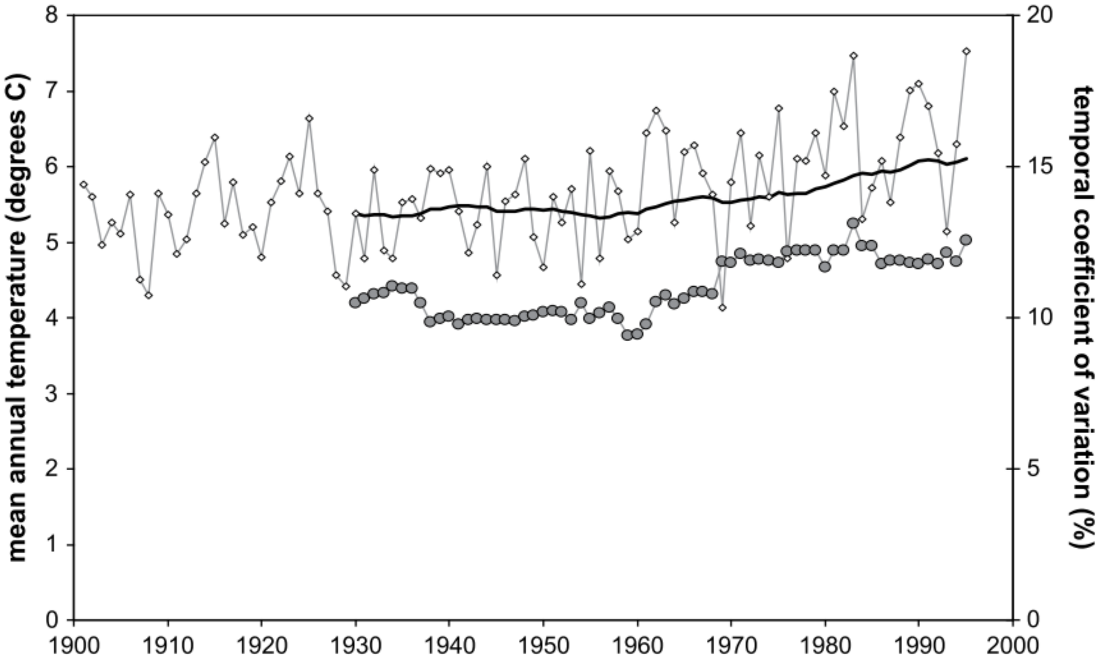

Figure 2.3: Inter-annual variability and change in the mean annual temperature over Central Asia during the 20th Century (Lioubimtseva and Henebry, 2009)**.**

In contrast to temperature trends, the precipitation trends in the region are highly variable, reflecting the region's high diversity of landscapes and climate. Precipitation records available in this region since the end of the 19th century show a slight decrease during the past 50–60 years in the western part of the region, little or no change throughout most of the region, and a relatively significant increase in precipitation recorded by the stations surrounded by irrigated lands (Lioubimtseva and Henebry, 2009).

2.3 Climate change projections for the project area

Climate change impact studies depend on projections of future climate provided by climate models. Due to their coarse spatial resolution, outputs from General Circulation Models (GCMs) are usually directly downscaled to higher resolution using empirical-statistical downscaling methods, or used as boundary conditions for Regional Climate Models (RCMs), with their outputs being downscaled to higher resolution subsequently. The downscaled outputs are then used to assess future climatic changes and to drive other sector-specific models for climate change impact studies. Outcomes from these studies are used by policymakers to support decisions on climate change adaptation measures.

The number of GCMs available for climate change projections is increasing rapidly. For example, the CMIP3 archive (Meehl et al., 2007), which was used for the 4th IPCC Assessment Report (IPCC, 2007) contains outputs from 25 different GCMs, whereas the CMIP5 archive (Taylor et al., 2012), which was used for the 5th IPCC Assessment Report (IPCC, 2013), contains outputs from 61 different GCMs. These GCMs often have multiple ensemble members resulting in an even larger number of available model runs.

Despite improvements in the CMIP5 models compared to CMIP3 in terms of process representation (e.g. Blázquez and Nuñez, 2013; Sperber *et al.*, 2013), uncertainty about the future climate remains large (e.g. Knutti and Sedláček, 2012), and locally even increases with the larger number of models available (e.g. Joetzjer *et al.*, 2013; Lutz *et al.*, 2013). Considering the large number of available climate models and constraints in the available computational and human resources, detailed climate change impact studies cannot include all projections. In practice, rather one climate model or a small ensemble of climate models is selected for the assessment. Despite the importance of using an ensemble that is representative for the region of interest and shows the full uncertainty range, the selection of models to be included in the ensemble is not straightforward, and can be based on multiple criteria.

One approach is the so-called envelope approach, where an ensemble of models covering a wide range of projections for one or more climatological variables of interest is selected from the pool of available models. This approach aims at covering all possible futures as projected by the entire pool of climate models. For this CRVA, such a climate model selection approach, based on the approach developed by (Lutz et al., 2016), is used to select four marker from the pool corresponding GCM runs from the CMIP5 RCP4.5 and RCP8.5 ensembles (Figure 2.4, Figure 2.5, Table 2.1).

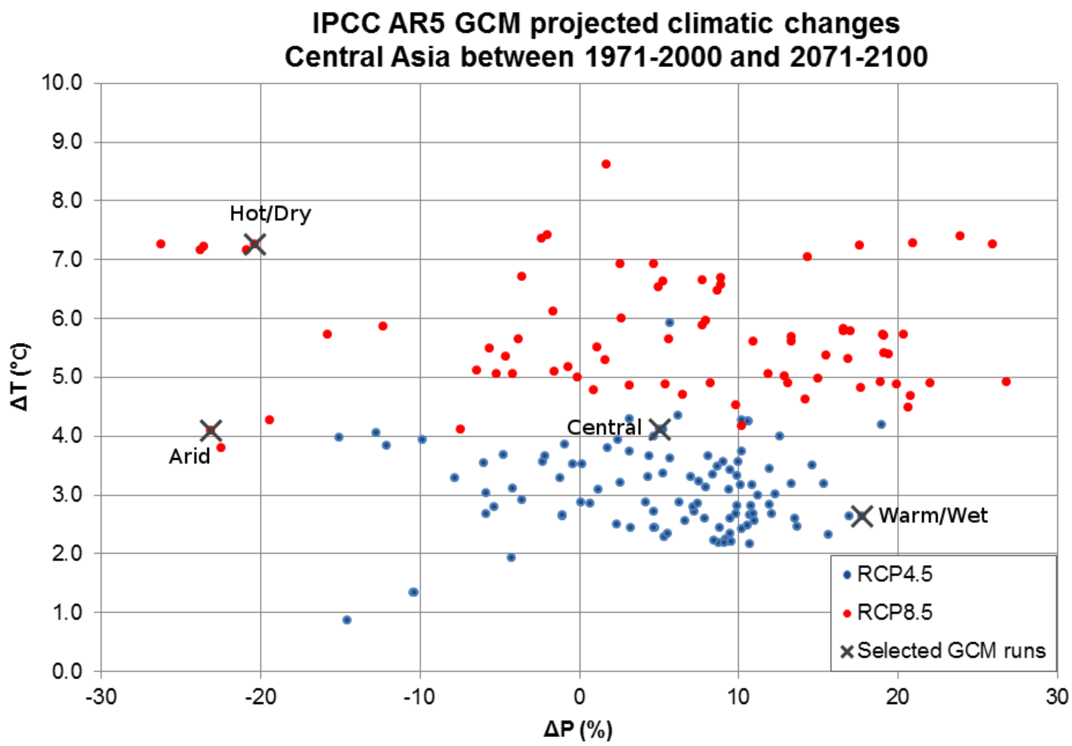

Figure 2.4: Projected changes in temperature and precipitation for the upstream Amu Darya and Syr Darya basins in Central Asia between 1971-2000 and 2071-2100. All AR5 GCM runs for RCP4.5 and RCP8.5 are shown. Values are average for extent shown in Figure 2.5. GCM runs that were selected based on proposed marker scenarios are indicated with black crosses.

Figure 2.5: Area for which GCM analysis was conducted (Figure 2.4).

Table 2.1: Selected GCM runs for each of the four marker scenarios and their projected changes in temperature and precipitation averaged over the Central Asian region between 1971-1990 and 2071-2100.

Marker scenario	GCM run	RCP	ΔT (°C)	ΔP (%)
Arid	FIO-ESM_r2i1p1	RCP8.5	+4.1	-23.1
Hot/dry	IPSL-CM5A-LR_r1i1p1	RCP8.5	+7.3	-20.3
Central	HadGEM2-ES_r2i1p1	RCP4.5	+4.1	+5.0
Warm/Wet	GISS-E2-H_r4i1p2	RCP4.5	+2.6	+17.7

In most climate types, but especially in climate types with large spatial variation, such as the climate in mountainous regions, the GCM resolution is generally not sufficient to satisfactory simulate the climate, because climatic variables vary strongly over short distances due to orographic effects. Many processes such as local circulation patterns cannot be resolved by GCMs (Christensen and Christensen, 2002). Besides a gap in resolution, GCMs exhibit biases with respect to observed climate data. To try to overcome these two problems, additional empirical-statistical downscaling and error correction techniques are required to account for the scale differences between GCMs and hydrological models, and to correct for systematic biases between GCMs and local-scale observations. Empirical-statistical methods are based on statistical relationships between large-scale predictors (climate model data) and local-scale observations (Fowler et al., 2007; Maraun et al., 2010; Wilby and Wigley, 1997). Advantages of statistical downscaling methods include the possibility to provide point-scale climatic variables derived from GCM scale climate model output, the ability to directly incorporate observed data and the computational efficiency compared to dynamical downscaling. Important disadvantages on the other hand, include the requirement of a sufficiently long and reliable observed historical data series for calibration and the assumption that the statistical relationship between the large-scale data and the local-scale data stays constant in the future (Fowler et al., 2007; Wilby and Wigley, 1997).

The selected GCM runs are downscaled using the 'delta change' approach (Kay et al., 2008; Prudhomme et al., 2002) to generate model forcing for the upstream SPHY model and downstream WEAP model until 2100, using change factors. Differences between a future and control GCM run are superimposed on a local-scale baseline observation dataset. The downscaling process is described in detail in Appendix I.

Summarizing, the following downscaled climate change scenarios are analyzed:

1. No climate change
2. Hot/Dry: the most extreme climate scenario for water availability
3. Arid, with low precipitation but a more moderate temperature increase than the Hot/Dry.
4. Central, reflecting a small increase in precipitation and a temperature increase.
5. Warm/wet, which reflects a modest temperature increase but a large precipitation increase

Analyzing these downscaled climate change scenarios for the study area shows the climatic change which can be expected for the direct vicinity of the project location (Table 2.2, Table 2.3). The range of projections clearly shows strong increases in temperature for all scenarios for the study area, indicating the urgent need to adapt to warming in the study area. Maximum air temperature (not shown here) is likely to increase stronger than mean air temperature in most places in the world, which implies even further increases in heat stress.

Table 2.2: Projected changes in air temperature for different climate change scenarios at the study area (Urgenc_Nukus_Aralsea in WEAP model)

Period	Tmean (°C)				ΔT (°C)			
Reference (2001-2010)	13.9				-			
	Arid	*Central*	*Hot/dry*	*Warm/wet*	*Arid*	*Central*	*Hot/dry*	*Warm/wet*
2010s	14.2	14.3	14.4	14.1	0.3	0.4	0.5	0.2
2030s	16.3	16.6	16.9	16.0	2.4	2.7	3.0	2.1
2050s	15.3	15.9	16.6	14.7	1.4	2.0	2.7	0.8
2070s	16.1	16.9	17.9	15.2	2.2	3.0	4.0	1.3
2090s	16.7	17.8	19.1	15.5	2.8	3.9	5.2	1.6

Table 2.3: Projected changes in precipitation for different climate change scenarios at the study area (Urgenc_Nukus_Aralsea in WEAP model)

Period	P (mm/yr)				ΔP (%)			
Reference (2001-2010)	193				-			
	Arid	*Central*	*Hot/dry*	*Warm/wet*	*Arid*	*Central*	*Hot/dry*	*War/wet*
2010s	186	188	187	190	-3.6	-2.8	-3.2	-2.0
2030s	116	127	118	133	-39.8	-34.3	-39.2	-31.3
2050s	182	200	189	212	-5.9	3.3	-2.1	9.7
2070s	176	202	187	220	-9.0	4.4	-3.5	13.9
2090s	176	211	190	236	-9.0	9.0	-1.5	22.2

For precipitation, different scenarios indicate different changes in precipitation: increases as well as decreases. It is hard to tell which of the climate change scenarios is the most likely; in theory they have equal probability. Given the small amount of precipitation falling near the study area, the changes in surface water coming from upstream are more important for the water availability at the study area.

2.4 Climate impacts on hydrology and water use upstream of the project

2.4.1 Upstream hydrology

The hydrological model SPHY (Spatial Processes in Hydrology (Terink et al., 2015a)) was used to simulate the dynamics under the four climate change marker scenarios described earlier. Figure 2.6 and Figure 2.7 show how for two upstream catchments in the Amu Darya basin, the annual mean streamflow under the Warm/wet and the Arid marker scenario (for the other scenarios and other catchments, see Appendix IV). These two catchments were selected from the total of twelve upstream catchments, as they are most indicative for what happens downstream.

Figure 2.6 and Figure 2.7 show the different sources of water: glacier melt, snow melt, direct rainfall and baseflow. For most watersheds, glacier melt is the largest component. Thus, trends in glacier melt are most relevant for water availability downstream. This trend is generally negative: considerable reductions in water coming from glaciers are expected by the end of this century, compared to current. Highest negative trends are observed for the Dry scenario (Figure 2.6). For the warm-wet scenario (Figure 2.7), the water coming from glacier melt is more or less stable until the 2030s, and then decreases.

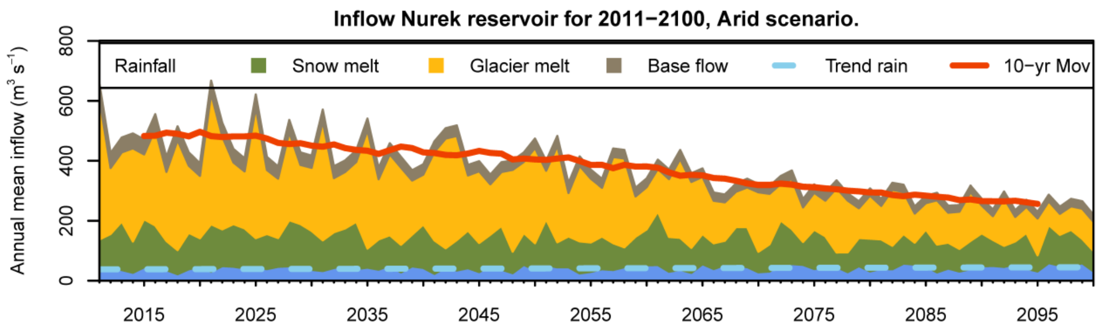

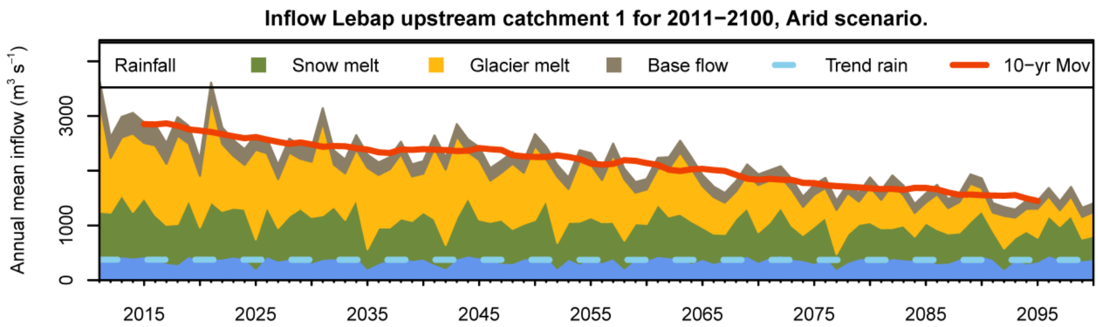

Figure 2.6. Future mean annual streamflow and its partitioning in snow, glacier, rainfall and baseflow, for Nurek reservoir inflow and the Lebap catchment, under the Arid scenario

The figures show also the 10-year moving average of the total streamflow (red-line). The dry scenario shows a clear downward trend. The warm-wet scenario (Figure 2.7) is generally less pessimistic for the first two decades but then also shows decreasing flows all catchments.

The blue dashed line in the figures shows the trend in the streamflow component that is coming from direct rainfall. For almost all watersheds, this component is relatively small compared to the water coming from glacier melt. Under the warm/wet scenario (Figure 2.7) this trend can be slightly positive because of two reasons: firstly because of the small projected increase in total precipitation, and secondly due to higher temperatures that cause more precipitation to fall as rainfall instead of snow. The complex interaction between precipitation and temperature changes in high mountain environments leads to sometimes contradictory outcomes: reductions in precipitation but increase in temperature may lead higher streamflow due to melting glaciers. Also the change from rainfall to snowfall can cause significant changes in the seasonality of the streamflow.

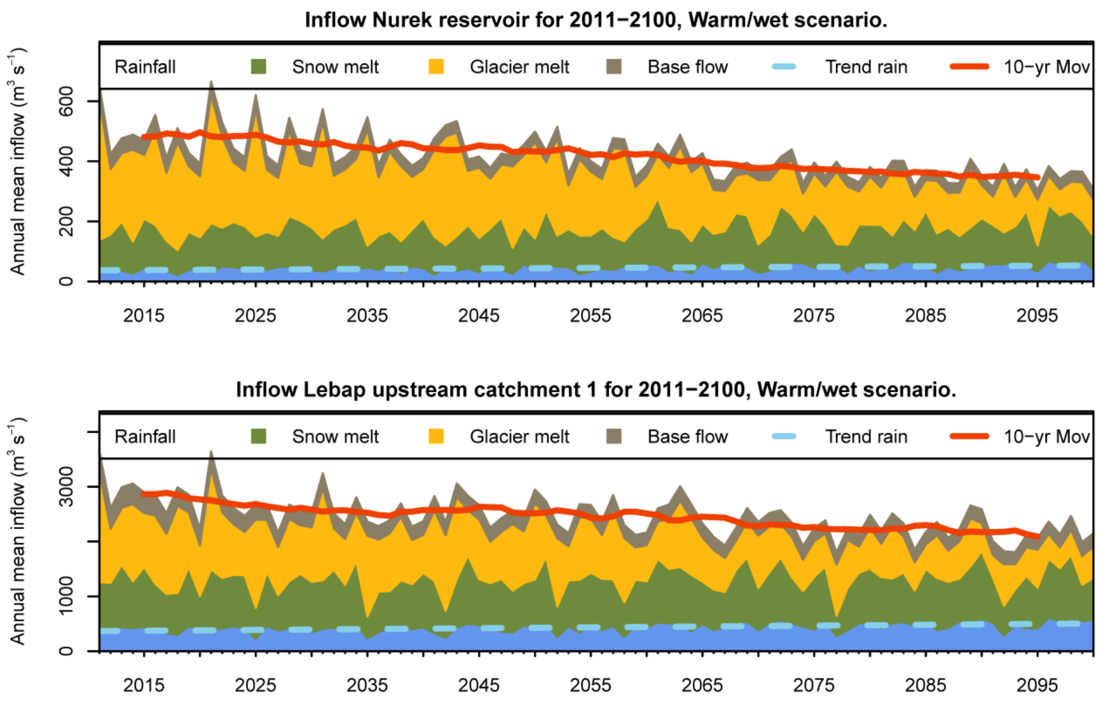

Figure 2.7. Future mean annual streamflow and its partitioning in snow, glacier, rainfall and baseflow, for Nurek reservoir inflow and the Lebap catchment, under the Warm/wet scenario

Also the monthly flow regime is affected by climate change as is shown in Figure 2.8 for the Nurek reservoir. The range of future projections indicate that the high flow season is flattened out for the Nurek reservoir, so August and September will have comparable flows as in July.

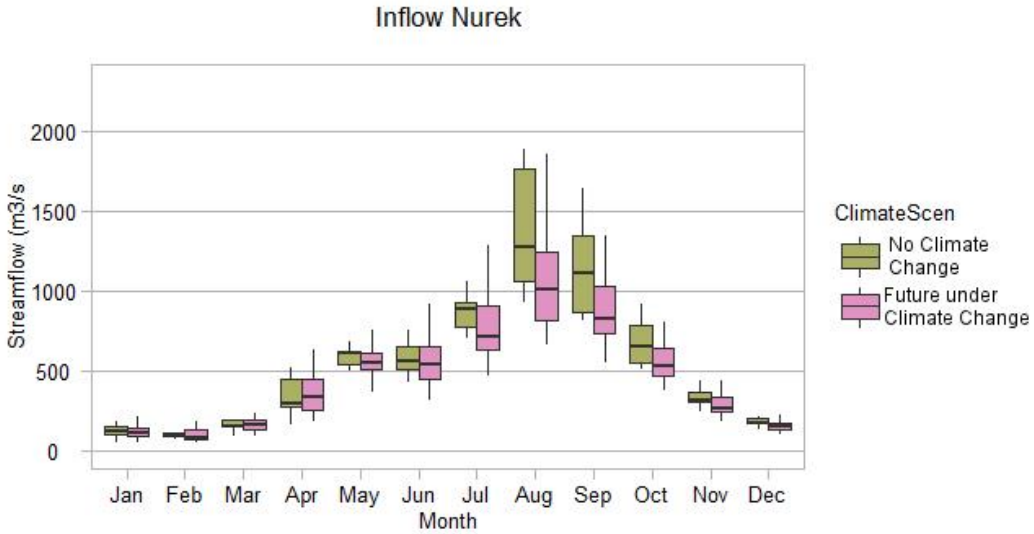

Figure 2.8. Monthly inflow for the Nurek reservoir under the current climate and the range of future climate change marker scenarios.

2.4.2 Upstream water users

The previous section illustrates how the upstream hydrology will change under climate change, affecting the water availability in the basin. Downstream of the mountains, but upstream of the project area, also water demands will change due to climate change. This demand can potentially increase considerably, especially for agricultural areas where increased temperatures and other climate factors (humidity, wind) will increase crop water requirements. This increase in demand and water use, upstream of the project area will further decrease water availability for the project area and should be accounted for.

Figure 2.9 and Figure 2.10 show the water supply under future climate change (including the current climate) for two key agricultural areas in the Amu Darya basin. For all the other agricultural areas these figures are included in the appendix. For these areas, model simulations suggest that water supply will be reduced significantly under future climate change. Outcomes suggest that adaptation measures are necessary for downstream areas in order to cope with reduced water supply. For other areas similar patterns are projected, as shown in Appendix V.

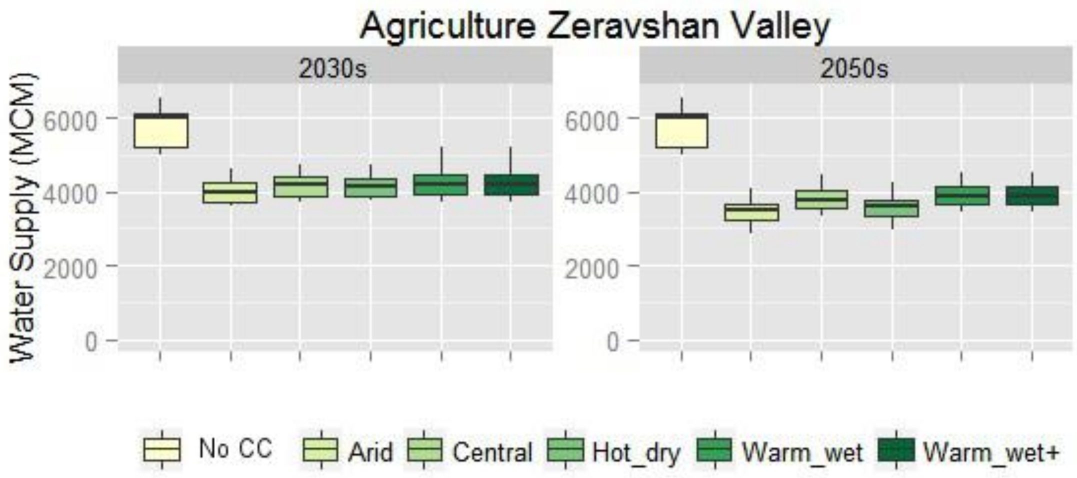

Figure 2.9. Annual variability of water supply to agriculture in the Zeravshan Valley.

Figure 2.9 shows that agriculture in Zeravshan Valley is likely to suffer considerably decreasing water availability. Water supplies will be reduced drastically in the 2030s and even more in the 2050s.

Figure 2.10 for agriculture in the downstream part of the Surkhandarya region shows that water supply might decrease in the future (Arid scenario for example), but might also increase slightly due to increasing crop water requirements in the 2050s (Warm_wet+ scenario).

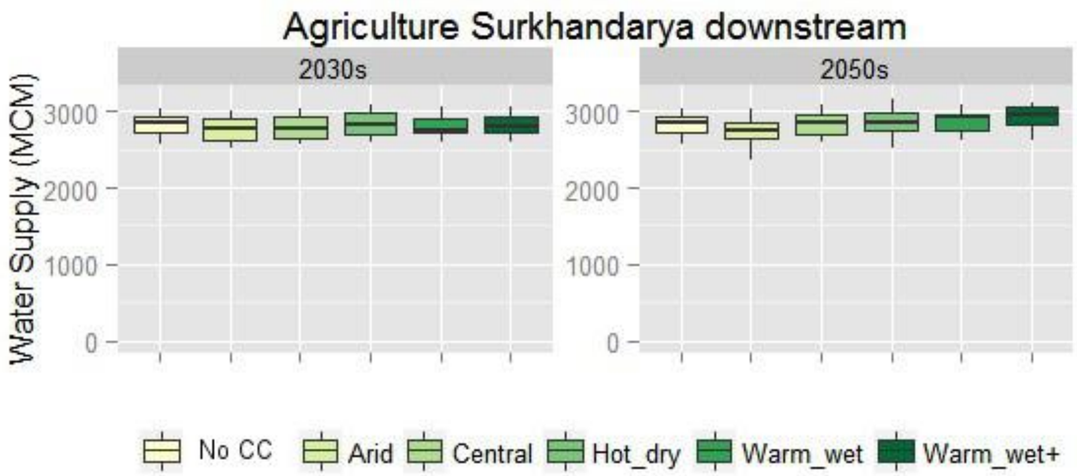

Figure 2.10. Annual variability of water supply to agriculture in the downstream part of the Surkhandarya area.

At the same time that water supply to agricultural areas upstream of the project location is likely to decrease, the water demand of agricultural areas increases as a result of climate warming. Crops demand more water under higher temperatures; evapotranspiration rates increase (Table 2.4). Agricultural water demand in all agricultural areas upstream of the project area is projected to increase by 0.3 to 6.2%, depending on the climate change scenario. This is a substantial increase for a region already facing water stress issues. Note that these projections assume that the surface area of different crops in the future remains the same as in the current situation, therefore they do not take into account possible future increases in agricultural areas or intensification of agricultural production per area. This would imply a further increase in water demand.

Table 2.4: Future changes in agricultural water demand upstream of project area under different climate change scenarios.

Scenario	Current Demand (2010s, (Mm^3/yr)	Demand 2020s (Mm^3/yr)	Δ2020s vs. current	Demand 2030s (Mm^3/yr)	Δ2030s vs. current	Demand 2040s (Mm^3/yr)	Δ2040s vs. current
No Climate Change	40747	40283	-1.1%	40160	-1.4%	40858	0.3%
Arid		40876	0.3%	41156	1.0%	42267	3.7%
Central		40842	0.2%	41097	0.9%	42190	3.5%
Hot/Dry		41294	1.3%	41858	2.7%	43266	6.2%
Warm/Wet		40538	-0.5%	40586	-0.4%	41468	1.8%

2.5 Climate change impacts on water resources of project area

Taking into account changes in upstream hydrology of the mountains, and water allocation changes under climate change in the agricultural and domestic areas upstream of the project area, projections for changes in water resources at the project site can be made.

2.5.1 Inflow Tuyamuyun reservoir

The Tuyamuyun reservoir is the principal reservoir of the project area. Inflow into this reservoir will be affected in the future by changes in upstream hydrology and upstream water demands, as was shown previously. Figure 2.11 shows reservoir inflow for the different future scenarios and different decades. It is clear from the figure that total inflows into the reservoir are likely to decline in the future, for each of the climate changes scenarios. Interannual variability in flows (the error bars in Figure 2.11) show that very low flows, are more likely to occur in the future, compared to the situation without climate change.

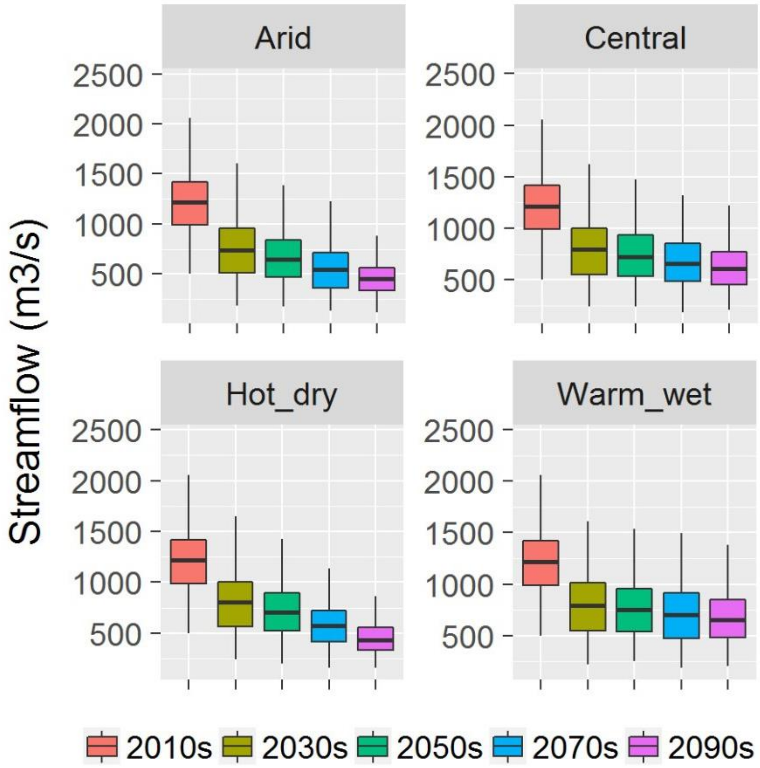

Figure 2.11. Observed (2010s) and projected (2030s-2090s) annual variability of inflow into Tuyamuyun reservoir.

2.5.2 Offtake points

Besides the pumping station drawing water from Tyuyamuyun reservoir, offtake locations are located at the reach of the Amu Darya downstream of the reservoir. The hydrological model simulations indicate increasing variability in flows, with variability increasing especially for the lower flows (Figure 2.12). It is especially the change in low flows, which are of interest in the light of possible future water scarcity. Looking at these changes per month of the year (Figure 2.13), indicates that the months with low flows are more subject to decreases in flows and increases in variability compared to the months with high flows. For most climate change scenarios, months with very low flows are likely to occur in January, February, November and December during dry years.

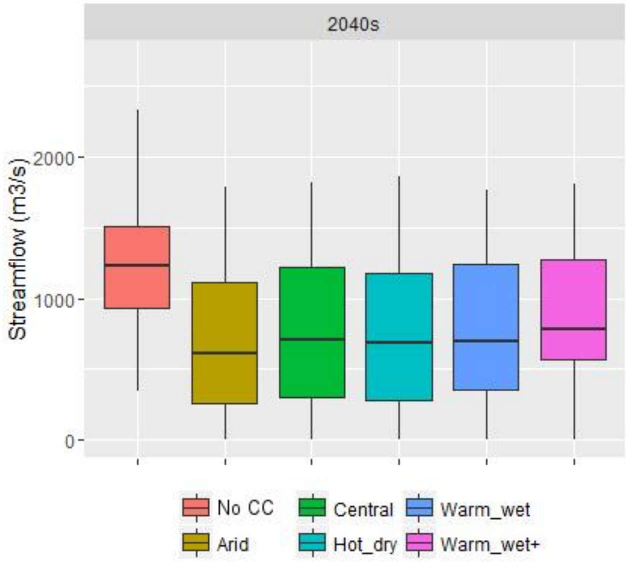

Figure 2.12: Projected streamflow variability in the 2040s for the Amu Darya reach downstream of Tyuyamuyun reservoir, for different climate change scenarios.

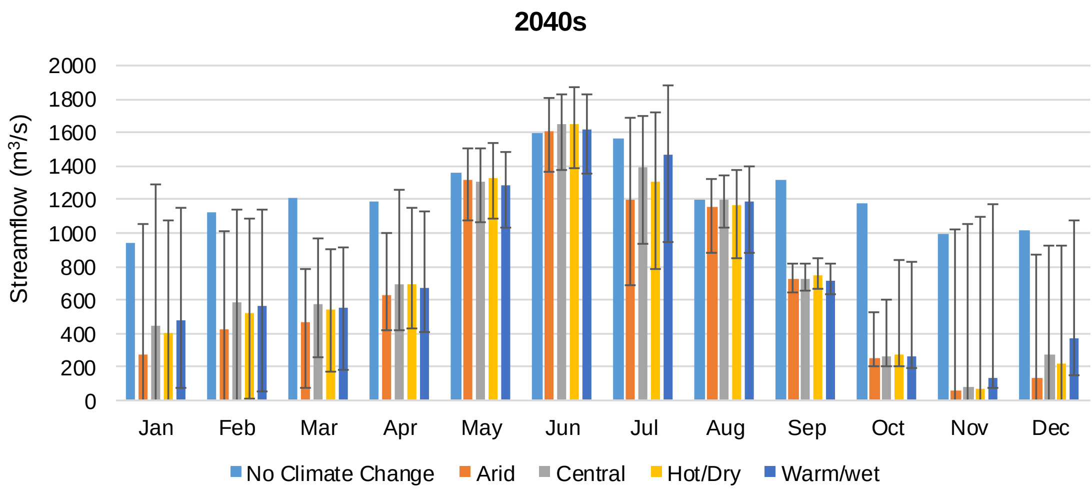

Figure 2.13: Projected streamflow variability per month in the 2040s for the Amu Darya reach downstream of Tyuyamuyun reservoir, for different climate change scenarios. Error bars indicate the interannual variablility of monthly flows.

2.5.3 Groundwater

Groundwater is used in areas where no surface water is available through water supply or canals, and constitutes a minor source of domestic water in the enitre project area, but a major source in remote areas outside the district center towns. Historical records of groundwater extractions for different wellfields in the project area do not provide clear trends (Figure 2.14). The record from the Berunyi wellfield is very constant, whereas the Abai wellfield shows a decreasing trend. For the Urazbai wellfield the trend was decreasing and extraction stopped completely in 2009. The reason for this is unknown. The much larger extractions in the wellfields in the Nukus district show a small increasing trend towards the end of the records.

Although no clear trends in groundwater can be derived from the historical abstraction records, groundwater recharge will decrease in the future because of decreases in Amu Darya flows (being the main source of groundwater recharge), increased evapotranspiration rates, and possible decrease in precipitation.

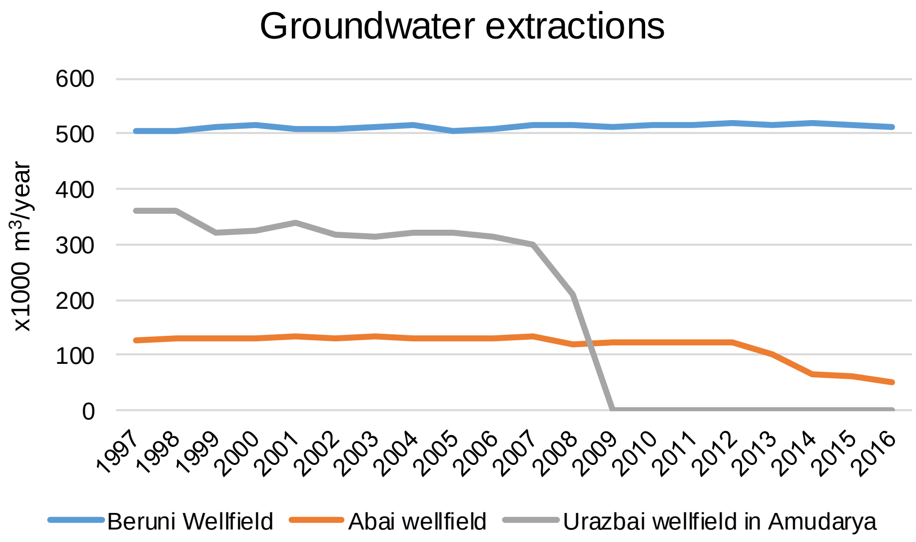

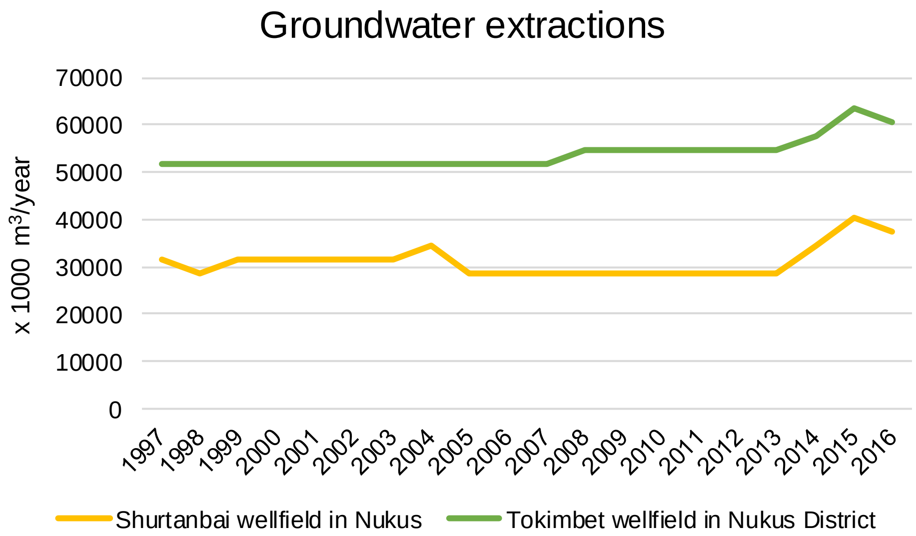

Figure 2.14: Groundwater extractions for different wellfields in the project area. Data source: PPTA team.

During a site visit it was reported that the groundwater is very saline during dry periods. This is also indicated by surveys under the local population. The project's inception report (9286, 2017) indicated that groundwater quality in the area in general is degrading due to highly salinized soils and increased use of agrochemicals. With dry periods likely to become more frequent and more severe in the future in the context of climate change, a decrease in relying on groundwater sources for domestic water supply is desirable.

3 Climate Risks and Adaptation

The potential water-related climate risks for the project beneficiaries – the population of the six districts in Karakalpakstan which are considered as the Project area – can be summarized as follows:

1. People in remote areas need to be connected to a centralized water supply system, because their current water sources are unsustainable under climate change.
2. Flows in the Amu Darya are likely to decrease towards the project horizon and be more variable, with low flows more frequent to occur
3. Because of future increases in air temperature, per capita water consumptions will increase.
4. Climatic extremes are very likely to increase in frequency and magnitude. This may lead to more damage to infrastructure.
5. Increases in air temperature lead to deterioration of water quality

These 5 principal climate risks are further detailed in separate sections, including an analysis of how strong or applicable these risks are in the context of the project's baseline design. Furthermore, required corresponding climate adaptation measures are proposed.

3.1 Water supply service coverage

The scarce amount of precipitation falling in the region may decrease further. This combined with increased evaporation rates leads to a decrease in groundwater recharge and increased competition with other water sectors and water users (industry and agriculture) in the project area. More people in remote areas will need to be connected to the water supply system, because less groundwater is available, and its quality is insufficient.

With an exception for Nukus, the Capital town, in the Republic of Karakalpakstan (RKP) centralized water supply service coverage is low, with a cover of 22.5% in the Amudarya district, and 32.6% in Berunyi district. Particularly in towns and settlements the water service is provided only a few hours daily. The water supply system will be designed for a service coverage of 100% of the region's districts.

The current population in the Project area is estimated at 360,000. Future population projections to the project's horizon 2045, indicate a projected population around 520,000 in 2045 (Table 3.1). This is an increase of almost 45% with respect to the current situation, and in line with the historical development of the population in Uzbekistan (Figure 3.1).

A population of 170,000 out of the total 360,000 lives in remote areas, outside the district's center towns. These are the most vulnerable people in the region, living in areas with population densities at or below 50 cap/km^2. Constructing water supply connections to these areas has high costs per connected household, and would therefore need to be strongly subsidized.

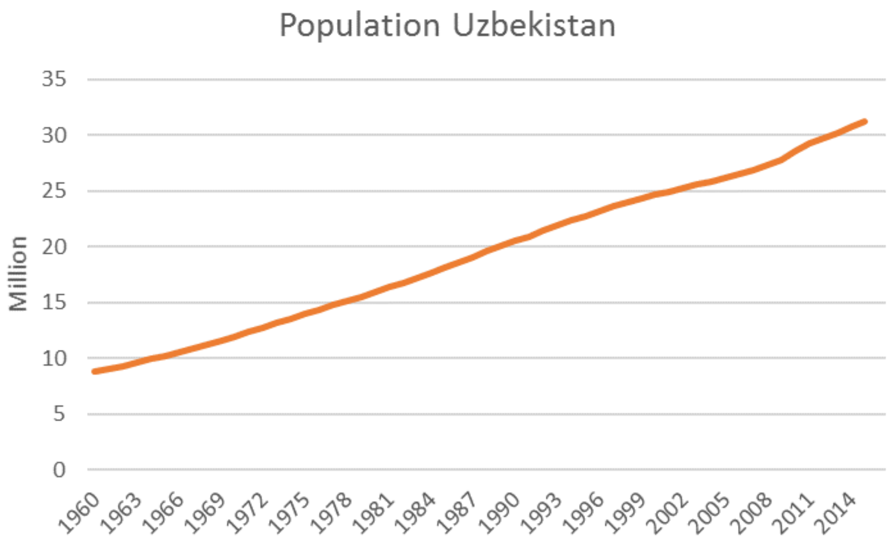

Figure 3.1: Historical population in Uzbekistan. Source: World Development Indicators, World Bank Group.

Table 3.1: Current and projected future population (x 1000 cap) in the project area's districts of Karakalpakstan. Source: ADB PPTA 9286 Feasibility Report.

Districts	Total population 2016	Population in remote areas 2016	Population in remote areas, % of total	Projected total population 2045	Projected population in remote areas 2045
Amudarya	78.5	43.9	56%	118.1	66.0
Beruniy	95.9	37.2	39%	149.2	57.9
Karauzak	31.3	16.3	52%	45.6	23.7
Kungrad	94.9	28.2	30%	130.9	38.9
Muynak	23.7	10.5	44%	31.0	13.7
Nukus	33.1	23.4	71%	43.8	31.0
Total	**357.4**	**159.5**	**45%**	**518.6**	**231.2**

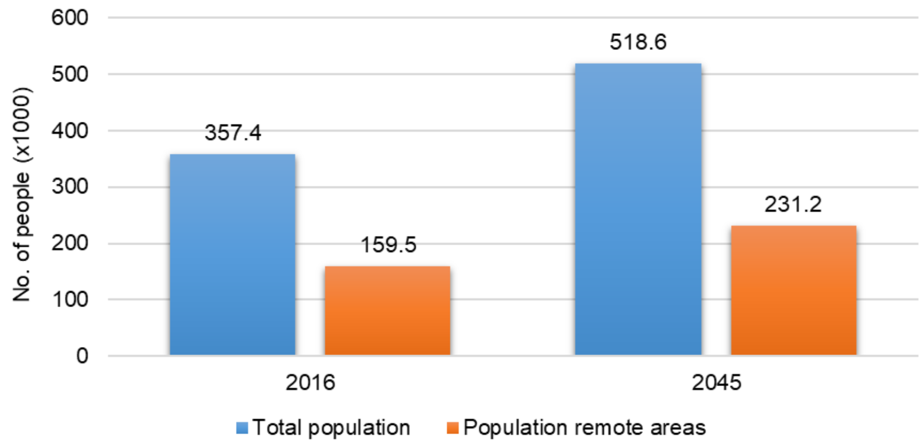

Figure 3.2: Project area's total population and population living in remote areas in 2016 and 2045.

Precipitation projections for the region indicate that precipitation is likely to change from 193 mm/yr to 182-212 mm/yr, depending on the climate change scenario (section 2.3). Thus, potentially there will be a small decrease in precipitation. Combined with other climatic changes, the model calculations show that evapotranspiration rates in the area are likely to increase by 5.3-8.0%, depending on the climate change scenario (Figure 3.3). The combination of changes in precipitation and changes in evapotranspiration rates will lead to a significant reduction in groundwater recharge and filling of local surface water storage. The earlier mentioned decreases in stream flow in the Amu Darya river, further lead to a decrease in recharge of groundwater levels.

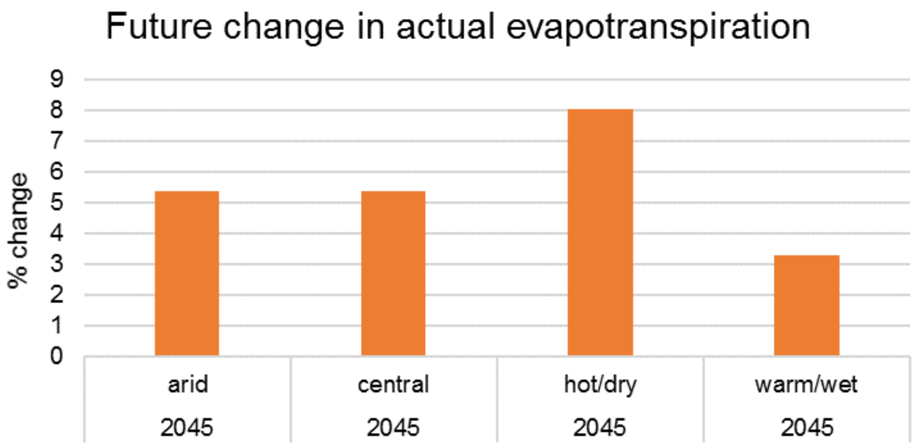

Figure 3.3: Future changes in evapotranspiration rates in the study area with respect to current situation.

Currently a significant share of the rural areas rely on groundwater abstractions for water supply. Reduced availability of resources in the aquifers due to climate change will mean that a relatively higher number of settlements and rural areas need to be connected to the distribution system to be resilient to climate-change induced water shortages. Besides, the reported groundwater quality in the current situation is low. With future climate change imposing more droughts and less groundwater recharge, this quality will further reduce. The only sustainable option for sufficient and safe domestic water would be to connect the remote areas to water supply drawn from the Amu Darya river and phasing out the use of groundwater for domestic purposes.

The average household size in rural areas in Uzbekistan is 5.9 cap (Government of the Republic of Uzbekistan, 2005). This implies that ~27,000 households in rural areas need to be connected to be resilient to climate change. At the project horizon 2045, this number will have increased to ~40,000 households.

3.2 Increased supply variability

As described in section 2.4.1 inflows into the upstream domains of the Amu Darya are likely to decrease gradually throughout the 21st century, for each of the climate change scenarios. This decrease in inflows is combined with increasing water demands in the areas upstream of Karakalpakstan. Large irrigated agricultural areas, will require more water as increasing temperatures lead to increased crop evapotranspiration. Besides, increases in population and standards of living lead to increased domestic water use.

In the end, these combined factors lead to strong decreases in inflows into Tyuyamuyun reservoir, as indicated in Figure 2.11 and Table 3.2. This is the principal reservoir from which the proposed water supply systems take surface water. The annual variability in inflows changes strongly, and each scenario shows low inflows during dry years. The inflow during dry years decreases by 34-48%, when 10-year periods are compared.

The storage capacity of Tyuyamuyun reservoir is 5400 Mm^3 (CA-Water database). The current annual water demand for domestic water in the project area is estimated at 29.2 Mm^3 or 0.5 % of the total reservoir storage capacity. An estimated 98% of the reservoir's water is used for agriculture, whereas the remaining 2% is used for domestic and industrial purposes. Since domestic water supply should always have priority over agricultural water supply, even with future inflow into the reservoir decreasing strongly, the amount of water available for domestic water use is sufficient. This also holds for the project horizon 2045. However, this is only valid if the basin's waters are managed in an integrated way, meaning that agricultural water supply in areas upstream of Tuyamuyun reservoir are rationed timely when dry periods and low reservoir levels are expected, to avoid the domestic water supply from running dry. Reservoir management should be improved using weather forecasts, optimizing releases and operational rules so spills are minimized.

Another, but much more costly mitigation measure is to increase existing water storage possibilities or construct new storage capacity. This option is not advised at this stage, since the risk can be mitigated by improving management and operations alone. However, this option should be reconsidered in the future if management and operational practices do not improve and if Tuyamuyun reservoir's capacity decreases in the future due to further siltation.

Table 3.2. Annual mean inflow into Tuyamuyun reservoir

Period	Scenario	Minimum annual average flow during 10-year period (m^3/s)	% change
2015	Reference (no Climate Change)	945	
2045	arid	492	-48%
2045	central	602	-36%
2045	hot/dry	554	-41%
2045	warm/wet	627	-34%

3.3 Per capita water consumption

Maximum temperatures and the occurrence of heat waves have an influence on per capita water consumption. Especially during heat waves, which are projected to occur more frequently and more severe under climate change, human water consumption will increase strongly. Thus, peaks in water consumption will become more extreme and frequent. Such peaks are determinative for the production and transport capacity of drinking water. Besides, it is also likely that more water is required for other domestic purposes, such as irrigation of gardens, with future increase in standards of living.

Thus, an increase in daily maximum temperatures and heat wave frequency (see also section 2.4) will lead to higher peak demands. This requires water supply infrastructure that is capable of meeting the peak demands. The water supply system is designed to supply 820,000 people continuously in 2045 (Table 3.1). Without accounting for climate change impacts, the estimated water use per capita in Uzbekistan would be 109 m^3 per capita per year (Aldaya et al., 2010).

To adapt the project to this climate change-induced risk, the design should include sufficient production and transportation capacity. Few studies assessed relationships between climate change induced changes in air temperature and domestic water consumption (Arnell, 1999; Herrington, 1996; New, 2002; Sadiq and Karney, 2005). (Herrington, 1996) estimates a 5% increase in per capita domestic demand due to 1 °C of warming, for the United Kingdom, and (New, 2002) used the same approach for the more arid Western Cape region in South Africa. (Sadiq and Karney, 2005) suggest a more non-linear relation between air temperature and domestic water demand, with stronger demand increases under climate change for higher temperatures. Considering the hot climate in the Project area, a 10% increase in domestic demand per 1 °C of warming can be assumed. In the case of a hot/dry climate change scenario that would imply that 27% more water needs to be supplied compared to the situation without climate change (Figure 3.4). In the most optimistic case (the warm/wet scenario), still, 8% more water needs to be supplied compared to the situation without climate change.

To mitigate this risk two options can be considered:

1) Increase the water supply capacity
2) Decrease domestic water demand per capita

In the demand projections used for the project's feasibility study (9286, 2017), the decrease in water use per capita as a result of providing metered connections and the proposed climate awareness programme, and capacity building has not been taken into account. The decrease in water use resulting from these two measures is estimated to be in the same order as the climate change-induced increase in domestic water demand. This therefore compensates and eventually mitigates this risk. Besides, the baseline design of the water supply system is to have a supply capacity of 250,000 m^3/day, which is sufficient to supply 820,000 people in 2045.

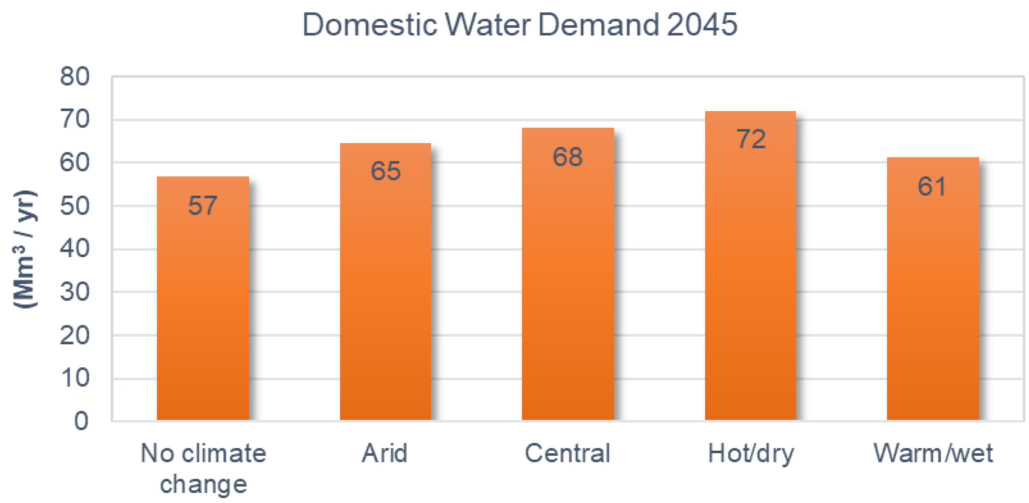

Figure 3.4: Total estimated domestic water use in the supplied area in 2045 without climate change, and for 4 climate change scenarios.

3.4 Damage to infrastructure

Almost all climate change scenarios indicate increases in frequency and magnitude of extreme events in the future. These extreme events (floods, heat waves, storms) lead to increase in damage to existing infrastructure. To make the infrastructure climate proof, additional investment is required to make the infrastructure resilient to future climate change.

Floods can have a serious impact on the maintenance and life expectancy of infrastructure. A major negative impact on the water infrastructure during floods is related to the increased water flows in the river bed at the intake facilities which need proper physical protection provisions. Other aspects are the potential flooding of treatment facilities and pumping stations located close to the river or in exposed areas, and landslides at riverbanks caused by flooding which often cut water pipes and power supply, prevent from access to water supply facilities or directly damage them.

Based on the climate projections and model simulations it is estimated that the frequency of peak flows that can lead to floods in the area will increase due to climate change between 0% and 90% (see Table 3.3).

These damages incur additional costs and require climate adaptation measures:

- Protection of water supply facilities against flooding and direct impact of the increased flow, by protecting the water intake facilities. Also, additional protection is required of pumping stations and the treatment plants or other facilities that are exposed to flooding or landslides
- Increased flooding leads to increased sedimentation and thus existing treatment plants need to be upgraded with installation of pre-sedimentation ponds.
- Also, there will be an increased need for risk-management and decision support tools that monitor water levels and provide early warnings.

Based on estimates in similar areas and for similar conditions (Guiu et al., 2015; Pouget et al., 2012), and assuming the scenario with the highest impact (Warm/wet), it is estimated that these adaptation measures could increase project costs by 20%.

Also heat waves and increased storm can potentially lead to increased damage to infrastructure, especially those facilities that rely on electricity supply (e.g. pumps). Typical measures that will need to be taken are:

- Additional need to use underground cables where possible
- Identify and use overhead transmission line routes less exposed to storms risks
- Install back-up power supply for WSS infrastructure (back-up power connection or generator)

From the climate projections studied for the project area, it was estimated that heat wave frequency will increase between 64% and 178%. Thus, costs related to protecting electricity supply for water supply infrastructure is likely to increase substantially. Assuming the scenario with the highest impact (Hot/dry), it is estimated that these costs can increase by around 10%.

Table 3.3: Changes in flooding and heat wave frequency under current and future climate change (hot/dry and warm/wet scenario)

Hazard	Indicator	Current	Hot_dry	Warm_wet
Flooding	Days/decade with daily rainfall > 20 mm	5	5	9.5
	Difference with current climate	0%	0%	90%
Heat waves	Days/year with daily max temp. > 38ºC	20	57	33
	Difference with current climate	0%	174%	64%

The baseline design of the infrastructure in the project is estimated to comply with the requirements imposed by the above mentioned climate change risks. Inspection in the field showed that the risk of damage by flooding is nihil. No structures are placed at or near the river banks, but intakes are located at side canals of the main river, and water levels can be largely regulated through the headworks. The risk of heat waves and associated dust storms prevails, but current design standards used in the baseline project are estimated to be sufficiently high to cope with these. It is however advised to include strong focus on maintenance of the infrastructure in the capacity building program to ensure long-lasting resilience.

3.5 Water quality

Increases in air temperature lead to a decline in the quality of surface water (Delpla et al., 2009). Observed adverse effects include increases in pH and decrease in dissolved oxygen solubility (Ducharne et al., 2007). Warming of soils and increases in droughts lead to increases in nitrogen mineralization and increases in extractable organic carbon. Pathogens spread more quickly in warmer water, causing immediate threats for human health. These adverse effects are already observed at small temperature increases in the order of 0.5 °C. Wïth projected temperature increases for the study area of +0.8 to + 2.7 °C between the present and the 2045 project horizon, this could have a significant impact in this area.

To cope with this climate change-induced risk, additional investments are generally required in the drinking water treatment facilities and there are increased costs related to water quality monitoring and health risk assessments. Based on studies in similar conditions (climate and socio-economic), it is estimated that these issues could lead to a 5-15% increase in costs in the design of water treatment facilities with sufficient large capacities and increased health risk monitoring, compared to a future without climate change, depending on the scenario. Similar as for the climate change risk imposed on infrastructure, the baseline design of the project’s water treatment infrastructure is resilient to the projected increases in temperature and associated increase in treatment capacity.

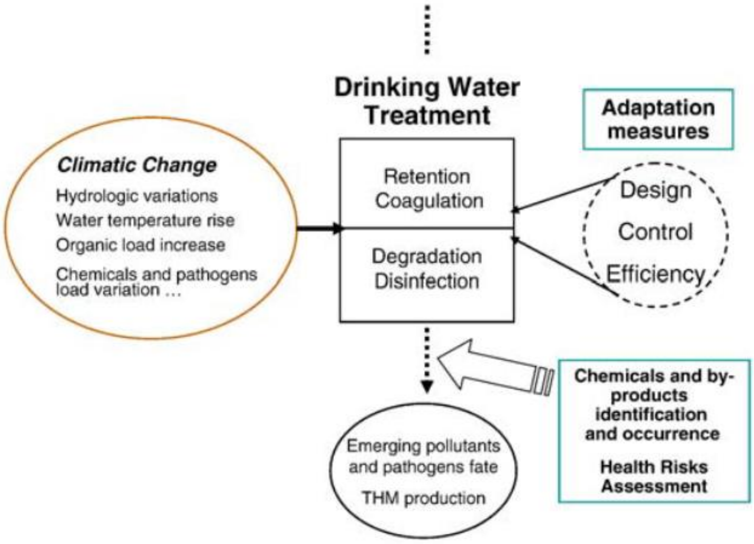

Figure 3.5: Climate change impacts and drinking water treatment issues (Delpla et al., 2009)**.**

3.6 Overview of recommended adaptation measures

To summarize the analysis of the potential climate change-induced risks for the project it can be concluded that adaptation measures are required to make the project climate-resilient up to the project horizon 2045. The adaptation measures are divided in two groups of measures:

1. Hard measures: Construction of new infrastructure
2. Soft measures: Increase awareness and capacity

The major risk identified considers the absence of connection to the centralized water supply system in remote areas outside the district's centers. By connecting these areas, the climate resilience of the inhabitants of these areas increases drastically. The total costs for constructing the connections to the remote areas is estimated at 35.8 million US$ (Table 3.4).

Table 3.4: Estimated costs of connections to remote areas.

District	Population in remote areas (x1000 cap)			Costs of connections to remote areas (million US$)
	2016	**2022**	**2045**	
Amudarya	43.9	48.1	66.0	7.5
Beruniy	37.2	41.0	57.9	8.3
Karauzak	16.3	17.7	23.7	5.1
Kungrad	28.2	30.2	38.9	6.5
Nukus	23.4	24.9	31.0	4.9
Muynak	10.5	11.1	13.7	3.5
Total	159.5	173.0	231.2	35.8

The other risks identified can be mitigated by soft measures. These measures should lead to changes in operational protocols, communicate the risks and generate awareness on climate change, and implement long-term consideration, including climate change, in the development of strategies. Operations of the water supply must change drastically to make the system climate resilient and operators should be trained for this. This will require substantial efforts as stationarity in operations should shift towards dynamic and pro-active operations. Intensive training of staff of the TN is needed to make this paradigm-shift in operating their systems in a re-active (by complaints) modus towards a pro-active way by considering short and long-term forecasts in demand and supply.

To reduce the water consumption per capita, public awareness campaigns targeting schools, kindergarten, water users (especially women), and other stakeholders should be implemented. These should be aimed at educating the population to better appreciate and understand to value of water and to ensure sustainable and productive use of water supplied. Besides this basic water related education, a real-time communication system should be setup so that water users can be informed on a day-to-day base about expected water delivery. This will build trust and will avoid disruption of the system by e.g. excessive storage by users, illegal withdrawals, non-sustainable source development, etc.

Strategic monitoring and development should not stop after the Project design and construction. On a regular base (annual) past performance and near-future strategic decisions need to be made to ensure optimal distribution of water and maintenance. Similarly, a system should be established to evaluate on a five-years' base the longer term strategic decisions to ensure that the system is still climate resilient. Substantial capacity building and institutional refocussing is needed to achieve this. The costs to implement these soft measures are estimated at 4 million US$.

4 Conclusions and Recommendations

This Climate Risk Vulnerability Assessment (CRVA) identifies the risks and vulnerabilities associated with future climate change for Asian Development Bank's proposed project to expand water supply in Western Uzbekistan in six districts of Karakalpakstan.
Water availability in the project area depends largely on water brought from the high Pamir mountain ranges by the Amu Darya river. Therefore, this CRVA constitutes a basin-wide climate change impact assessment, using a suite of coupled state-of-the-art hydrological models, and an ensemble of representative marker scenarios from the most recent pool of IPCC climate change scenarios.

Climate change projections for the area show continuing increases in temperature, and variation in projections of future precipitation. For water supplied from the mountainous upstream areas, the hydrological projections show a steady decrease in flows, starting in the coming decades, accelerating towards the end of the century. These trends will already have effects at the project's horizon year in 2045. Taking into account changes in inflow form the mountains, and changes in domestic and agricultural water demand and water use in the agricultural and domestic areas upstream of the project site, it is likely that inflows into Tyuyamuyun reservoir and the Amu Darya reaches downstream of the reservoir will decrease in the coming decades. Interannual variability is likely to increase especially for low flows, indicating increases in water shortage during dry years. The people most vulnerable to climate change, living in the remote areas of Karakalpakstan, currently cannot rely on a sustainable source of water supply.

The risk assessment analysed five major potential climate-change related risks for the proposed project:

1. People in remote areas need to be connected to a centralized water supply system, because their current water sources are unsustainable under climate change.
2. Flows in the Amu Darya are likely to decrease towards the project horizon and be more variable, with low flows more frequent to occur
3. Because of future increases in air temperature, per capita water consumptions will increase.
4. Climatic extremes are very likely to increase in frequency and magnitude. This may lead to more damage to infrastructure.
5. Increases in air temperature lead to deterioration of water quality

The analysis indicates that risk 1, 2, and 3 require adaptation measures, which are additional to the Project's baseline design. Taking into account the spread in the climate change scenarios, following measures are proposed for climate proofing of the proposed water supply project:

- Construct infrastructure to connect 160,000 (230,000 in 2045) people to the centralized water supply system taking water from the Amu Darya river. Thereby the use of groundwater and other unsafe water sources can be phased out, thus making the most vulnerable groups of the population in the Project area climate resilient. The costs of implementing this infrastructure are estimated at 35.8 million US$
- Implement programs aimed at changing operational protocols, generating awareness of climate change-induced risks, and implementation of long-term considerations, including climate change, in the development of strategies. The costs for implementing such programs is estimated at 4 million US$.

References

9286, A. P.: ADB TA 9286 - UZB: Western Uzbekistan Water Supply System Development Project - Feasibility Study, Tashkent, Uzbekistan., 2017.
ADB: Central Asia Regional Economic Cooperation: Power Sector Regional Master Plan, ADB., 2012a.

ADB: Consultant's Report Regional Technical Assistance : Water and Adaptation Interventions in Central and West Asia., 2012b.

Aldaya, M. M., Munoz, G. and Hoekstra, A. Y.: Water Footprint of cotton, wheat and rice production in Central Asia, Delft., 2010.

Arnell, N. W.: Climate change and global water resources, Glob. Environ. Chang., 9, S31–S49, 1999.

Bernauer, T. and Siegfried, T.: Climate change and international water conflict in Central Asia, J. Peace Res., 49(1), 227–239, doi:10.1177/0022343311425843, 2012.

Blázquez, J. and Nuñez, M. N.: Analysis of uncertainties in future climate projections for South America: Comparison of WCRP-CMIP3 and WCRP-CMIP5 models, Clim. Dyn., 41(3–4), 1039–1056, doi:10.1007/s00382-012-1489-7, 2013.

Chen, Y., Li, W., Deng, H., Fang, G. and Li, Z.: Changes in Central Asia's Water Tower: Past, Present and Future, Sci. Rep., 6(October), 35458, doi:10.1038/srep35458, 2016.

Chen, Y., Li, W., Fang, G. and Li, Z.: Review article: Hydrological modeling in glacierized catchments of Central Asia: status and challenges, Hydrol. Earth Syst. Sci., 21, 669–684, doi:10.5194/hess-2016-325, 2017.

Christensen, J. H. and Christensen, O. B.: Severe summertime flooding in Europe, Nature, 421(February), 805–806, 2002.

Delpla, I., Jung, A. V., Baures, E., Clement, M. and Thomas, O.: Impacts of climate change on surface water quality in relation to drinking water production, Environ. Int., 35(8), 1225–1233, doi:10.1016/j.envint.2009.07.001, 2009.

Deque, M.: Frequency of precipitation and temperature extremes over France in an anthropogenic scenario: Model results and statistical correction according to observed values, Glob. Planet. Change, 57(1–2), 16–26, doi:10.1016/j.gloplacha.2006.11.030, 2007.

Droogers, P. and Allen, R. G.: Estimating reference evapotranspiration under inaccurate data conditions, Irrig. Drain. Syst., 16, 33–45, 2002.

Ducharne, A., Baubion, C., Beaudoin, N., Benoit, M., Billen, G., Brisson, N., Garnier, J., Kieken, H., Lebonvallet, S., Ledoux, E., Mary, B., Mignolet, C., Poux, X., Sauboua, E., Schott, C., Théry, S. and Viennot, P.: Long term prospective of the Seine River system: Confronting climatic and direct anthropogenic changes, Sci. Total Environ., 375(1–3), 292–311, doi:10.1016/j.scitotenv.2006.12.011, 2007.

Fowler, H. J., Blenkinsop, S. and Tebaldi, C.: Linking climate change modelling to impacts studies : recent advances in downscaling techniques for hydrological modelling, Int. J. Climatol., (September), 1547–1578, doi:10.1002/joc, 2007.

Government of the Republic of Uzbekistan: Welfare Improvement Strategy Paper of the Republic of Uzbekistan for 2005-2010, Tashkent, Uzbekistan., 2005.

Guiu, R., Pouget, L. and Termes, M.: Selecting an Efficient Adaptation Level to Uncertain Water Scarcity by Coupling Hydrological Modeling and Economic Valuation, Water Econ. Policy, 1(3), 1550008, doi:10.1142/S2382624X15500083, 2015.

Harris, I., Jones, P. D., Osborn, T. J. and Lister, D. H.: Updated high-resolution grids of monthly climatic observations - the CRU TS3.10 Dataset, Int. J. Climatol., doi:10.1002/joc.3711, 2013.

Herrington, P.: Climate Change and the Demand for Water, p. 164, HMSO., 1996.

Hock, R.: Glacier melt: a review of processes and their modelling, Prog. Phys. Geogr., 29(3), 362–391, doi:10.1191/0309133305pp453ra, 2005.

Immerzeel, W. W. and Lutz, A. F.: Regional knowledge sharing on climate change scenario downscaling. FutureWater technical report 116., Wageningen, The Netherlands., 2012.

Immerzeel, W. W., Lutz, A. F. and Droogers, P.: Climate Change Impacts on the Upstream Water Resources of the Amu and Syr Darya River Basins, Wageningen, The Netherlands., 2012.

IPCC: Climate change 2007: Synthesis Report. Contribution of Working Groups I, II and III to the Fourth Assessment Report of the Intergovernmental Panel on Climate Change, edited by R. K. Pachauri and A. Reisinger, Geneva, Switzerland. [online] Available from: http://www.worldcat.org/oclc/603555098 TS - WorldCat, 2007.

IPCC: Climate Change 2013: The Physical Science Basis. Contribution of Working Group I to the Fifth Assessment Report of the Intergovernmental Panel on Climate Change, Cambridge, UK., 2013.

Joetzjer, E., Douville, H., Delire, C. and Ciais, P.: Present-day and future Amazonian precipitation in global climate models: CMIP5 versus CMIP3, Clim. Dyn., 41(11–12), 2921–2936, doi:10.1007/s00382-012-1644-1, 2013.

Karssenberg, D., Burrough, P., Sluiter, R. and de Jong, K.: The PCRASTER software and course materials for teaching numerical modelling in the environmental sciences, Trans. GIS, 5, 99–110, doi:10.1111/1467-9671.00070, 2001.

Kay, A. L., Davies, H. N., Bell, V. A. and Jones, R. G.: Comparison of uncertainty sources for climate change impacts: flood frequency in England, Clim. Change, 92, 41–63, doi:10.1007/s10584-008-9471-4, 2008.

Knutti, R. and Sedláček, J.: Robustness and uncertainties in the new CMIP5 climate model projections, Nat. Clim. Chang., 3, 369–373, doi:10.1038/nclimate1716, 2012.

Lioubimtseva, E. and Henebry, G. M.: Climate and environmental change in arid Central Asia: Impacts, vulnerability, and adaptations, J. Arid Environ., 73(11), 963–977, doi:10.1016/j.jaridenv.2009.04.022, 2009.

Lioubimtseva, E., Cole, R., Adams, J. M. and Kapustin, G.: Impacts of climate and land-cover changes in arid lands of Central Asia, J. Arid Environ., 62(2), 285–308, doi:10.1016/j.jaridenv.2004.11.005, 2005.

Lutz, A. F. and Immerzeel, W. W.: Water Availability Analysis for the Upper Indus , Ganges , Brahmaputra , Salween and Mekong River Basins, Technical Report 127 FutureWater, Wageningen, The Netherlands., 2013.

Lutz, A. F., Droogers, P. and Immerzeel, W. W.: Climate Change Impact and Adaptation on the Water Resources in the Amu Darya and Syr Darya River Basins, FutureWater Report 110, Wageningen, Netherlands., 2012.

Lutz, A. F., Immerzeel, W. W., Gobiet, A., Pellicciotti, F. and Bierkens, M. F. P.: Comparison of climate change signals in CMIP3 and CMIP5 multi-model ensembles and implications for Central Asian glaciers, Hydrol. Earth Syst. Sci., 17(9), 3661–3677, doi:10.5194/hess-17-3661-2013, 2013.

Lutz, A. F., Immerzeel, W. W., Shrestha, A. B. and Bierkens, M. F. P.: Consistent increase in High Asia ' s runo due to increasing glacier melt and precipitation, Nat. Clim. Chang., (June), 1–6, doi:10.1038/NCLIMATE2237, 2014.

Lutz, A. F., ter Maat, H. W., Biemans, H., Shrestha, A. B., Wester, P. and Immerzeel, W. W.: Selecting representative climate models for climate change impact studies: an advanced envelope-based selection approach, Int. J. Climatol., 36, 3988–4005, 2016.

Maraun, D., Wetterhall, F., Ireson, A. M., Chandler, R. E., Kendon, E. J., Wildmann, M., Brienen, S., Rust, H. W., Sauter, T., Themeßl, M., Venema, V. K. C. and Chun, K. P.: Precipitation downscaling under climate change: recent developments to bridge the gap between dynamical models and the end user, Rev. Geophys., 48(RG3003), 1–34, 2010.

Meehl, G. A., Covey, C., Delworth, T., Latif, M., Mcavaney, B., Mitchell, J. F. B., Stouffer, R. J. and Taylor, K. E.: The WCRP CMIP3 multimodel dataset: A New Era in Climate Change Research, Bull. Am. Meteorol. Soc., 88(September), 1382–1394, 2007.

New, M.: Climate change and water resources in the southwestern Cape, South Africa, S. Afr. J. Sci., 98(7–8), 369–367, 2002.

Pouget, L., Escaler, I., Guiu, R., Mc Ennis, S. and Versini, P. A.: Global Change adaptation in water resources management: The Water Change project, Sci. Total Environ., 440, 186–193, doi:10.1016/j.scitotenv.2012.07.036, 2012.

Prudhomme, C., Reynard, N. and Crooks, S.: Downscaling of global climate models for flood frequency analysis: where are we now?, Hydrol. Process., 16(6), 1137–1150, doi:10.1002/hyp.1054, 2002.

Raskin, P., Hansen, E., Zhu, Z. and Stavisky, D.: Simulation of water supply and demand in the Aral Sea Region, Water Int., 17, 55–67 [online] Available from: http://www.tandfonline.com/doi/abs/10.1080/02508069208686127 (Accessed 28 December 2012), 1992.

Sadiq, W. A. and Karney, B. W.: Modeling Water Demand Considering Impact of Climate Change – a Toronto Case Study, Eff. Model. Urban Water Syst. Monogr. 13, 6062, 93–106, doi:10.14796/JWMM.R223-06, 2005.

Sorg, A., Huss, M., Rohrer, M. and Stoffel, M.: The days of plenty might soon be over in glacierized Central Asian catchments, Environ. Res. Lett., 9(104018), 8, doi:10.1088/1748-9326/9/10/104018, 2014.

Sperber, K. R., Annamalai, H., Kang, I. S., Kitoh, A., Moise, A., Turner, A., Wang, B. and Zhou, T.: The Asian summer monsoon: An intercomparison of CMIP5 vs. CMIP3 simulations of the late 20th century, Clim. Dyn., 41(9–10), 2711–2744, doi:10.1007/s00382-012-1607-6, 2013.

Taylor, K. E., Stouffer, R. J. and Meehl, G. A.: An Overview of CMIP5 and the Experiment Design, Bull. Am. Meteorol. Soc., 93(4), 485–498, doi:10.1175/BAMS-D-11-00094.1, 2012.

Terink, W., Lutz, A. F., Simons, G. W. H., Immerzeel, W. W. and Droogers, P.: SPHY v2.0 : Spatial Processes in HYdrology, Geosci. Model Dev., 8, 2009–2034, doi:10.5194/gmd-8-2009-2015, 2015a.

Terink, W., Lutz, A. F. and Immerzeel, W. W.: SPHY v2.0: Spatial Processes in Hydrology: Model theory and SPHY interface (v1.0) manual, Wageningen, The Netherlands., 2015b.

Wilby, R. L. and Wigley, T. M. L.: Downscaling general circulation model output: a review of methods and limitations, Prog. Phys. Geogr., 21(4), 530–548, doi:10.1177/030913339702100403, 1997.

Appendix I - Delta change downscaling approach

I.1 Approach

An efficient way to do downscale GCM projections is applying the ‘delta change’ approach. When applying this approach the final generated grids are monthly delta change data for a future period (e.g. 2071-2100) relative to a reference period (e.g. 1971-2000). The delta change values reflect the change in temperature and precipitation over a period years (in this case that would be 100 years. These change data are in Kelvin for temperature and in % for precipitation. This well established delta change approach is an efficient way to assess climatic changes (Arnell, 1999; Deque, 2007; Kay et al., 2008). This approach becomes necessary due to the large scale discrepancy between the climate models and the hydrological models operating at a much higher resolution. We cut out the grid cells of the climate models over the study region to calculate monthly climate change signals, which are subsequently superimposed on a local reference time series, which is available from the ADB project. The “delta change” approach removes large parts of model biases, which cancel out in the climate change signals. Based on these change data the annual change can be calculated (assuming linear change) and be used to generate transient time series to force the models.

The following paragraphs discuss the procedure in detail, and show examples how this was done for the Himalayan region (based on (Immerzeel and Lutz, 2012)).

I.2 Downloading of GCMs

The selected GCMs are downloaded from the CMIP5 portal. (http://cmip-pcmdi.llnl.gov/cmip5/data_portal.html). For the selected GCMs the files containing the monthly summed precipitation (pr, [$kgm^{-2}s^{-1}$]) and monthly averaged near-surface air temperature (tas, [K]) for the historical period (January 1971 – December 2000) and future period (January 2071 – December 2100) are downloaded. The data is available in netCDF format. Each file contains a time series of worldwide rasters for each month in the resolution specific for the GCM.

I.3 Downscaling of GCMs

The downscaling of the GCMs consists of the following processing steps:

- Extracting temperature and precipitation grid per month for study domain from NetCDF files
- Calculate average temperature and precipitation per month for Jan-Dec for 1971-2000
- Calculate average temperature and precipitation per month for Jan-Dec for 2071-2100
- Calculate delta change values for Jan-Dec for 2071-2100 compared to 1971-2000
- Interpolate delta change values from GCM resolution to 0.25° resolution

The processing steps are done using the ‘raster’ package in the open access R statistical computing software (http://www.r-project.org/), and ArcGIS scripting with Python. In the following paragraphs these processing steps are discussed in detail.

I.3.1 *Extracting one grid per month for study domain from NetCDF files*

For each month within the periods 1971-2000 and 2071-2100 a grid with temperature and a grid with precipitation is extracted for the rough extent of the study domain. This results for each GCM in:

- 360 temperature grids reference period (each month from January 1971 to December 2000)
- 360 temperature grids future period (each month from January 2071 to December 2100)
- 360 precipitation grids reference period (each month from January 1971 to December 2000
- 360 precipitation grids future period (each month from January 2071 to December 2100)

In total 4 * 360 * 8 = 11520 grids are extracted. Figure 0.1 shows examples of extracted temperature and precipitation grids for July 1971 for the CanESM2-r4ip1 RCP 4.5 projection.

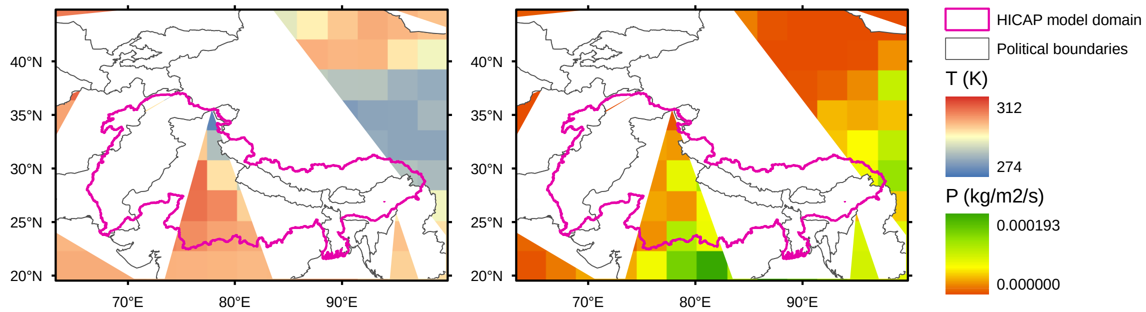

Figure 0.1: Average T (K) and summed P (kg/m²/s) for July 1971 (CanESM2-r4i1p1_rcp45).

I.3.2 *Calculate average monthly temperature and precipitation for Jan-Dec 1971-2000*

For each month in the reference period (1971-2000) a grid with the average temperature is calculated using the grids extracted in the previous step (section I.3.1). This is done by summing all temperature grids for the specific month and dividing by the number of summed months. For example for January this is:

1971-2000 January average = (January 1971 + January 1972 + … + January 2000) / 30

The same is done for the months February to December.

The same procedure is applied to calculate average precipitation per month. For each month in the reference period (1971-2000) a grid with the average monthly summed precipitation is calculated using the grids extracted in the previous step (section I.3.1). This is done by summing all precipitation grids for the specific month and dividing by the number of summed months. For example for January this is:

1971-2000 January average = (January 1971 + January 1972 + … + January 2000) / 30

The same is done for the months February to December.

This yields:

- 12 grids for average temperature (Jan-Dec)
- 12 grids for average summed precipitation (Jan-Dec)

The procedure is repeated for each of the selected GCMs resulting in a total of 24 x 8 = 192 grids. Figure 0.2 shows examples of average July temperature and precipitation grids for the reference period (1971-2000) and the future period (2071-2100) for the the CanESM2-r4ip1 RCP 4.5 projection.

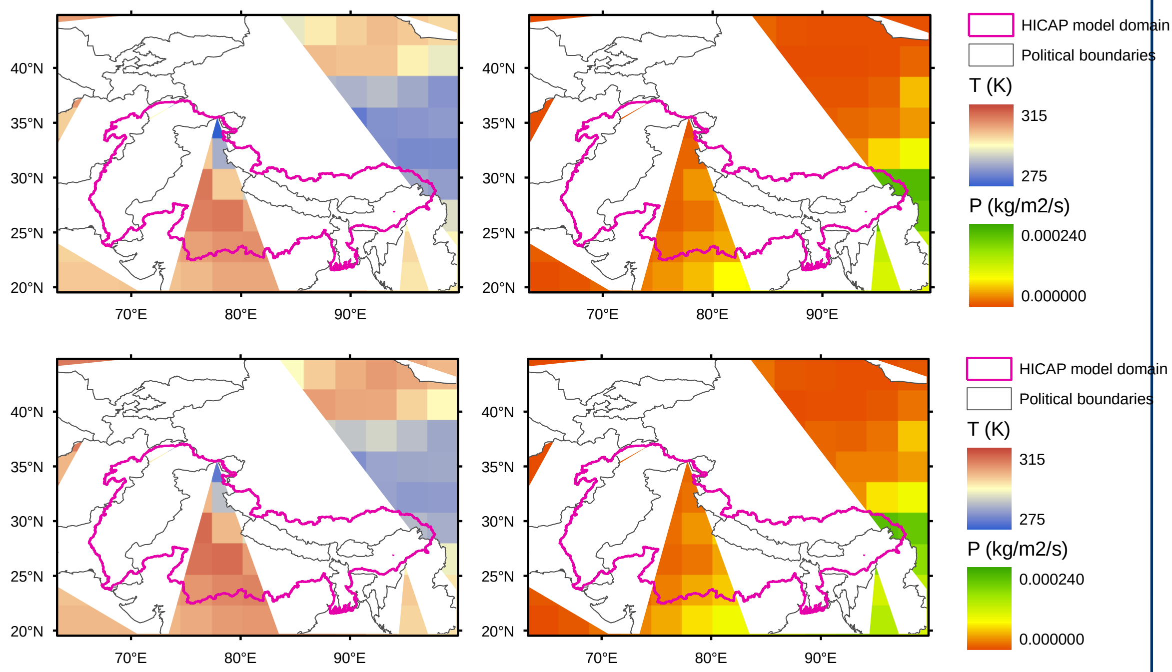

Figure 0.2: Average July temperature and average July precipitation 1971-2000 (upper panels) and 2071-2100 (lower panels) (CanESM2-r4i1p1_rcp45).

I.3.3 Calculate average monthly temperature and precipitation for Jan-Dec for 2071-2100

Following the same procedure as in section I.3.2 average monthly temperature and precipitation grids are calculated for the future period (2071 – 2100).

For each month in the future period (2071-2100) a grid with the average temperature is calculated using the grids extracted in the previous step (section I.3.1). This is done by summing all temperature grids for the specific month and dividing by the number of summed months. For example for January this is:

2071-2100 January average = (January 2071 + January 2072 + … + January 2100) / 30

The same is done for the months February to December.

The same procedure is applied to calculate average precipitation per month. For each month in the future period (2071-2100) a grid with the average monthly summed precipitation is calculated using the grids extracted in the previous step (section I.3.1). This is done by summing all precipitation grids for the specific month and dividing by the number of summed months. For example for January this is:

2071-2100 January average = (January 2071 + January 2072 + … + January 2100) / 30

The same is done for the months February to December.

This yields:

- 12 grids for average temperature (Jan-Dec)
- 12 grids for average summed precipitation (Jan-Dec)

The procedure is repeated for each of the selected GCMs resulting in a total of 24 x 8 = 192 grids. Figure 0.2 shows examples of average July temperature and precipitation grids for the reference period (1971-2000) and the future period (2071-2100) for the the CanESM2-r4ip1 RCP 4.5 projection.

I.3.4 Calculate delta change values for Jan-Dec for 2071-2100 compared to 1971-2000

For each month (Jan-Dec) a delta change value (Arnell, 1999; Deque, 2007; Kay et al., 2008) is calculated using the grids calculated in sections I.3.2 and I.3.3. For temperature the delta change value is calculated in Kelvin and for precipitation the delta change value is calculated as a percentage.

For example, the ΔT value for January is calculated as follows:

ΔT Jan = T Jan 2071-2100 – T Jan 1971-2000

The same is done for February – December.

This leads to 12 (Jan-Dec) ΔT grids per selected GCM. For eight GCMs this means 12 x 8 = 96 ΔT grids. As an example, Figure 0.3 shows the ΔT grids for January and July for the CanESM2-r4ip1 RCP 4.5 projection.

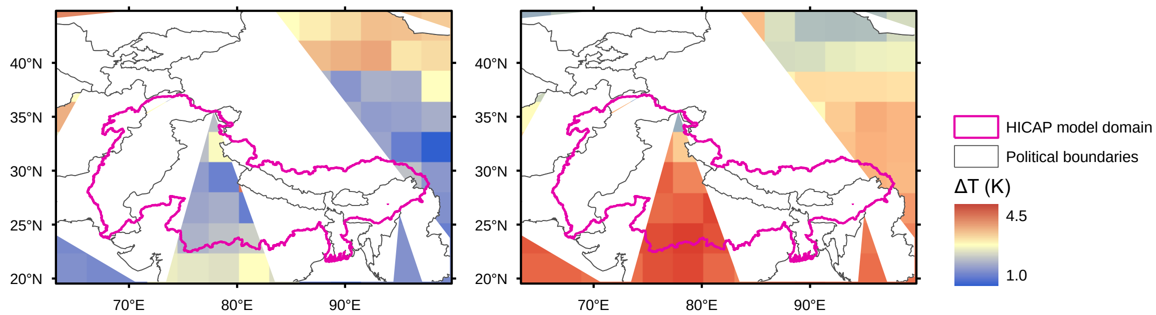

Figure 0.3: Delta change for temperature January (left panel) and July (right panel) (CanESM2-r4i1p1_rcp45).

For precipitation, the calculation of the delta change value requires extra steps. Because some parts of the study area are characterized by very low amounts of precipitation during parts of the year this can lead to very extreme values when calculating the ΔP value. To avoid this, the ΔP value for months with low precipitation (< 15 mm per month), is calculated using the annual precipitation instead of precipitation per month.

In addition, a maximum boundary is set at 200% of the precipitation value in the reference period.

For each selected GCM an annual ΔP value is calculated using the monthly precipitation grids calculated in sections I.3.2 and I.3.3. With these grids annual precipitation grids can be calculated for the reference period and the future period:

Annual P 1971-2000 = P Jan 1971-2000 + P Feb 1971-2000 + … + P Dec 1971-2000

Annual P 2071-2100 = P Jan 2071-2100 + P Feb 2071-2100 + … + P Dec 2071-2100

If monthly precipitation in 1971-2000 > 15 mm:

Jan ΔP = ((Jan P 2071-2100 – Jan P 1971-2000) / Jan P 1971-2000)) * 100

If monthly precipitation in 1971-2000 < 15 mm:

Jan ΔP = ((Annual P 2071-2100 – Annual P 1971-2000) / Annual P 1971-2000) * 100

If Jan ΔP < 200%:
Jan ΔP = Jan delta change P

If Jan ΔP > 200%:
Jan ΔP = 200%

The same is done for February – December.
This leads to 12 ΔP grids (Jan-Dec) for precipitation per selected GCM. For eight GCMs this means 12 x 8 = 96 ΔP grids.

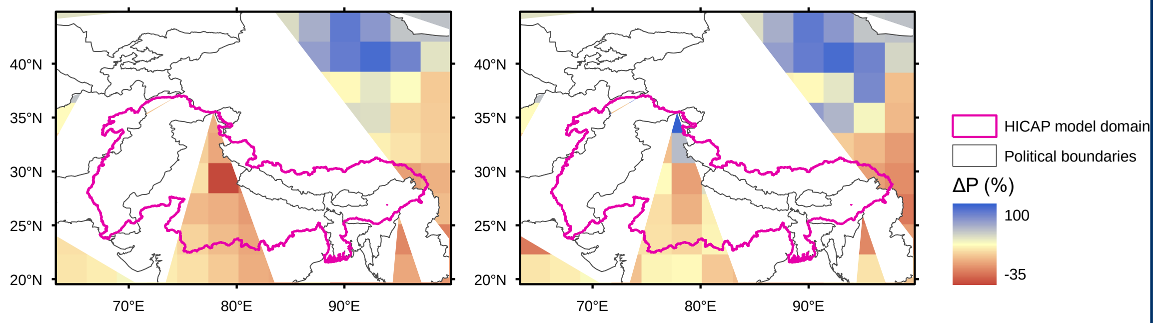

Figure 0.4: Delta change value for precipitation in January (left panel) and July (right panel) (CanESM2-r4i1p1_rcp45).

I.3.5 Interpolate delta change values from GCM resolution to 0.25° resolution

The 192 delta change grids calculated in section I.3.4 are spatially interpolated to 0.25° resolution using a spline interpolation. This interpolation is done from the central points of the grid cells. A tension spline with spline tension 10 and 4 neighbours is applied.

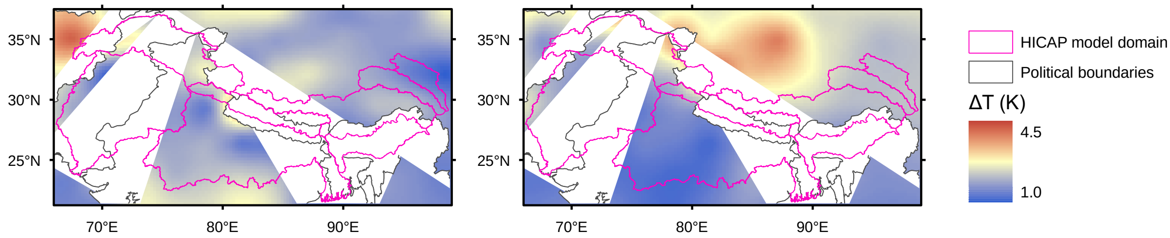

Figure 0.5: Delta change for temperature January (left panel) and July (right panel) at 0.25° resolution (CanESM2-r4i1p1_rcp45).

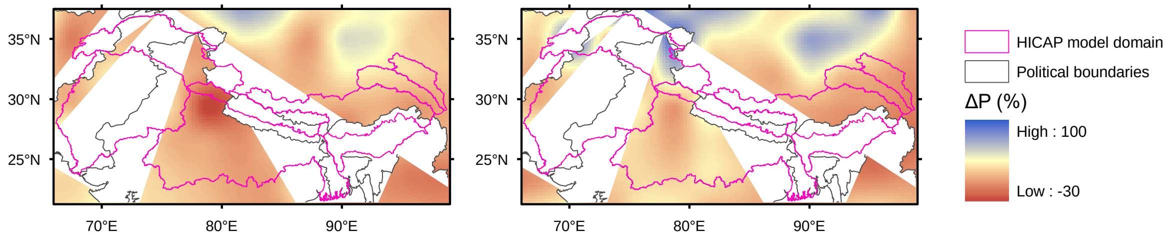

Figure 0.6: Delta change value for precipitation in January (left panel) and July (right panel) at 0.25° resolution (CanESM2-r4i1p1_rcp45).

II.1 SPHY model structure

The SPHY (Spatial Processes in Hydrology) model (Immerzeel et al., 2012; Lutz and Immerzeel, 2013; Terink et al., 2015b) is a raster based highly detailed full distributed cryospheric- hydrological model. The model is based on commonly accepted standards from multiple proven hydrological models. SPHY is created in PCRaster environmental modelling software (Karssenberg et al., 2001). PCRaster is a spatio-temporal environmental modelling language developed at Utrecht University, the Netherlands. The model runs at 1 x 1 km spatial resolution with daily time steps and incorporates all major hydrological processes as well as cryospheric processes. A full decription is available in the scientific journal publication by (Terink et al., 2015b)

The actual runoff which is calculated for each grid cell consists of four contributing factors. These are: runoff originating from rain, runoff originating from snow melt, runoff originating from glacial melt, and base flow, as visualized in Figure 0.7. With the daily air temperature and daily precipitation per grid cell as input the model evaluates how much precipitation falls and it is disaggregated into either snow or rain based on the air temperature distribution. The model evaluates the amount of glacier melt and snow melt or accumulation and which part of snow and glacier melt is directly transformed to runoff and which part refreezes. Rainfall-runoff processes are evaluated in a soil component in the model. The runoff from all contributing components is routed through the system using the DEM.

Each grid cell is divided in fractions. If a cell is (partly) glacierized, the cell has a glacier fraction between 0 and 1 (0: no glacier cover, 1: complete glacier cover). The other fraction of the grid cell can be either ‘snow’ or ‘rain’. This depends on the presence of snow cover, which is determined by the model. As long as snow cover is present, the snow module is active, while the rain module is active when no snow cover is present.

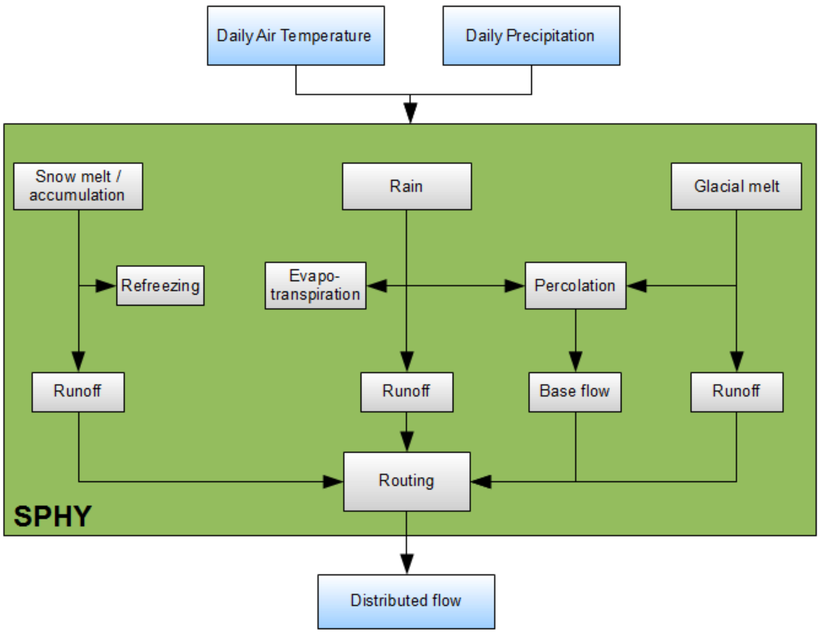

Figure 0.7: Model structure of SPHY model

II.2 Cryospheric processes

Since the model is set up for a 1 x 1 km resolution, the ice cover is described as a fraction varying from 0 (no glacial cover) to 1 (100% glacial cover). In this way, 1 x 1 km grid cells which are partly covered with ice can be simulated. A differentiation is made between clean ice glaciers and debris covered glaciers. Glaciers at lower altitude tend to have more debris cover because of the cumulative accumulation of debris from higher grounds and glacier parts with a small slope have more debris cover compared to steep-sloped parts of the glacier. The differentiation between clean ice glaciers and debris covered glaciers is then re-calculated to fractions of the 1 x 1 km grid cells used in the model. Summing the fractions of clean ice glacier and debris covered glacier will always result in a total fraction of one.

Initial conditions for snow cover are obtained directly from the model. A model run is done simulating several years to develop a balanced snow cover. The snow cover at the end of this model run is used as initial snow cover for further model runs. In the model calculations, the amounts of ice and snow are described as millimeters water equivalent. The modelling of processes involving glaciers is described in a schematic way in Figure 0.8. Melt from clean ice glaciers is defined as the air temperature (if above 0 °C) multiplied by the degree day factor for clean ice, multiplied by the clean ice fraction of the glacier cover and the cell fraction with glacier cover.

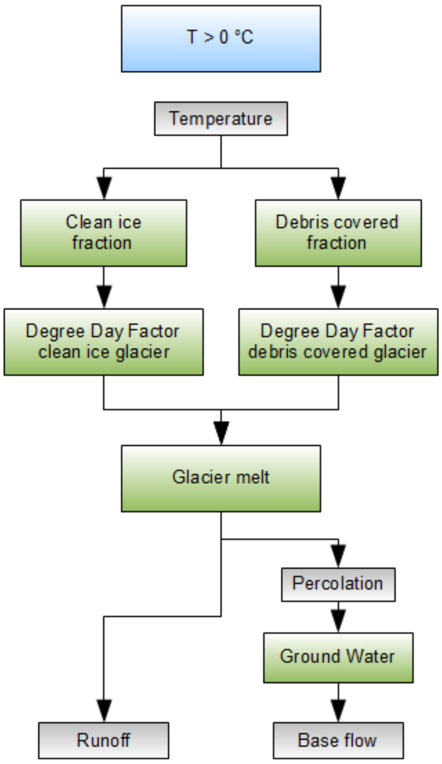

Figure 0.8: Schematic representation glacier related processes in the SPHY model

For the melt from debris covered glaciers the calculation is similar, although a different degree day factor for debris covered glaciers is specified. Melt rates for debris covered glaciers are lower, since the energy fluxes are partly blocked by the (thick) debris cover.

The use of temperature index or degree day models is widespread in cryospheric models to estimate ice and snow melt. In these models an empirical relationship between melt and air temperature based on a frequently observed correlation between the two quantities is assumed

(Hock, 2005). Degree-day models are easier to set up compared to energy-balance models, and only require air temperature, which is mostly available and relatively easy to interpolate.

The total glacier melt is then calculated by summing the two components from clean ice glacier melt and debris covered glacier melt. A part of glacial melt comes to runoff, while another part percolates to the ground water. This process is controlled by adjusting the glacial runoff factor.

For each cell the model determines if precipitation falls as snow or rain by comparing the actual air temperature to a critical temperature. When air temperature is below or equal to the critical temperature, precipitation will fall as snow. When air temperature is above the critical temperature, precipitation will fall as rain.

In the model a differentiation is made between the potential snow melt and the actual snow melt (Figure 0.9). The potential snow melt is defined as the air temperature (if above 0 °C) multiplied by a degree day factor for snow multiplied by the cell fraction covered with snow. The actual snow melt however, is limited by the thickness of the snow pack. No more snow can be melted than the amount of snow which is available at the considered time step. The snow storage is then updated, to be used for the next time step. The snow storage is updated by subtracting the melt and/or adding the freshly fallen snow or rain to the water storage in the snow pack. The updated snow storage is the 'old' snow storage with the fresh snow added and the actual snow melt subtracted.

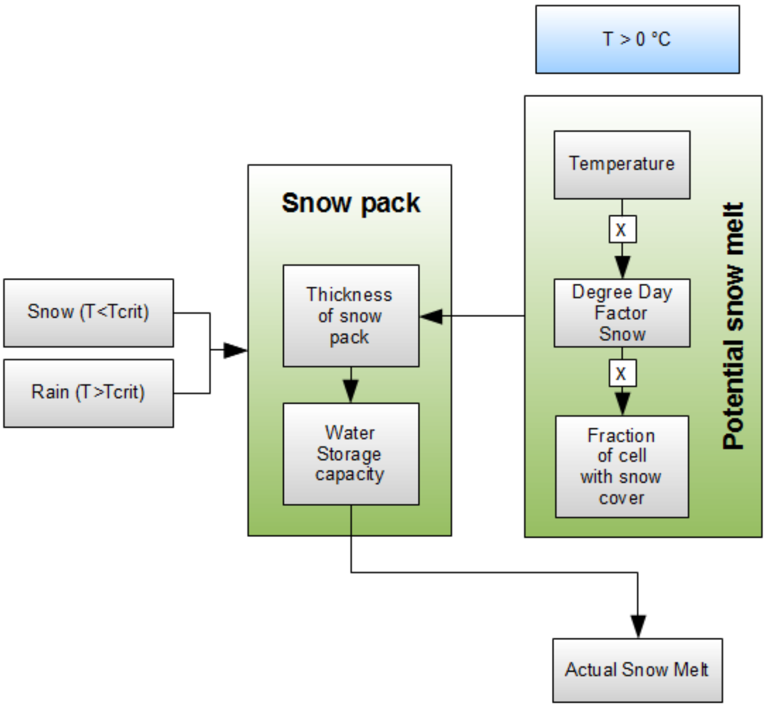

Figure 0.9 Schematic representation of snow related processes in the SPHY model

The water resulting from snow melt will partially refreeze as it infiltrates the underlying snow pack. The maximum amount of water that can refreeze is defined by the water storage capacity of the snow pack which depends on the thickness of the snow pack present and the storage capacity of snow (e.g. the total millimeters of melt water that can refreeze per millimeter of snow). The actual amount of water that is stored in the snow pack is defined as the water stored in the snow pack during the previous time step summed by the actual snow melt. Snow melt will become actual snow melt when the amount of snow melt exceeds the water storage capacity of the snow pack. When all snow in a grid cell has melted, the snow fraction is set to zero. If snow falls on a cell which had no snow during the previous time step the snow fraction is updated to 1.

II.3 Rainfall runoff

The modelling steps for rainfall in the SPHY model are represented in Figure 0.10. Precipitation in the model will fall as rain when the air temperature is above a critical temperature.

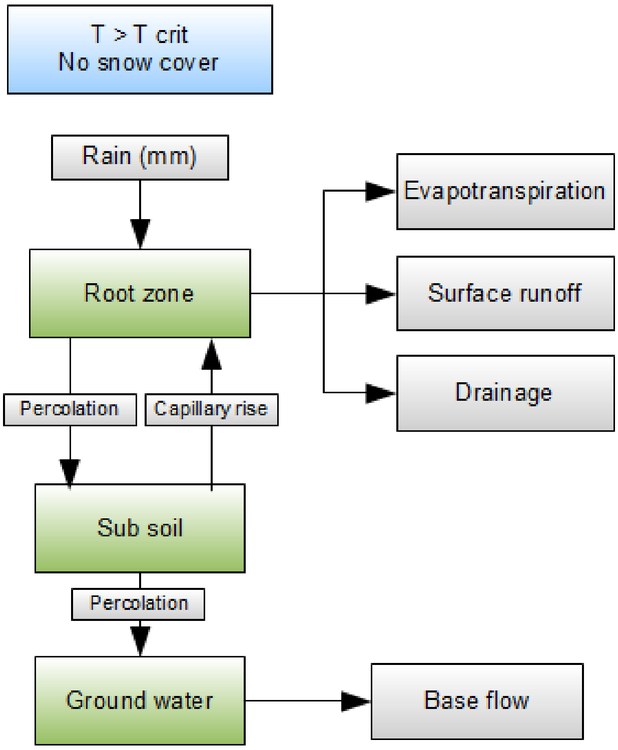

Figure 0.10: Schematic representation of rainfall-runoff modelling in the SPHY model

A soil module based on the saturation excess overland flow (also known as Hewlettian runoff) concept is incorporated in the SPHY model. The soil layer in the model is divided in a root zone and a sub soil. The thickness of the soil is slope dependent in the model. The soil properties are based on pedotransfer functions, to quantify soil properties for different soil types. The soil properties used in the SPHY model are listed in Table 0.1. Using these properties, the model evaluates how much water in the rootzone is available for evapotranspiration, surface runoff, lateral drainage and percolation/capillary rise to/from the subsoil.

Table 0.1: Soil properties used in SPHY model

Rootzone	Subsoil
Rooting depth (mm)	Subsoil depth (mm)
Saturated water content (mm/mm)	Saturated water content (mm/mm)
Field capacity (mm/mm)	Field capacity (mm/mm)
Wilting point (mm/mm)	Saturated conductivity (mm/day)
Permanent wilting point (mm/mm)	
Saturated conductivity (mm/day)	

The potential evapotranspiration (ET_{pot}) in the model is calculated using the reference evapotranspiration (ET_{ref}) and a crop coefficient (K_c):

$$ET_{pot} = ET_{ref} \cdot K_c$$

The reference evapotranspiration is calculated according to the Modified Hargreaves method (Droogers and Allen, 2002). This method requires average, maximum and minimum air temperature (T_{avg}, T_{max}, T_{min}), the summed precipitation (P) and incoming extraterrestrial radiation (Ra):

$$ET_{ref} = 0.0013 \cdot 0.408Ra \cdot (T_{avg} + 17.0) \cdot ((T_{max}\text{-}T_{min}) - 0.0123P)^{0.76}$$

Based on land use type, each grid cell is assigned a K_c factor to calculate the potential evapotranspiration. The actual evapotranspiration (ET_{act}) is the potential evapotranspiration limited by the water available in the rootzone (e.g. the saturation of the root zone).

Excess water is also leaving the rootzone as surface runoff, lateral drainage or percolation to the sub soil. The occurrence of capillary rise from the sub soil to the root zone or percolation from the root zone to the sub soil depends on differences in water saturation of both soil layers. Water percolates from the sub soil to the ground water.

At the moment a ‘rain fraction’ is covered with snow, it switches to ‘snow fraction’. As long as snow cover is present, the snow module (described in section II.2) is active. However, the soil component remains active, although no more precipitation is entering the soil and no more water is leaving the soil as surface runoff or evapotranspiration. Percolation to the subsoil and eventually to the ground water remains active.

II.4 Groundwater

A ground water reservoir generating base flow is incorporated in the model. During periods with low runoff the streams are fed by processes such as sustained ground water flow and/or slow throughflow through the deeper soil from earlier precipitation events. This is referred to as base flow. The ground water reservoir is active for each entire grid cell. The ground water is fed by percolation from the sub soil and percolation from the glacier fraction of a cell. These two components provide recharge to the ground water reservoir. The ground water recharge is translated into baseflow released from the reservoir with a certain time lag.

II.5 Routing

In the model, the generated runoff is routed through the basin according to a flow direction map based on the DEM. For each cell the local drain direction is defined. The runoff generated per grid cell accumulates with runoff generated in downstream grid cells. Using a linear regression with a regression constant, the time water needs to flow through the reservoir towards the outflow point is simulated.

Appendix III - Water resources modelling

III.1 The WEAP-ARAL model

WEAP ("Water Evaluation And Planning" system) is a well-known software tool that takes an integrated approach to water resources planning. Allocation of limited water resources between agricultural, municipal and environmental uses requires the consideration of the interdependent nature of supply, demand, water quality and ecological considerations. WEAP aims to incorporate these issues into a practical yet robust tool for integrated water resources planning. WEAP is developed by the Stockholm Environment Institute's U.S. Center. WEAP was originally developed for simulating water balances and evaluating water management strategies in the Aral Sea region (Raskin et al., 1992).

For a recent study carried out for the Asian Development Bank (Lutz et al., 2012) a water allocation model was developed in WEAP for the Amu Darya and the Syr Darya basin incorporating the agricultural and domestic demand sites, catchments, inflow points from upstream, reservoirs and the connections between them. The effects of future changes in temperature and precipitation for the future water availability and demand were simulated until 2050 and the effects of possible adaptation measures were explored. This version of the model is referred to in this report as ARAL-WEAP2011.

In WEAP, a database maintains water demand and supply information to drive a mass balance model on link-node architecture. Simulations calculate water demand, supply, runoff, infiltration, crop requirements, flows, and storage, and pollution generation, treatment, discharge and instream water quality under varying hydrologic and policy scenarios. Policy scenarios can be analysed to evaluate a full range of water development and management options, taking into account the multiple and competing uses of the different actors and sectors in the basin.

WEAP has a user-friendly GIS-based interface with flexible model output as maps, charts and tables. WEAP is available in also Russian and Farsi languages and it is already at use in the Aral Sea Basin. WEAP license is free of charge to non-profit, governmental or academic organization based in a country receiving development bank support (as all the Central Asian countries).[1]

[1] www.weap21.org

The ARAL-WEAP2011 model runs at a monthly time step for three time intervals: for the reference situation (2001-2010) and for two future time interval (2021-2030 and 2041-2050). The model was calibrated for the reference situation (2001-2010) (Lutz et al., 2012).

The WEAP model used for this CRVA is built upon the ARAL-WEAP2011 model, incorporating a list of modifications and advancements, and more recent climate change scenarios. The following changes and additions were made for this updated version:

- Additional irrigation reservoirs
- Incorporation of thermal power plants to analyze water availability for cooling water
- Transformation of a steady-state approach to a dynamic modelling approach
- Inclusion of reservoir evaporation
- Model performance assessment based on annual and monthly data on hydropower generation and reservoir releases
- Model runs until 2060

This methodological section details these updates and advancements carried out for ARAL-WEAP. For further details on ARAL-WEAP2011, please refer to the documentation in (Lutz et al., 2012).

III.2 Schematic setup

Figure 0.11 shows the schematic representation of the model setup for the Amu Darya basin. The figure includes all the demand sites (agricultural and urban), the reservoirs and the catchments and the links among them. For the upstream reservoirs, the inflow is simulated by the SPHY hydrological model, as indicated by the orange color of the triangle. The upstream catchments that do not drain into a reservoir in the upstream area are indicated with an orange hexagon symbol. In the downstream areas, the hydrology is simulated by a simplified rainfall-runoff model in WEAP.

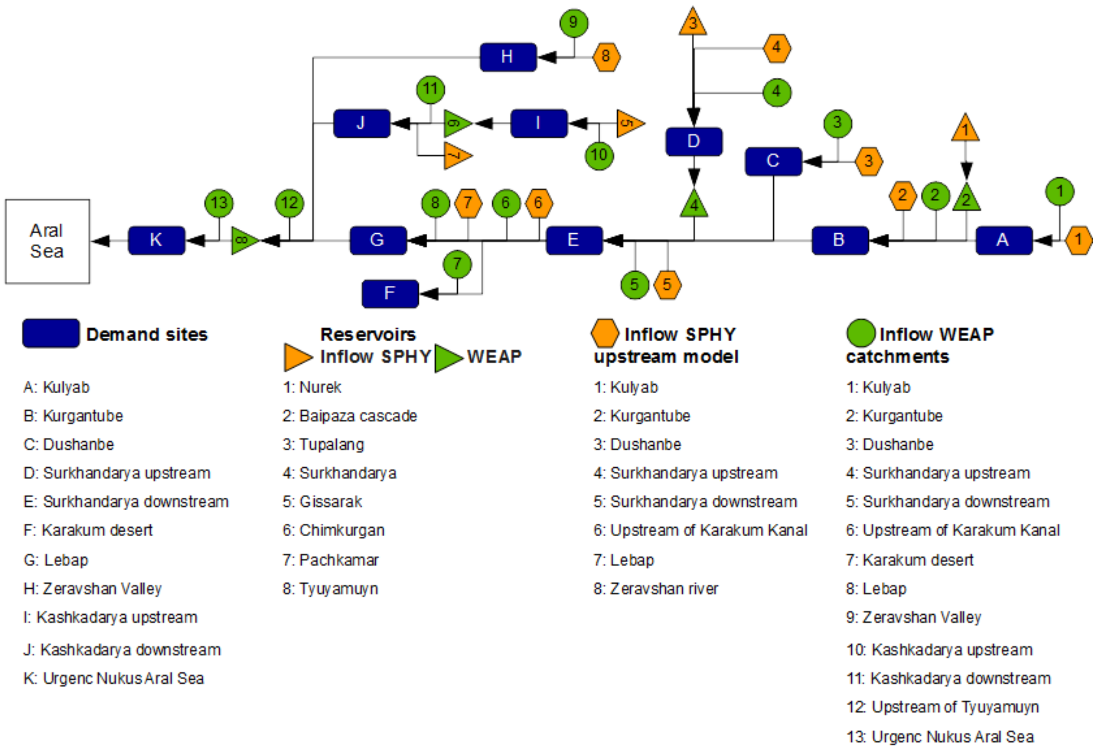

Figure 0.11: Schematic representation Amu Darya river basin in ARAL-WEAP model.

As explained previously (section 1.4 on Modelling approach), the division of the upstream and the downstream part approximates the division in areas without significant human interference and areas with significant human interference. Partly, this division is well defined where major reservoirs are located in the mountain ranges. Downstream of these locations, the stream flow is human-regulated. In some regions the division in upstream basin and downstream basin is less well defined. For those regions the division is made based on optical analysis of satellite imagery. This boundary approximates the division between the mountain environment and the lower land, extensively used by the human population. Figure 0.12 shows the upstream catchments for which the hydrological model SPHY was used. For the infrastructure scenarios the subcatchments draining to Nurek and Toktogul were further subdivided to obtain the flows at the upstream planned facilities.

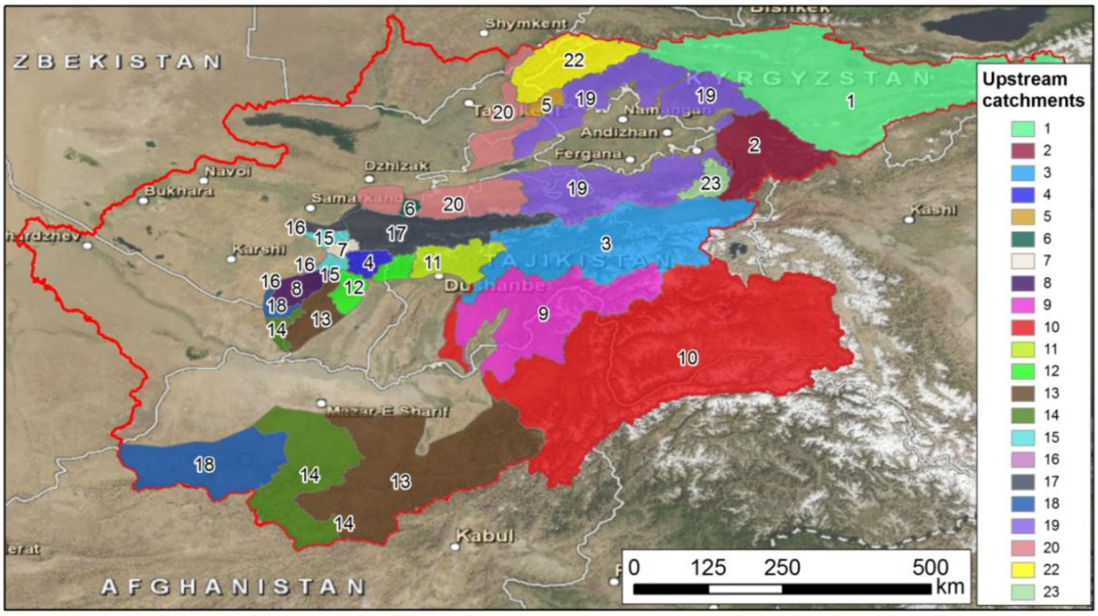

Figure 0.12: Subcatchments used in upstream model for input in downstream WEAP-model.

Figure 0.14 shows the geographical positioning of the rivers, demand sites, inflows, catchments, transmission links and return flows as represented schematically in Figure 0.11.

The runoff that is generated in the downstream areas is simulated by WEAP, by assigning catchments that coincide with the demand sites. For these catchments, monthly mean, maximum and minimum temperature and total monthly precipitation are extracted from the 2001-2010 climate data set prepared by the Finish Meteorological Institute (FMI). Based on this dataset, the monthly incoming water (from precipitation) and the water lost by evapotranspiration is calculated using the Modified Hargreaves method (Droogers and Allen, 2002). The rainfall-runoff scheme used is the FAO rainfall-runoff model, which is incorporated in WEAP. A detailed discussion on data set used, model calibration and performance as well as impact and adaptation results can be found in (Lutz et al., 2012).

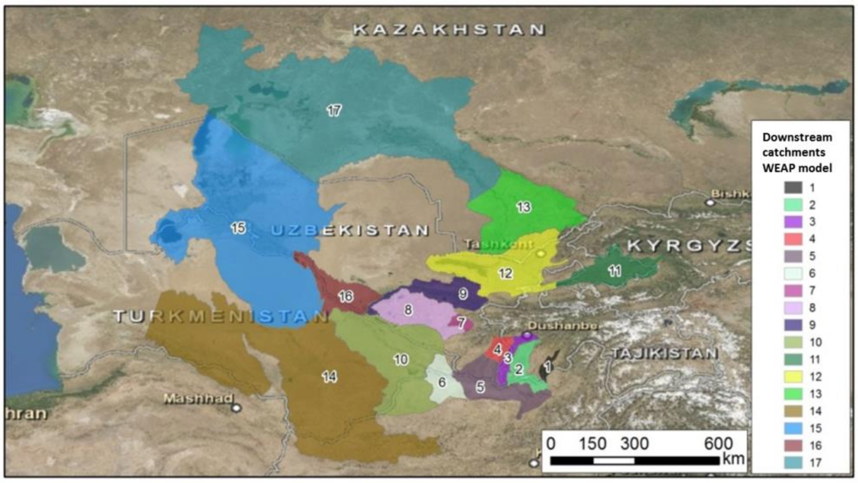

ID	Catchment name
1	Kulyab
2	KurganTube
3	Dushanbe
4	Surkhandarya upstream
5	Surkhandarya downstream
6	Karakum kanal
7	Kashkadarya upstream
8	Kashkadarya downstream
9	Zeravshan Valley
10	Lebap
11	Fergana Valley
12	Syrdaryo, Tashkent, Jizakh
13	South Kazakhstan
14	Karakum desert
15	Urgenc, Nukus, AralSea
16	Tyuyamuyn
17	Kzylorda

Figure 0.13: Downstream catchments used in WEAP model.

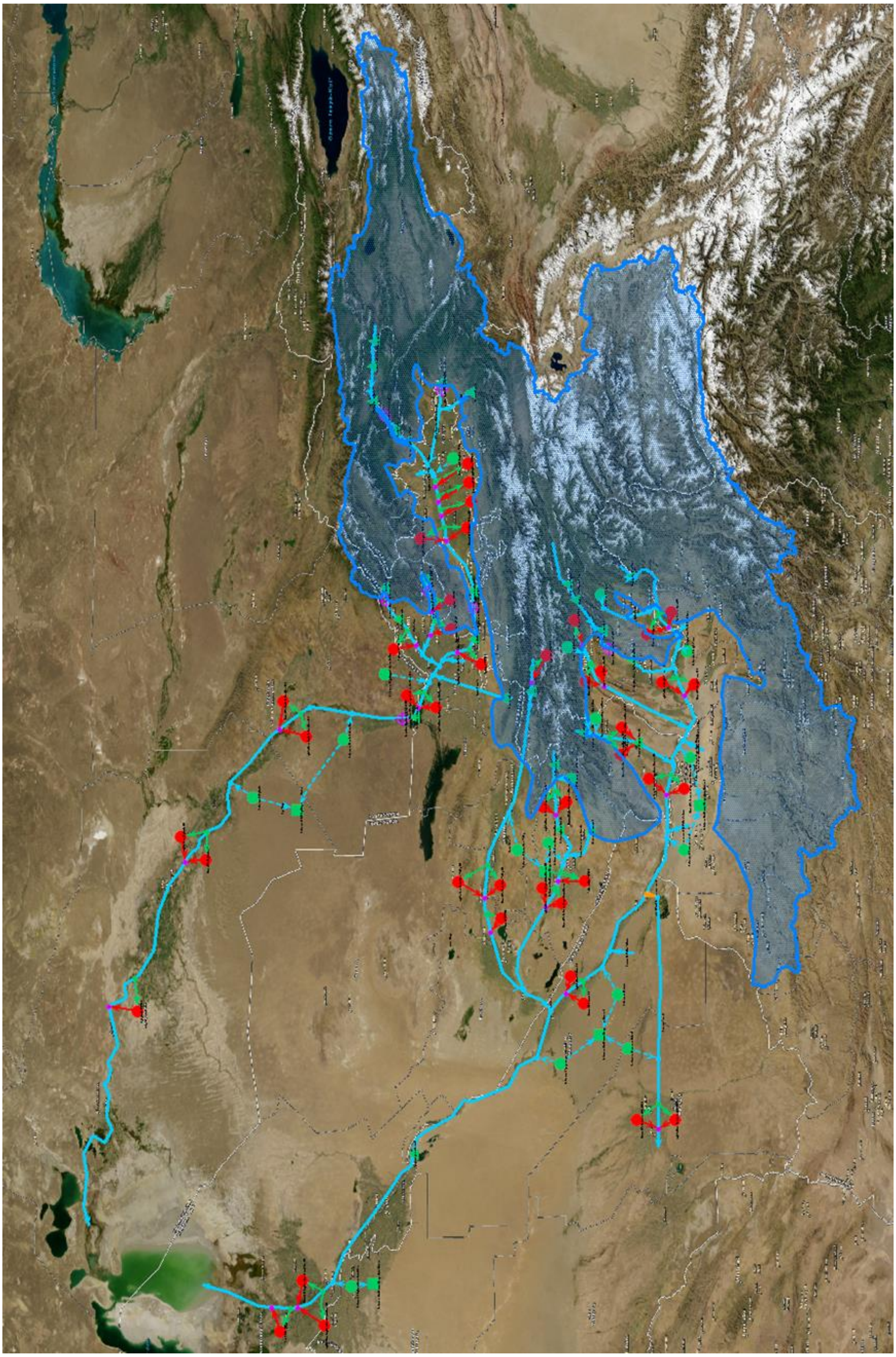

Figure 0.14: Geographical visualization of ARAL-WEAP2014 model. The spatial extent of the SPHY upstream model area is indicated with blue color. Demand sites are indicated with red dots, catchments are indicated with green dots.

III.3 Water demand: Domestic

For the reference situation, population figures for the year 2000 are assumed to be representative. The population figures per demand site are presented in Figure 0.15.

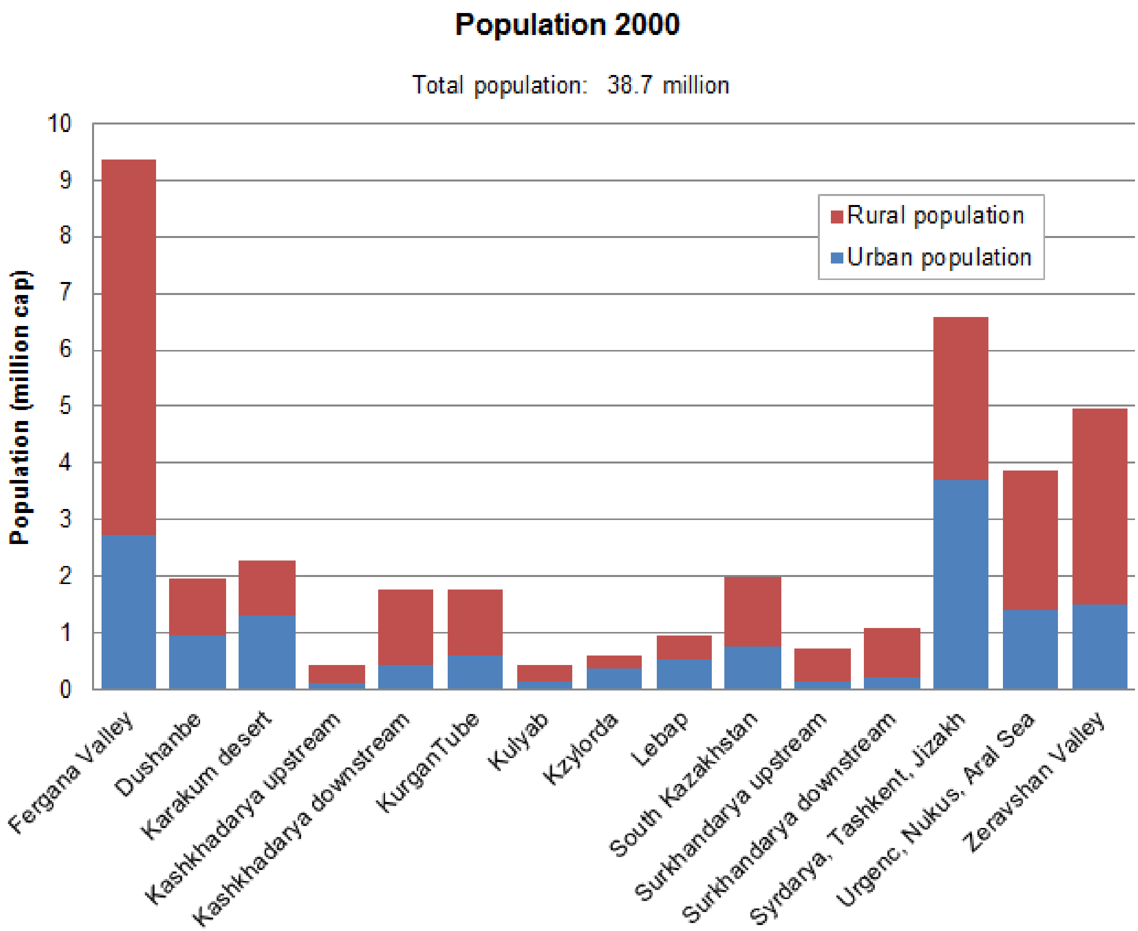

Figure 0.15: Population per demand site in 2000. Source: Central Asian Water Info database

Table 0.2: Domestic water allocation (Aldaya et al., 2010)

Country	Annual domestic water use (m^3/cap)	Monthly domestic water use (m^3/cap)
Kazakhstan	39	3.25
Kyrgyzstan	63	5.25
Tajikistan	69	5.75
Turkmenistan	74	6.17
Uzbekistan	109	9.08
Average	*70.8*	*5.9*

These population numbers are used in ARAL-WEAP to calculate monthly domestic water demand. The annual water use rate per capita in this study is assumed to be 70.8 m^3 per capita. This is the average rate for the five countries in the basin (Table 0.2). The effective domestic consumption is estimated to be 10%, which means 90% of the water allocated for domestic purposes is returned to the system and is available downstream.

III.4 Water demand: Agriculture

Data on agricultural land use at the province level was taken from the online Central Asian Waterinfo portal.[1] for the five countries in the Amu Darya and Syr Darya river basins (Uzbekistan, Kazakhstan, Tadzhikistan, Kyrgyzstan and Turkmenistan). No data is available in the database for Afghanistan. These data, combined with FAOSTAT data on production and irrigated areas was used to define agricultural demand sites in WEAP. Table 0.3 shows the translation of provinces to demand sites as used in the model.

Table 0.3: Division of provinces over WEAP demand sites.

<table>
<tr><th>Demand site in WEAP</th><th colspan="2">Provinces</th></tr>
<tr><td>Dushanbe</td><td colspan="2">Rayons of republican subordination (TJK)</td></tr>
<tr><td rowspan="3">Fergana Valley</td><td>Andijan (UZB)</td><td>Jalalabad (KGZ)</td></tr>
<tr><td>Namangan (UZB)</td><td>Osh (KGZ)</td></tr>
<tr><td colspan="2">Fergana (UZB)</td></tr>
<tr><td rowspan="2">Karakum desert</td><td colspan="2">Mary (TKM)</td></tr>
<tr><td colspan="2">Akhal (TKM)</td></tr>
<tr><td>Kashkhadarya upstream</td><td colspan="2">20% of Kashkhadarya (UZB)</td></tr>
<tr><td>Kashkhadarya downstream</td><td colspan="2">80% of Kashkhadarya (UZB)</td></tr>
<tr><td>Kurgantube</td><td colspan="2">80% of Khatlon (TJK)</td></tr>
<tr><td>Kulyab</td><td colspan="2">20% of Khatlon (TJK)</td></tr>
<tr><td>Kzylorda</td><td colspan="2">Kzylorda (KAZ)</td></tr>
<tr><td>Lebap</td><td colspan="2">Lebap (TKM)</td></tr>
<tr><td>South Kazakhstan</td><td colspan="2">South Kazakhstan (KAZ)</td></tr>
<tr><td>Surkhandarya upstream</td><td colspan="2">40% of Surkhandarya</td></tr>
<tr><td>Surkhandaraya downstream</td><td colspan="2">60% of Surkhandarya</td></tr>
<tr><td rowspan="2">Syrdarya, Tashkent, Jizakh</td><td>Jizakh (UZB)</td><td>Tashkent (UZB)</td></tr>
<tr><td>Syrdarya (UZB)</td><td>20% of Sughd (TJK)</td></tr>
<tr><td rowspan="3">Urgenc, Nukus, Aral Sea</td><td colspan="2">Khorezm (UZB)</td></tr>
<tr><td colspan="2">Karakalpakistan (UZB)</td></tr>
<tr><td colspan="2">Dashoguz (TKM)</td></tr>
<tr><td rowspan="3">Zeravshan Valley</td><td colspan="2">Bukhara (UZB)</td></tr>
<tr><td colspan="2">Navoiy (UZB)</td></tr>
<tr><td colspan="2">Samarkand (UZB)</td></tr>
</table>

In several agricultural demand nodes, reservoirs regulate and store water for irrigation. In some areas there are multiple smaller reservoirs, while also some bigger reservoirs exist in the region.

[1] www.cawater-info.net

The smaller reservoirs were aggregated to one single reservoir node in WEAP. Table 0.4 shows the characteristics of the irrigation reservoir nodes included in ARAL-WEAP2014.

Table 0.4: Irrigation reservoirs and their capacities included in WEAP-ARAL

Country	Reservoir	Full storage capacity (MCM)	Dead storage (MCM)	Basin
TUR	Turkmenistan reservoirs	4200	800	Amu Darya
UZB	Chimkurgan	500	50	Amu Darya
UZB	Pachkamar	260	10	Amu Darya
UZB	Surkhandarya	800	100	Amu Darya
UZB	Zaamin	51	21	Syr Darya
UZB	Fergana Valley reservoirs	1155	10	Syr Darya

The WEAP-ARAL2014 model assumes that domestic demand has always a higher priority than agricultural demand. Therefore, if not enough water is available in a certain river segment for domestic and agricultural demand, all unmet demand will go to the agricultural node in that particular river segment.

III.5 Modelling performance

The total annual power simulated over the reference period 2001-2010 was compared with the data available on power production of several of the major hydropower facilities (source: (ADB, 2012a)). Figure 0.16 compares the average annual power production that was simulated for these facilities compared with the actually produced ("observed") power for the reference period. As can be seen, the WEAP model simulates very similar production levels as actually produced.

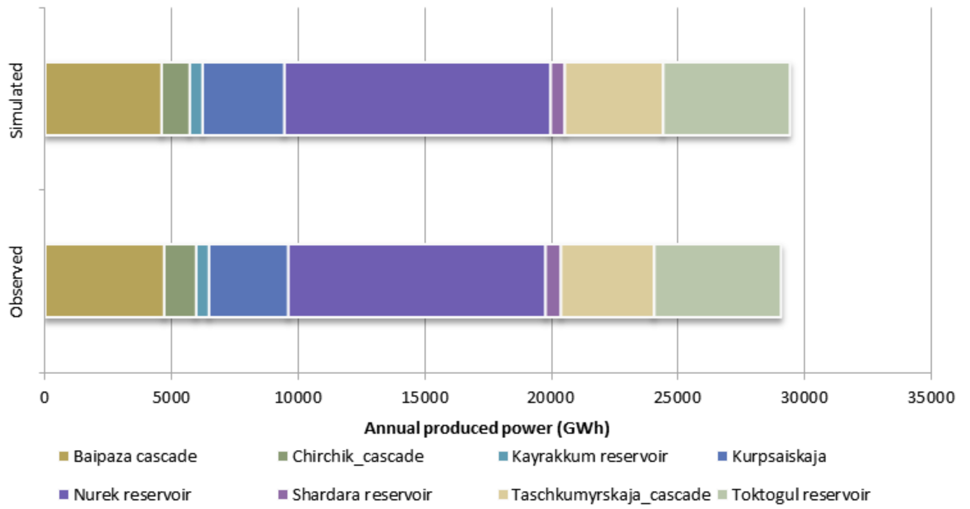

Figure 0.16. Produced versus simulated annual power production for the main reservoirs

Figure 0.17 is based on the same data but represented in the form of a scatterplot, indicating also the annual variability in power production (error bars based on the standard deviation of the annual series). Generally, the variability in simulated production levels are very much in the same range as actually produced power. This gives confidence in the model that it is able to mimic reasonably well the annual variability in production, mainly a function of water availability.

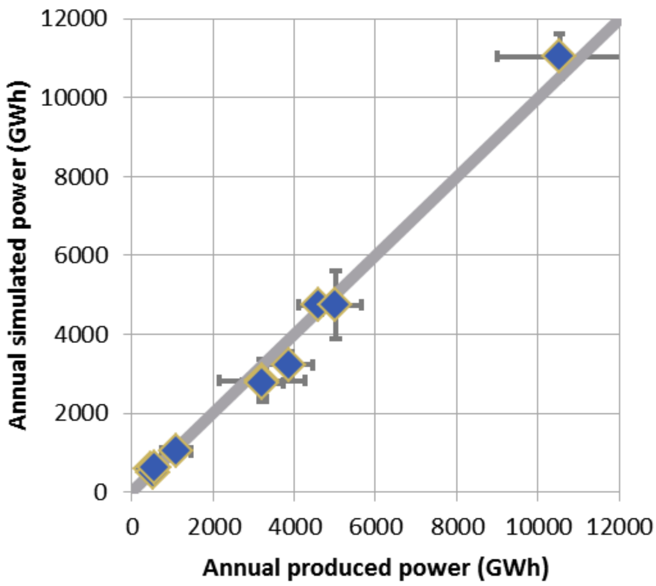

Figure 0.17. Scatterplot of produced versus simulated annual power production (GWh).

No data on monthly power production of the hydropower facilities is available. However, monthly data is available of the releases of most of the reservoirs (CAWATER database), being a good indicator of production levels. Figure 0.18 shows the average monthly release for several reservoirs. As can be seen in this figure, for these reservoirs the monthly pattern is quite similar between simulated and observed releases. The R^2 are ranging between 0.62 and 0.99 for these main reservoirs. This gives an indication that WEAP adequately mimics the outflow regime and operational rules in the current situation.

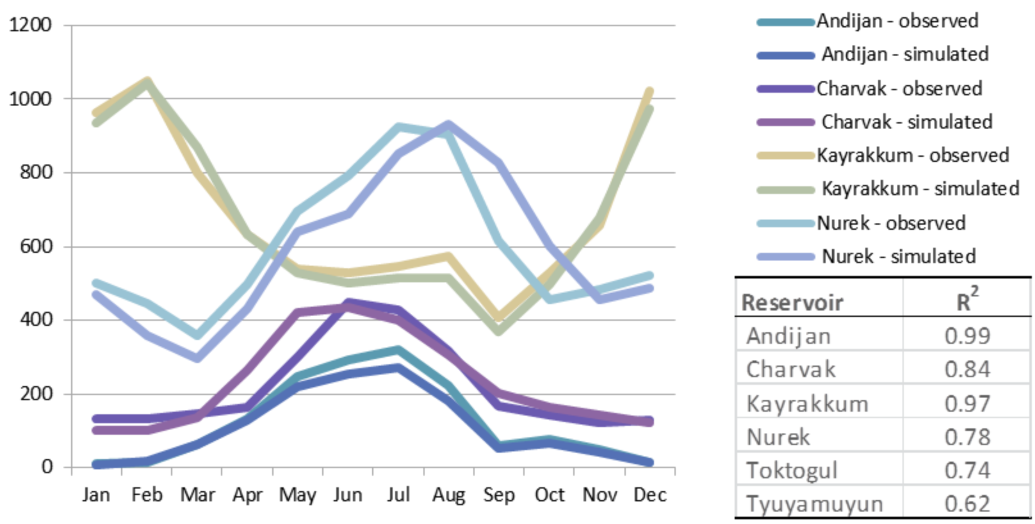

Reservoir	R^2
Andijan	0.99
Charvak	0.84
Kayrakkum	0.97
Nurek	0.78
Toktogul	0.74
Tyuyamuyun	0.62

Figure 0.18. Comparison of observed against simulated monthly reservoir releases

Appendix IV – Annual hydrographs under climate change

IV.1 Marker scenario: Arid

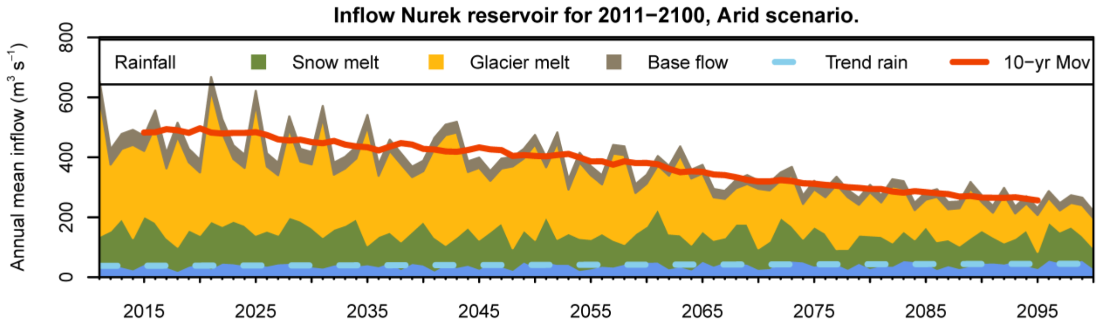

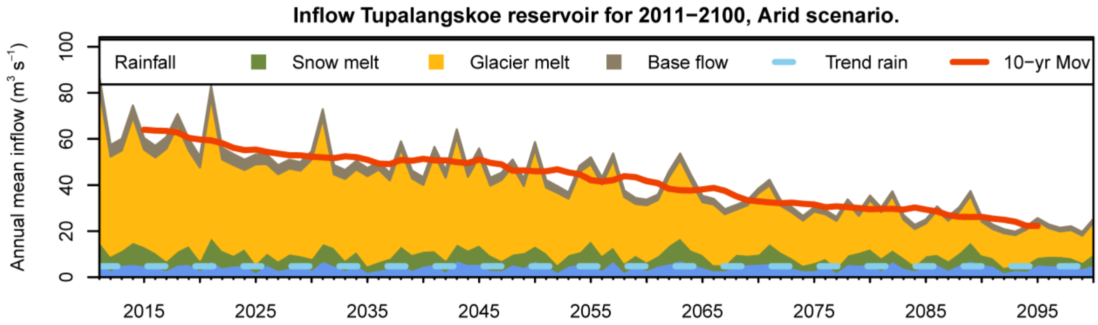

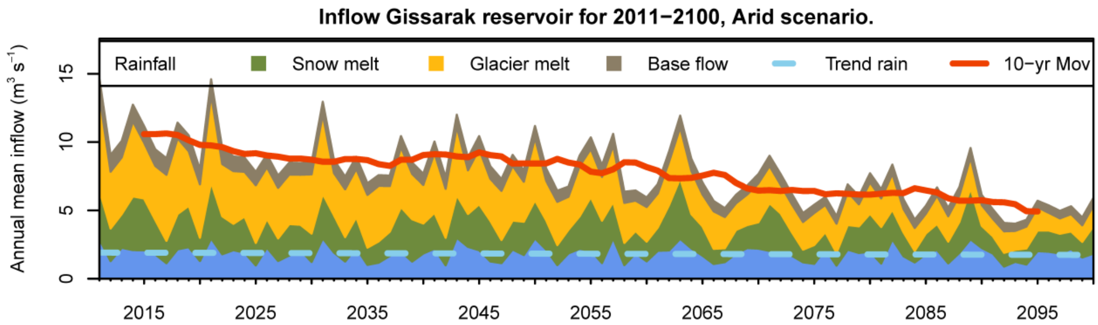

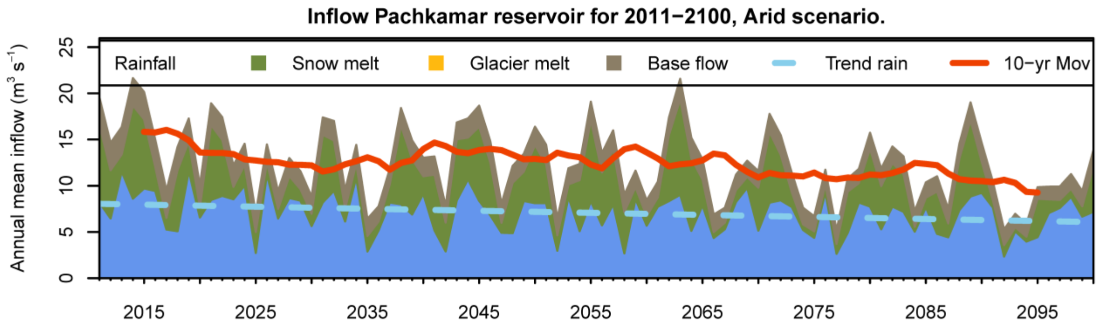

Inflow Kulyab catchment for 2011–2100, Arid scenario.

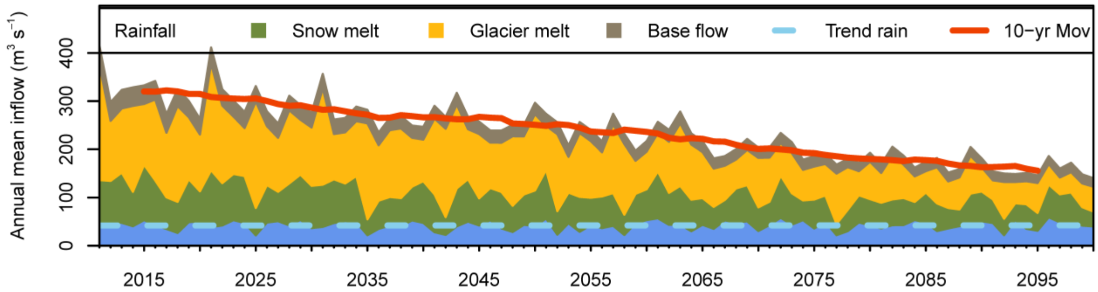

Inflow Kurgantube catchment for 2011–2100, Arid scenario.

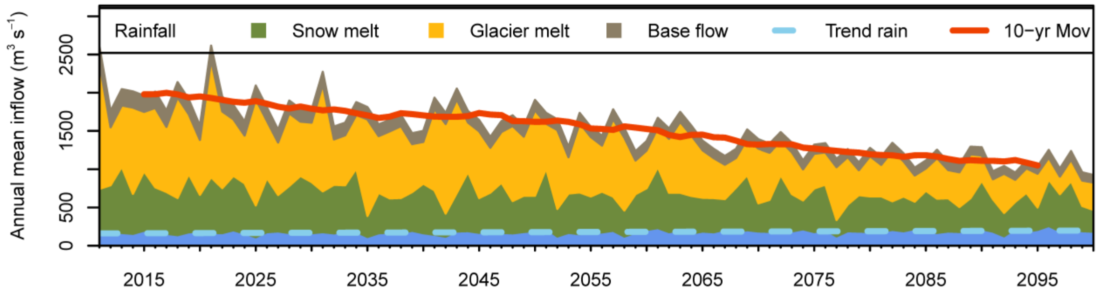

Inflow Dushanbe catchment for 2011–2100, Arid scenario.

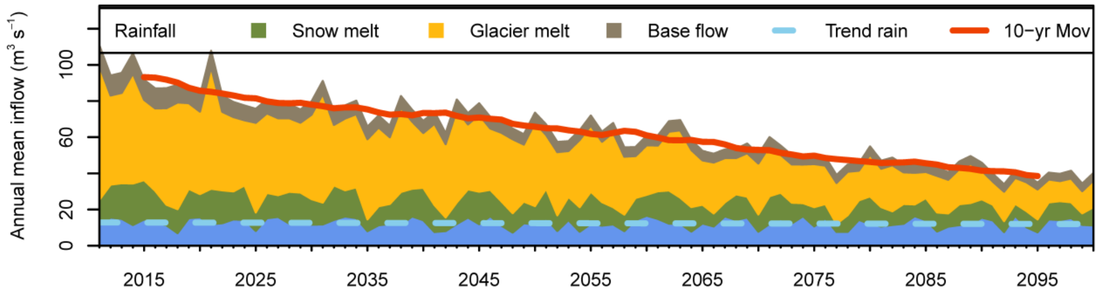

Inflow Surkhandarya upstream catchment for 2011–2100, Arid scenario.

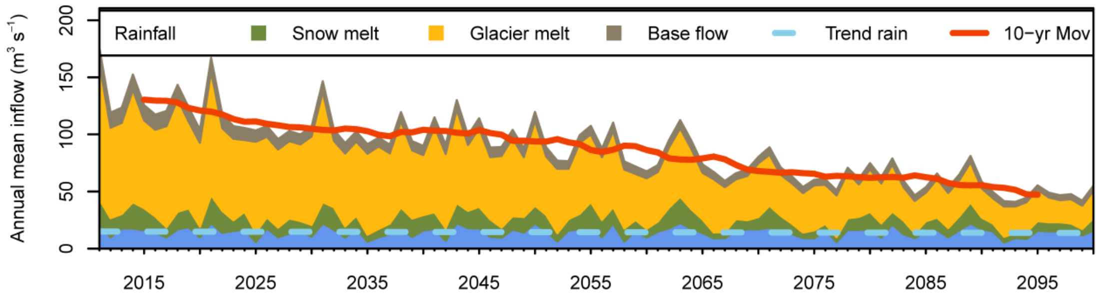

Inflow Surkhandarya downstream catchment for 2011–2100, Arid scenario.

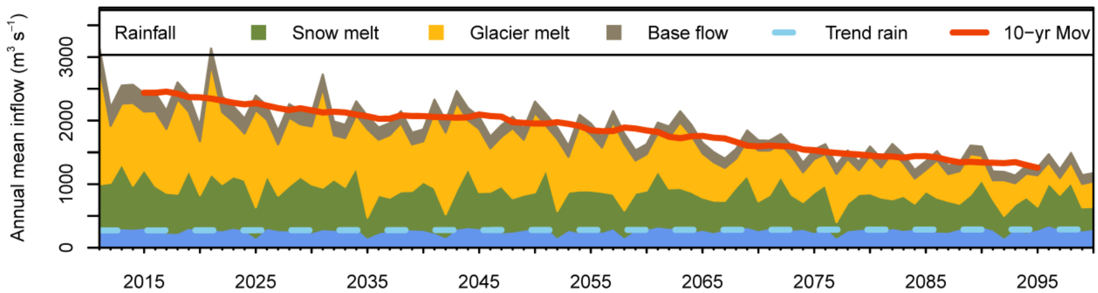

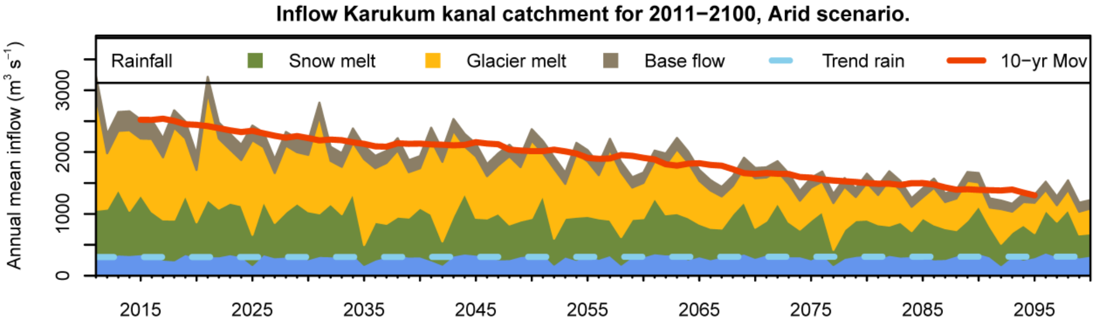
Inflow Karukum kanal catchment for 2011−2100, Arid scenario.
Rainfall
Snow melt
Glacier melt
Base flow
Trend rain
10−yr Mov
Annual mean inflow (m3 s−1)
0
1000
2000
3000
2015
2025
2035
2045
2055
2065
2075
2085
2095

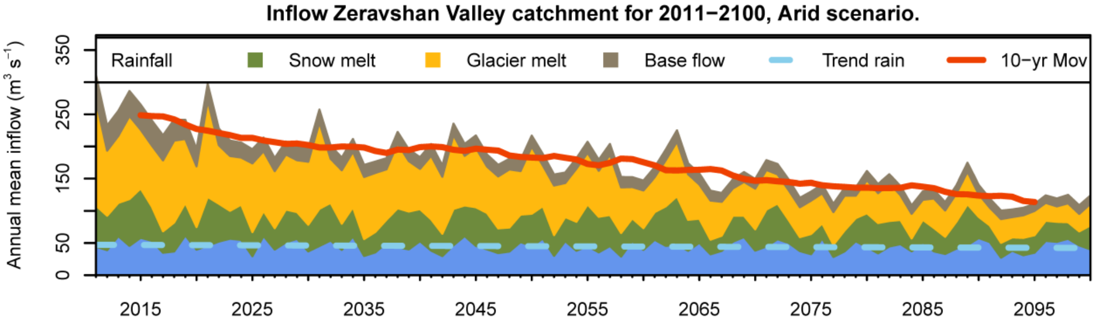
Inflow Zeravshan Valley catchment for 2011−2100, Arid scenario.
Rainfall
Snow melt
Glacier melt
Base flow
Trend rain
10−yr Mov
Annual mean inflow (m3 s−1)
0
50
150
250
350
2015
2025
2035
2045
2055
2065
2075
2085
2095

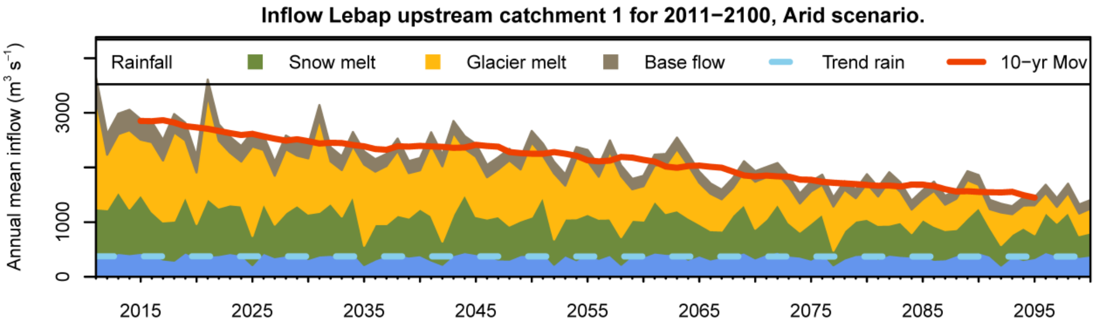
Inflow Lebap upstream catchment 1 for 2011−2100, Arid scenario.
Rainfall
Snow melt
Glacier melt
Base flow
Trend rain
10−yr Mov
Annual mean inflow (m3 s−1)
0
1000
3000
2015
2025
2035
2045
2055
2065
2075
2085
2095

IV.2 Marker scenario: Hot/dry

Inflow Nurek reservoir for 2011–2100, Hot/dry scenario.

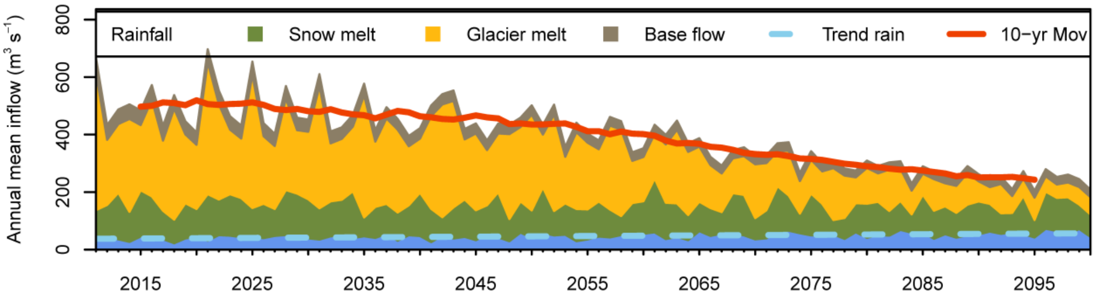

Inflow Tupalangskoe reservoir for 2011–2100, Hot/dry scenario.

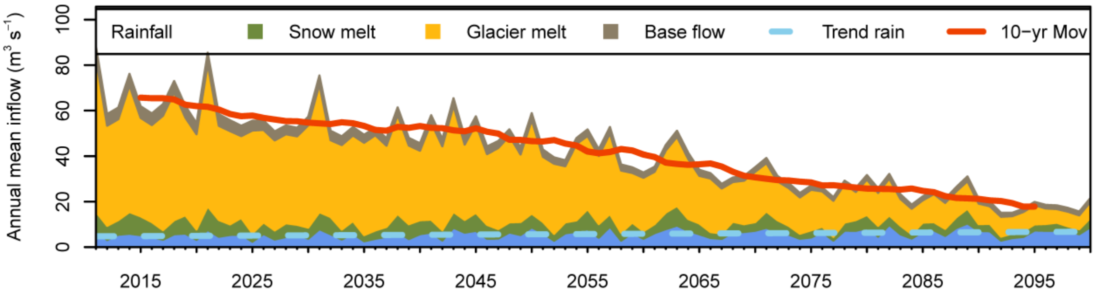

Inflow Gissarak reservoir for 2011–2100, Hot/dry scenario.

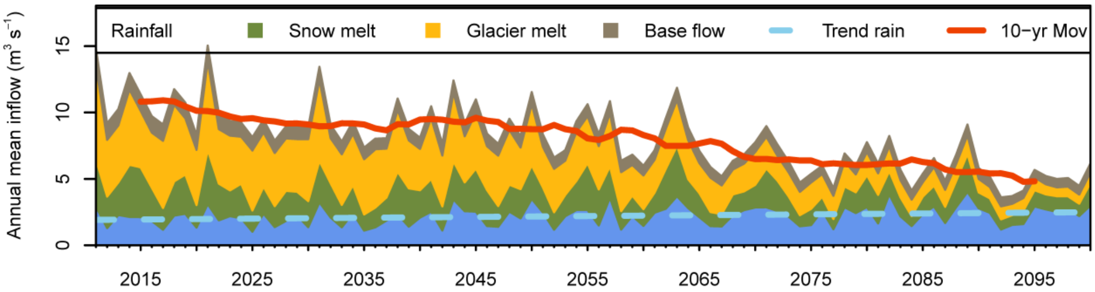

Inflow Pachkamar reservoir for 2011–2100, Hot/dry scenario.

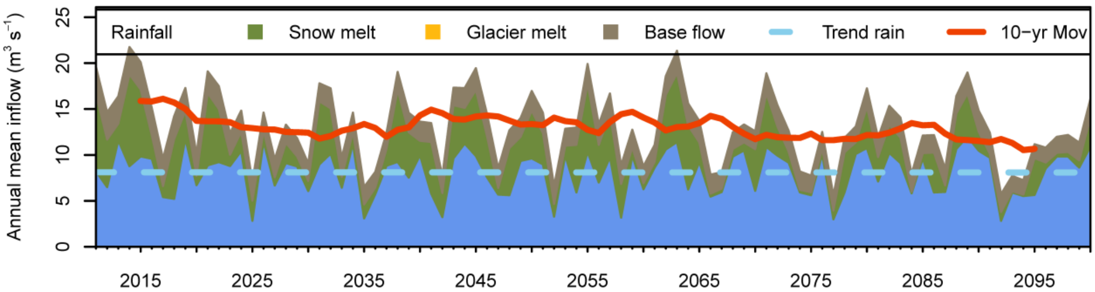

Inflow Kulyab catchment for 2011−2100, Hot/dry scenario.

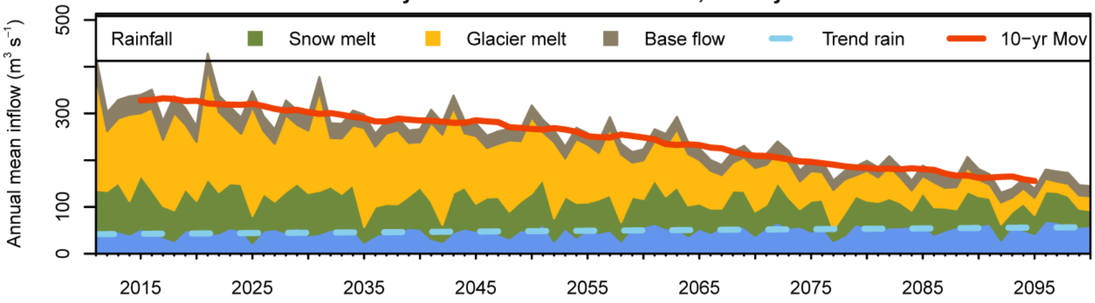

Inflow Kurgantube catchment for 2011−2100, Hot/dry scenario.

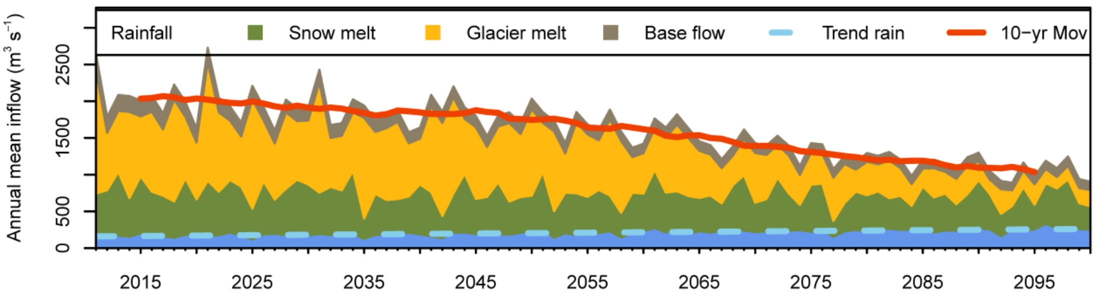

Inflow Dushanbe catchment for 2011−2100, Hot/dry scenario.

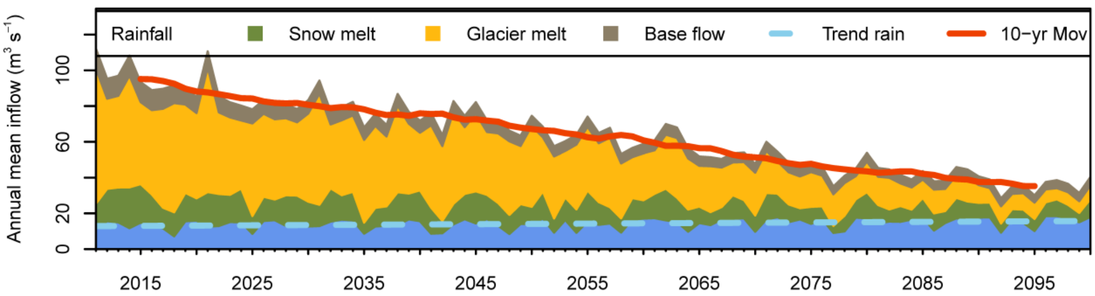

Inflow Surkhandarya upstream catchment for 2011−2100, Hot/dry scenario.

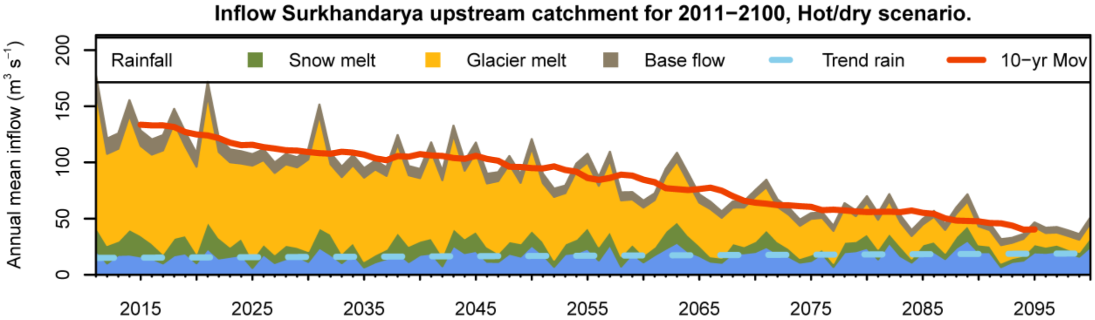

Inflow Surkhandarya downstream catchment for 2011−2100, Hot/dry scenario.

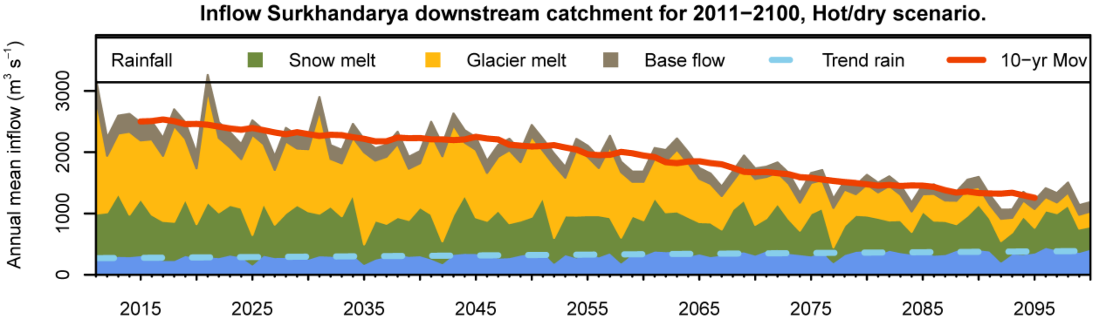

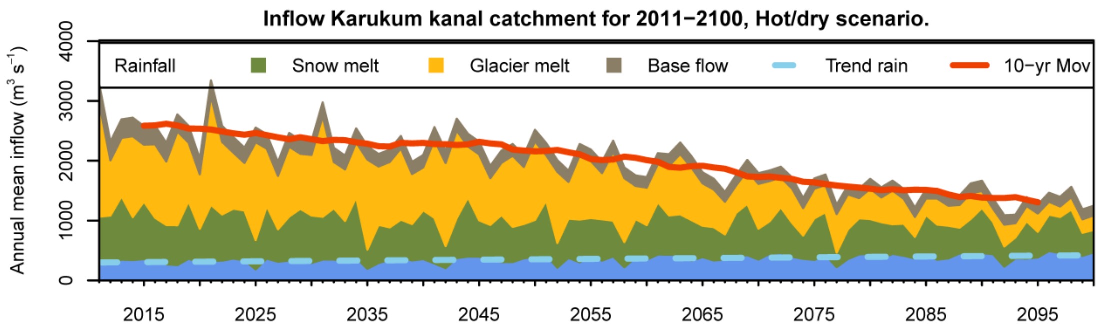
Inflow Karukum kanal catchment for 2011−2100, Hot/dry scenario.
Rainfall
Snow melt
Glacier melt
Base flow
Trend rain
10−yr Mov
Annual mean inflow (m3 s−1)
0
1000
2000
3000
4000
2015
2025
2035
2045
2055
2065
2075
2085
2095

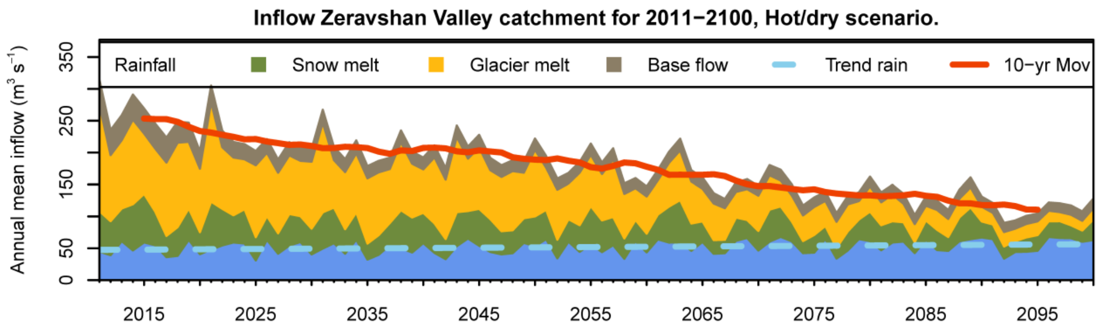
Inflow Zeravshan Valley catchment for 2011−2100, Hot/dry scenario.
Rainfall
Snow melt
Glacier melt
Base flow
Trend rain
10−yr Mov
Annual mean inflow (m3 s−1)
0
50
150
250
350
2015
2025
2035
2045
2055
2065
2075
2085
2095

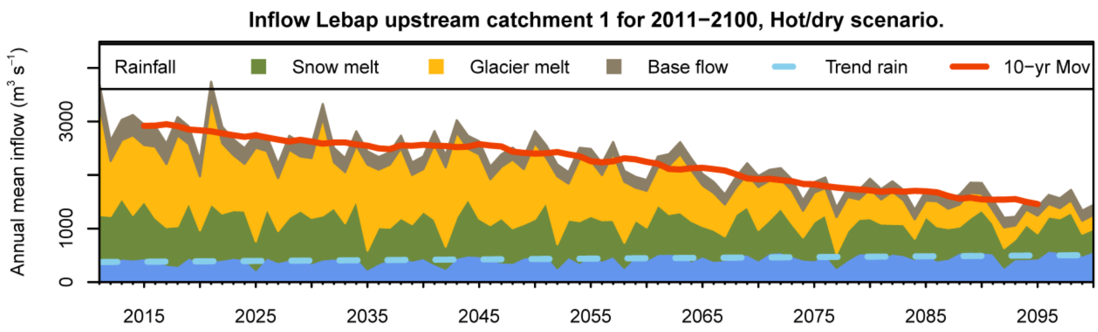
Inflow Lebap upstream catchment 1 for 2011−2100, Hot/dry scenario.
Rainfall
Snow melt
Glacier melt
Base flow
Trend rain
10−yr Mov
Annual mean inflow (m3 s−1)
0
1000
3000
2015
2025
2035
2045
2055
2065
2075
2085
2095

IV.3 Marker scenario: Central

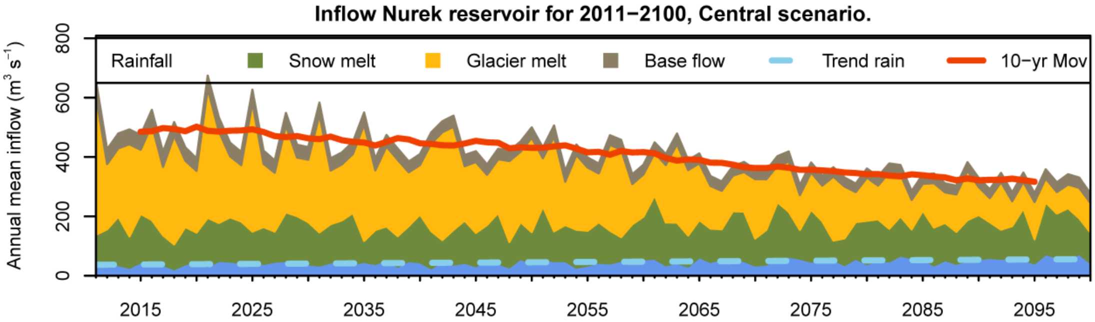

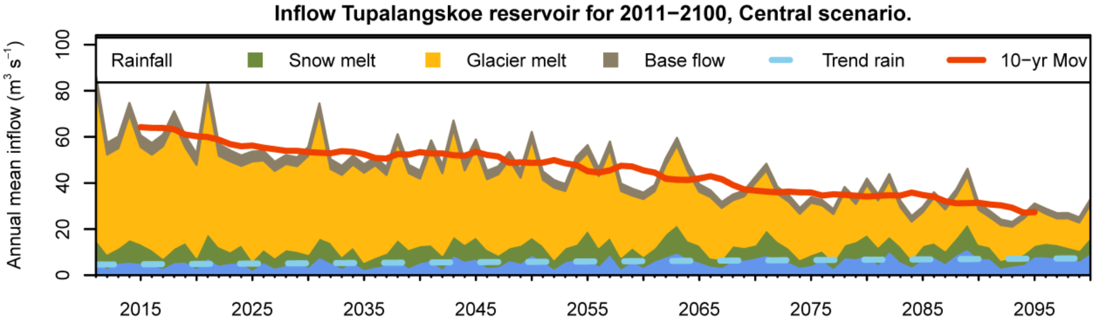

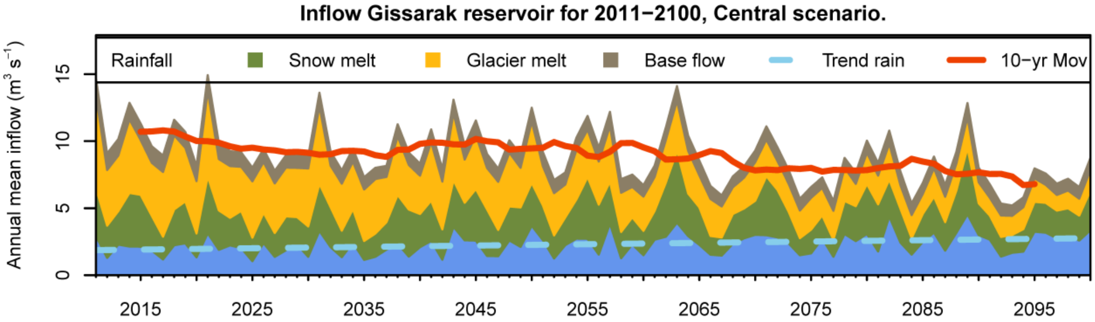

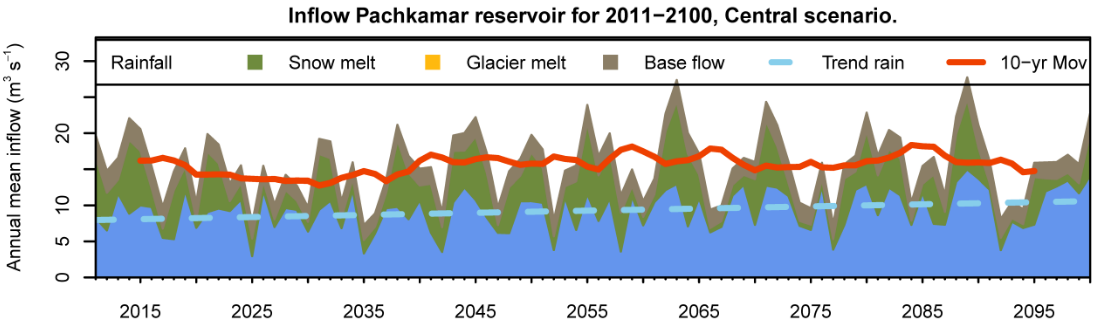

Inflow Kulyab catchment for 2011−2100, Central scenario.

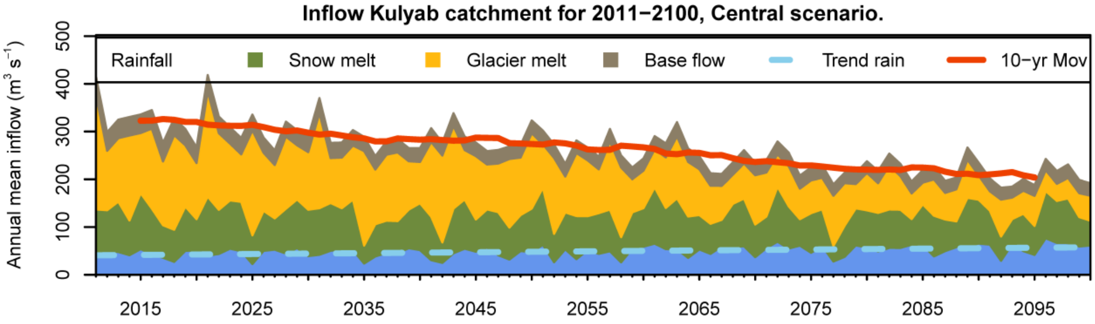

Inflow Kurgantube catchment for 2011−2100, Central scenario.

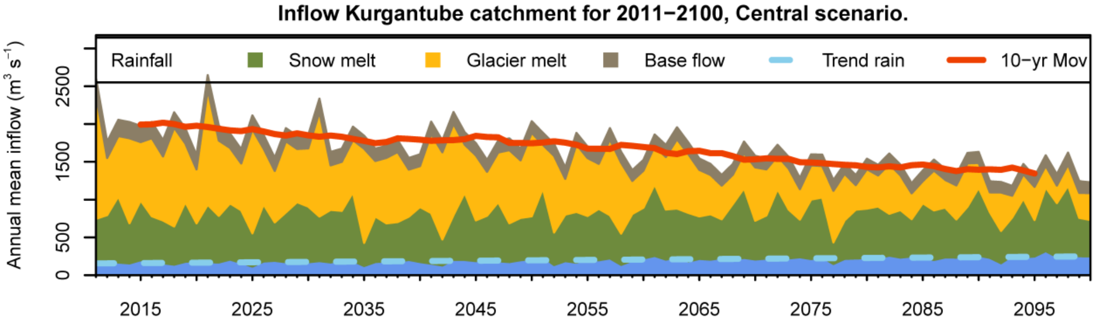

Inflow Dushanbe catchment for 2011−2100, Central scenario.

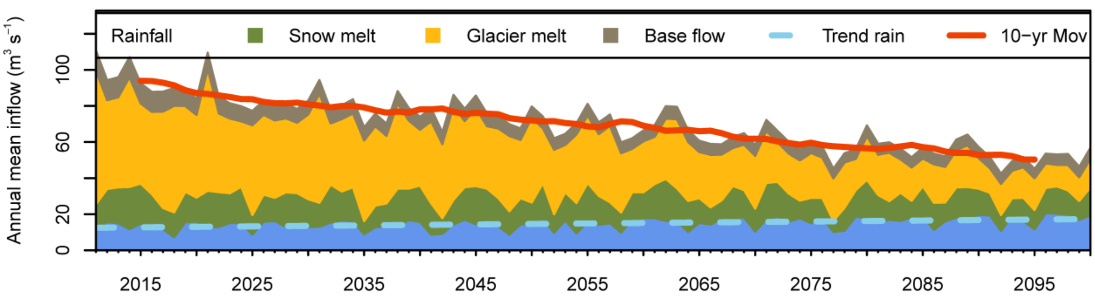

Inflow Surkhandarya upstream catchment for 2011−2100, Central scenario.

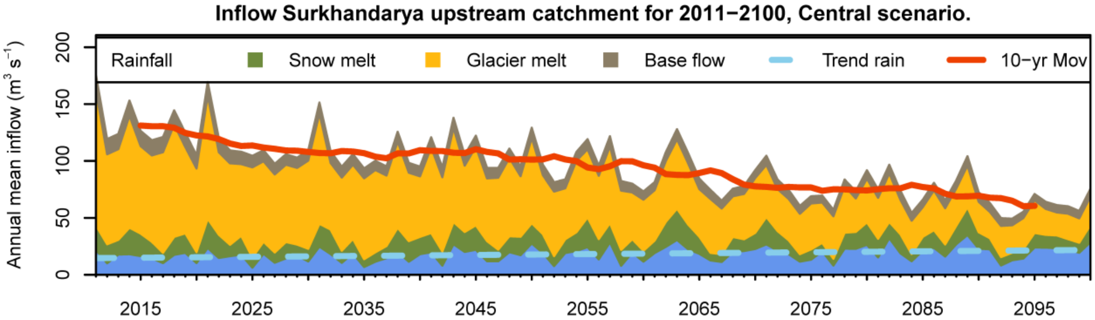

Inflow Surkhandarya downstream catchment for 2011−2100, Central scenario.

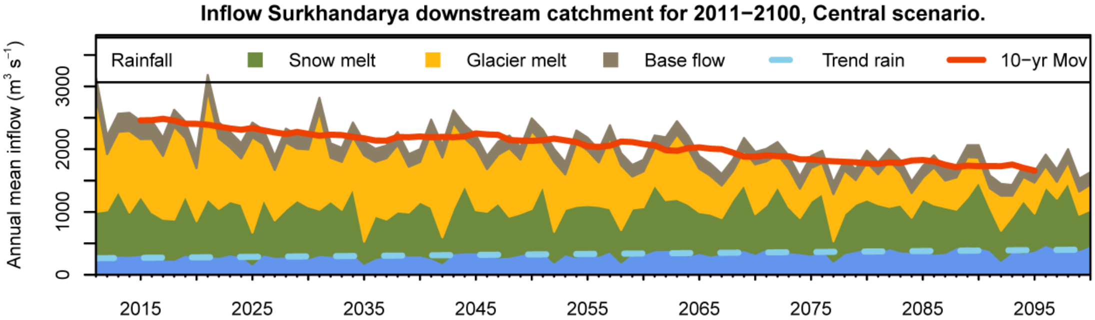

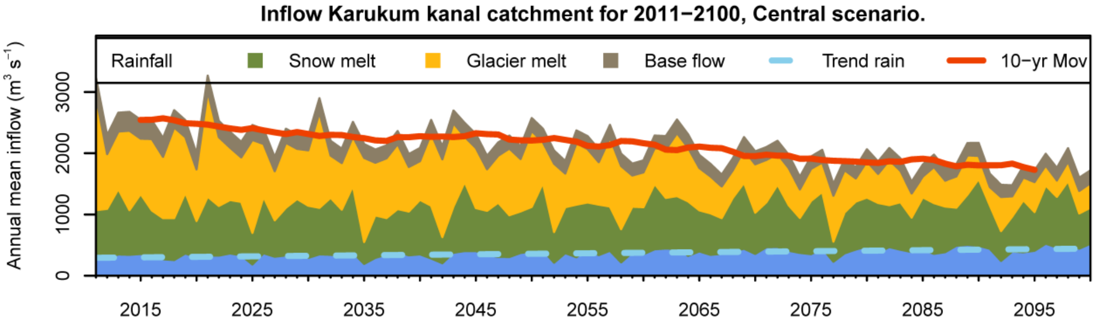
Inflow Karukum kanal catchment for 2011−2100, Central scenario.
Rainfall
Snow melt
Glacier melt
Base flow
Trend rain
10−yr Mov
Annual mean inflow ($m^3 s^{-1}$)
0
1000
2000
3000
2015
2025
2035
2045
2055
2065
2075
2085
2095

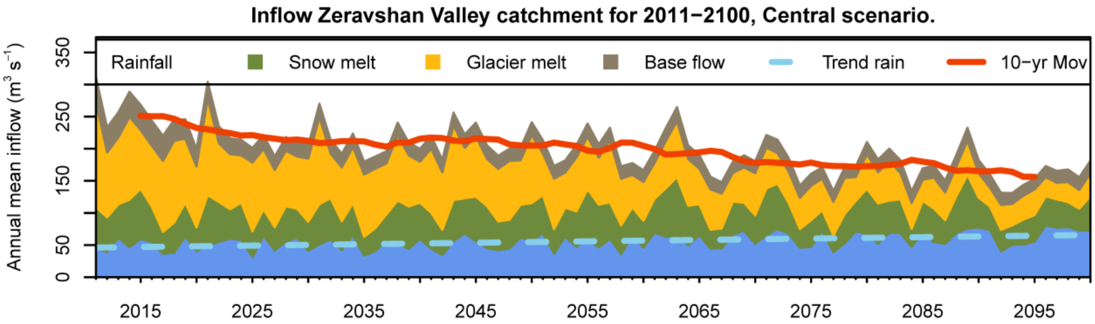
Inflow Zeravshan Valley catchment for 2011−2100, Central scenario.
Rainfall
Snow melt
Glacier melt
Base flow
Trend rain
10−yr Mov
Annual mean inflow ($m^3 s^{-1}$)
0
50
150
250
350
2015
2025
2035
2045
2055
2065
2075
2085
2095

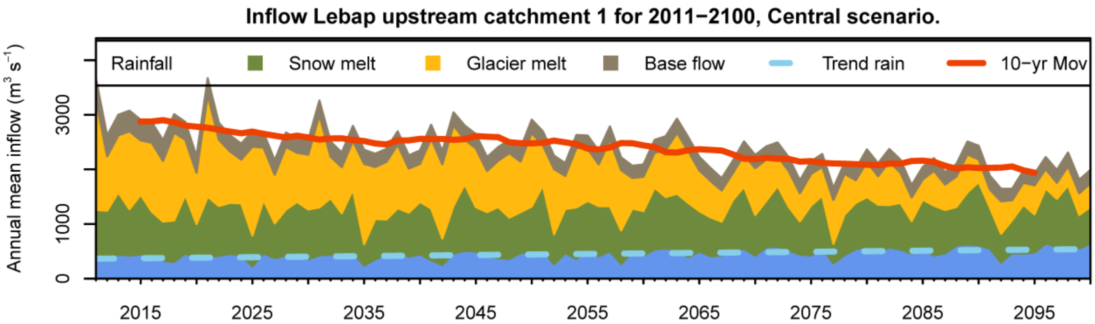
Inflow Lebap upstream catchment 1 for 2011−2100, Central scenario.
Rainfall
Snow melt
Glacier melt
Base flow
Trend rain
10−yr Mov
Annual mean inflow ($m^3 s^{-1}$)
0
1000
3000
2015
2025
2035
2045
2055
2065
2075
2085
2095

IV.4 Marker scenario: Warm/wet

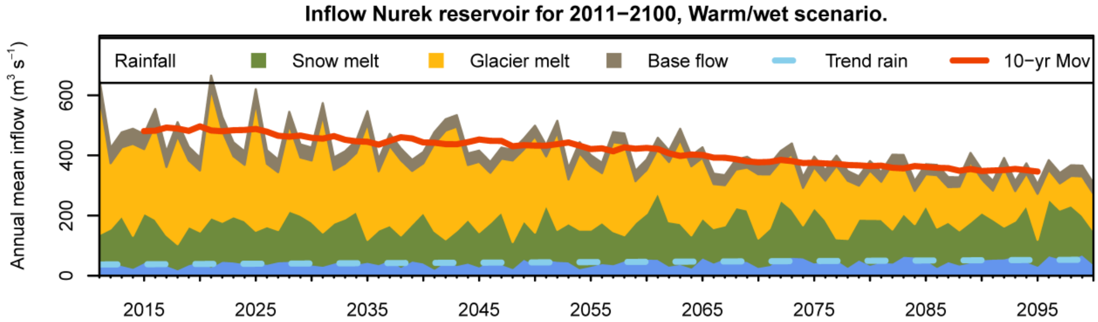

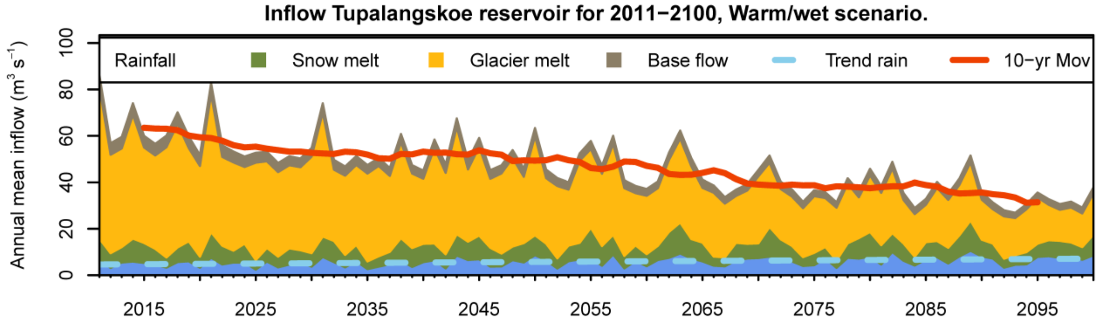

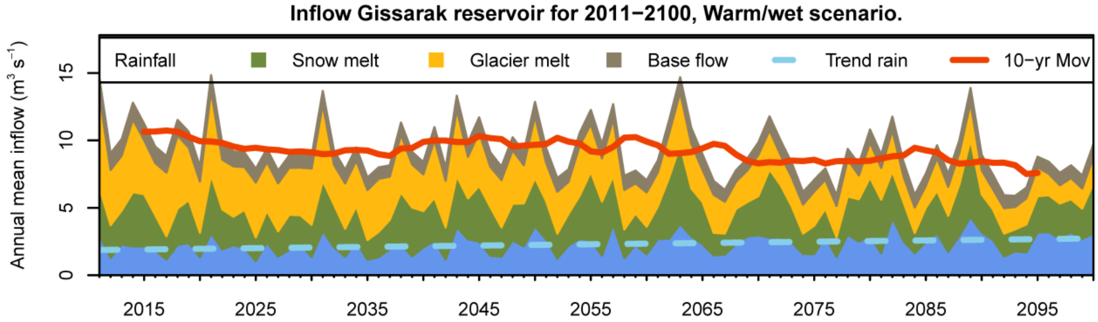

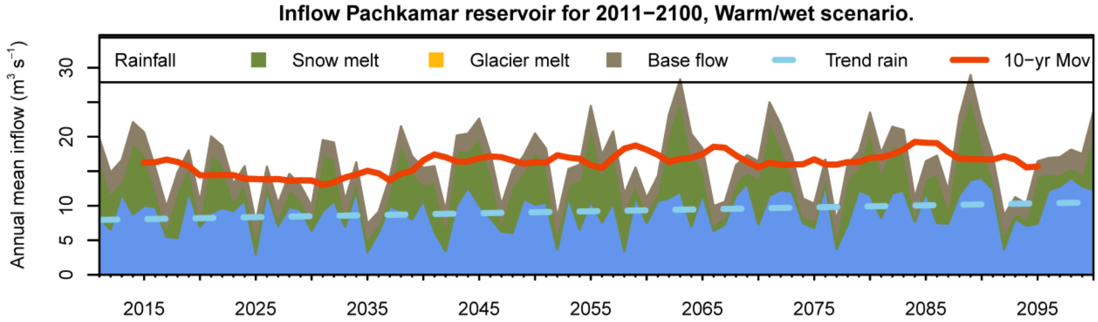

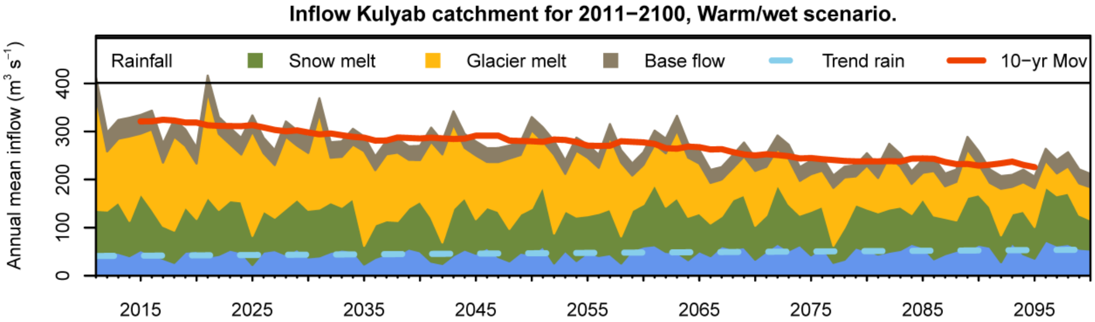
Inflow Kulyab catchment for 2011−2100, Warm/wet scenario.
Rainfall
Snow melt
Glacier melt
Base flow
Trend rain
10−yr Mov
Annual mean inflow ($m^3 s^{-1}$)
0 100 200 300 400
2015 2025 2035 2045 2055 2065 2075 2085 2095

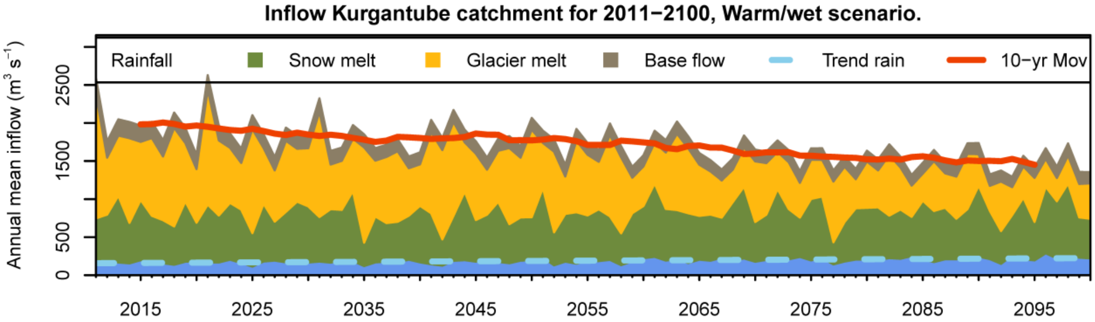
Inflow Kurgantube catchment for 2011−2100, Warm/wet scenario.
Rainfall
Snow melt
Glacier melt
Base flow
Trend rain
10−yr Mov
Annual mean inflow ($m^3 s^{-1}$)
0 500 1500 2500
2015 2025 2035 2045 2055 2065 2075 2085 2095

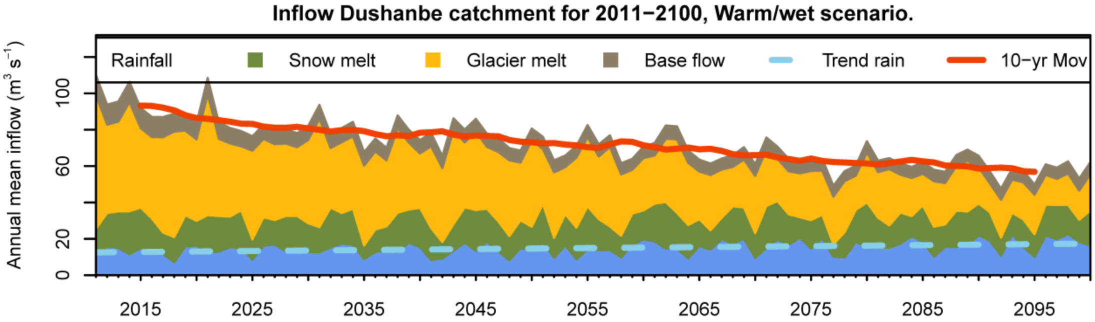
Inflow Dushanbe catchment for 2011−2100, Warm/wet scenario.
Rainfall
Snow melt
Glacier melt
Base flow
Trend rain
10−yr Mov
Annual mean inflow ($m^3 s^{-1}$)
0 20 60 100
2015 2025 2035 2045 2055 2065 2075 2085 2095

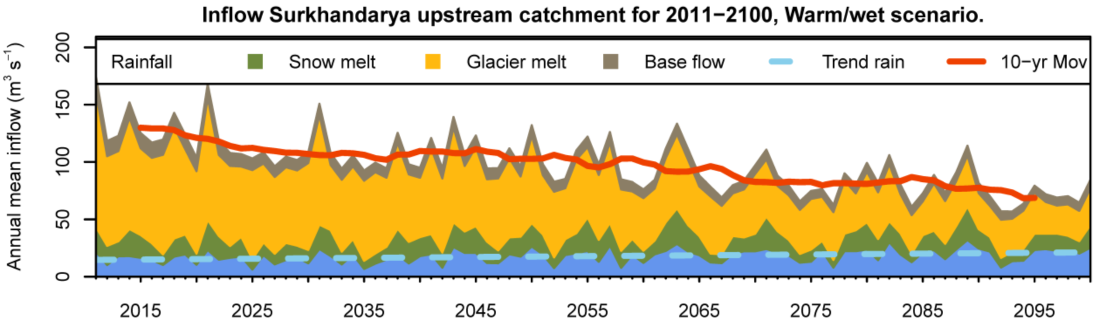
Inflow Surkhandarya upstream catchment for 2011−2100, Warm/wet scenario.
Rainfall
Snow melt
Glacier melt
Base flow
Trend rain
10−yr Mov
Annual mean inflow ($m^3 s^{-1}$)
0 50 100 150 200
2015 2025 2035 2045 2055 2065 2075 2085 2095

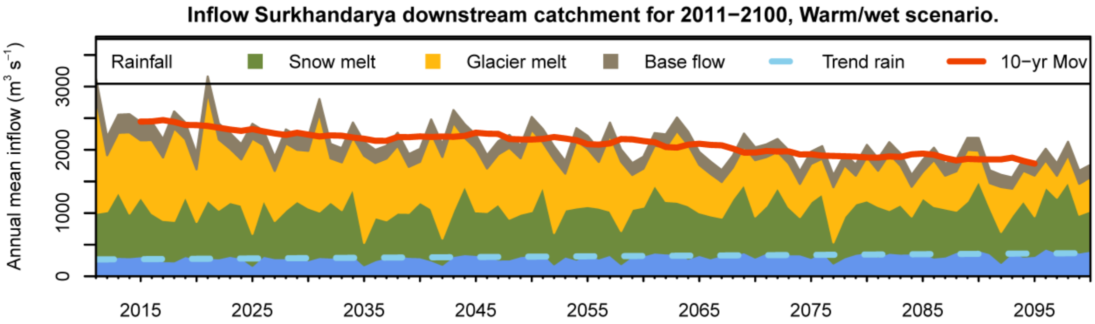
Inflow Surkhandarya downstream catchment for 2011−2100, Warm/wet scenario.
Rainfall
Snow melt
Glacier melt
Base flow
Trend rain
10−yr Mov
Annual mean inflow ($m^3 s^{-1}$)
0 1000 2000 3000
2015 2025 2035 2045 2055 2065 2075 2085 2095

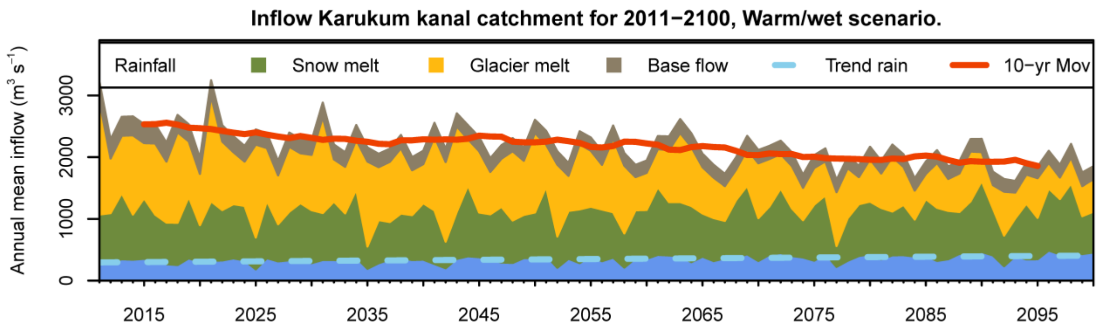
Inflow Karukum kanal catchment for 2011−2100, Warm/wet scenario.
Rainfall
Snow melt
Glacier melt
Base flow
Trend rain
10−yr Mov
Annual mean inflow (m³ s⁻¹)
0
1000
2000
3000
2015
2025
2035
2045
2055
2065
2075
2085
2095

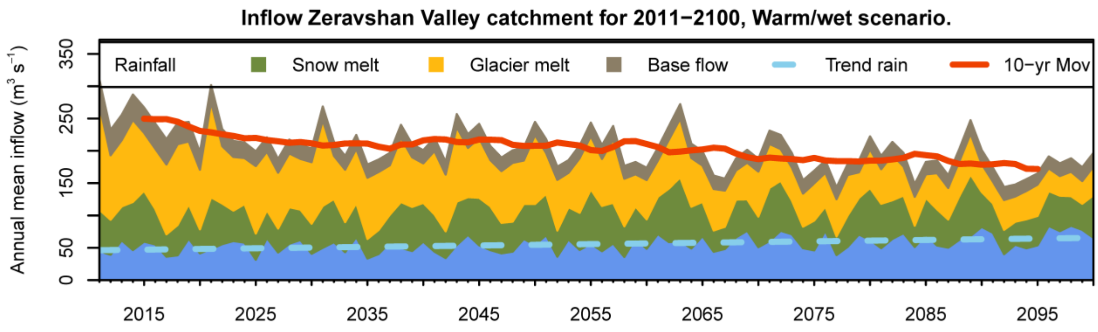
Inflow Zeravshan Valley catchment for 2011−2100, Warm/wet scenario.
Rainfall
Snow melt
Glacier melt
Base flow
Trend rain
10−yr Mov
Annual mean inflow (m³ s⁻¹)
0
50
150
250
350
2015
2025
2035
2045
2055
2065
2075
2085
2095

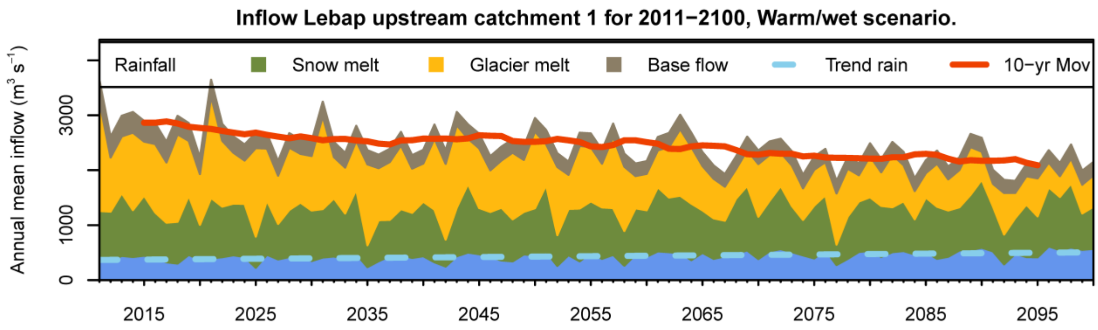
Inflow Lebap upstream catchment 1 for 2011−2100, Warm/wet scenario.
Rainfall
Snow melt
Glacier melt
Base flow
Trend rain
10−yr Mov
Annual mean inflow (m³ s⁻¹)
0
1000
3000
2015
2025
2035
2045
2055
2065
2075
2085
2095

Appendix V Agriculture Water Supply

Note: The scenario labeled ‘1Current’ refers to the ‘No Climate Change’ scenario.

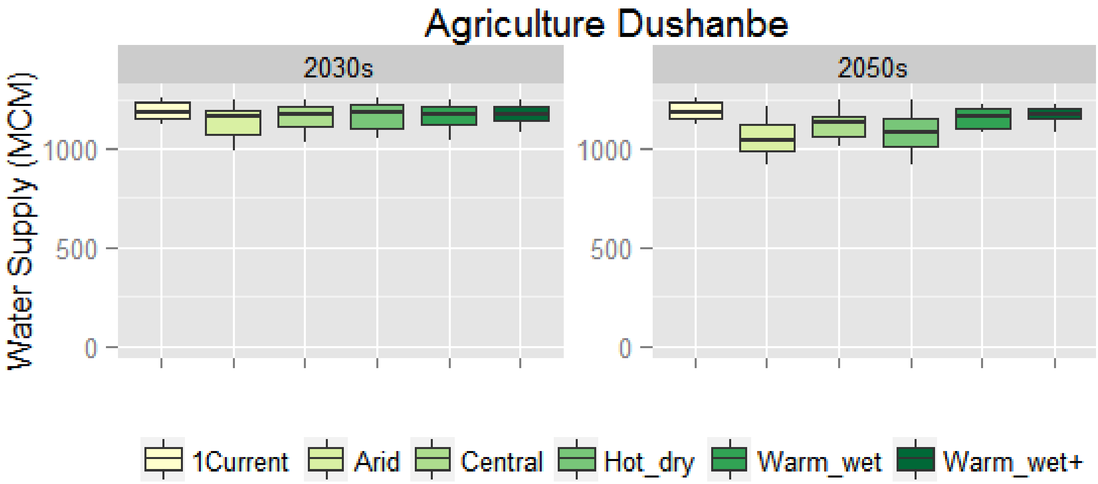

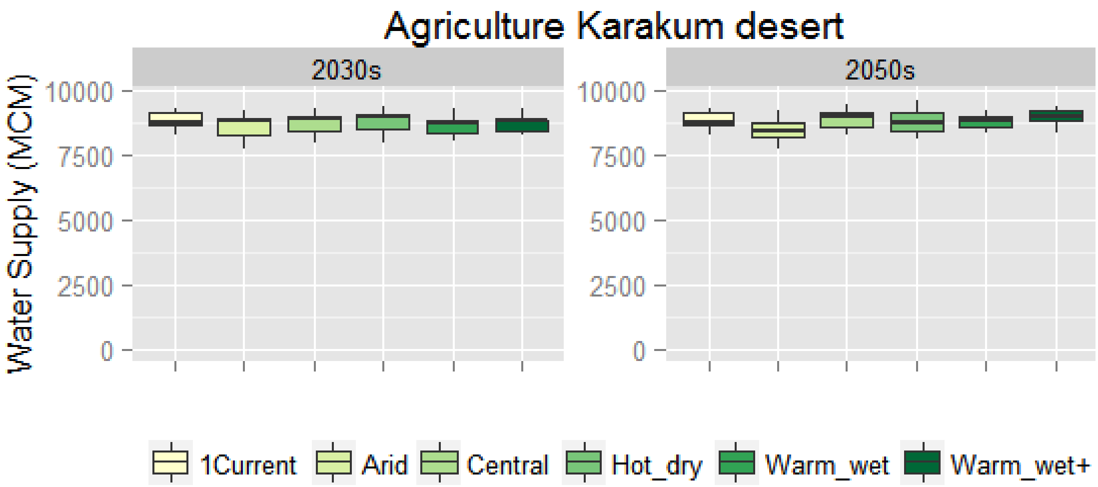

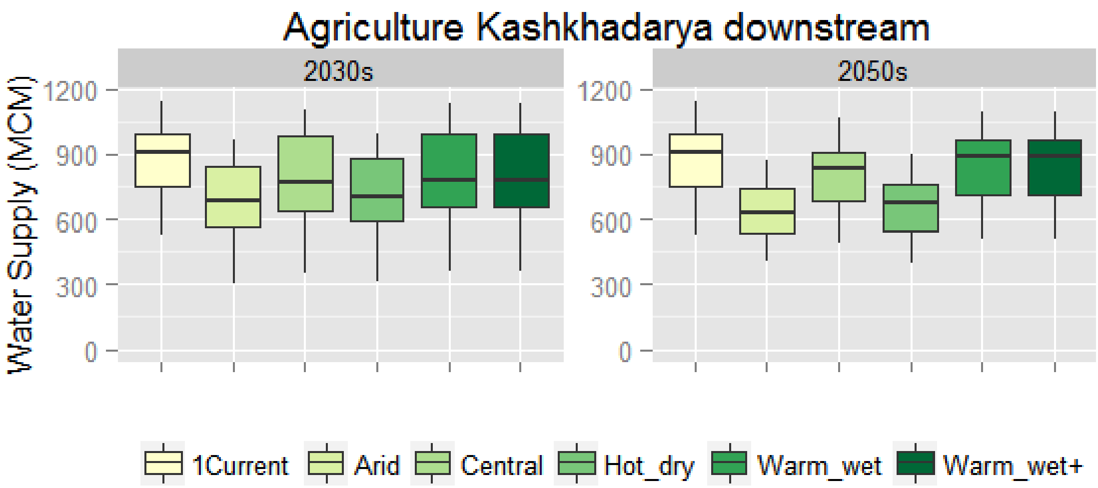

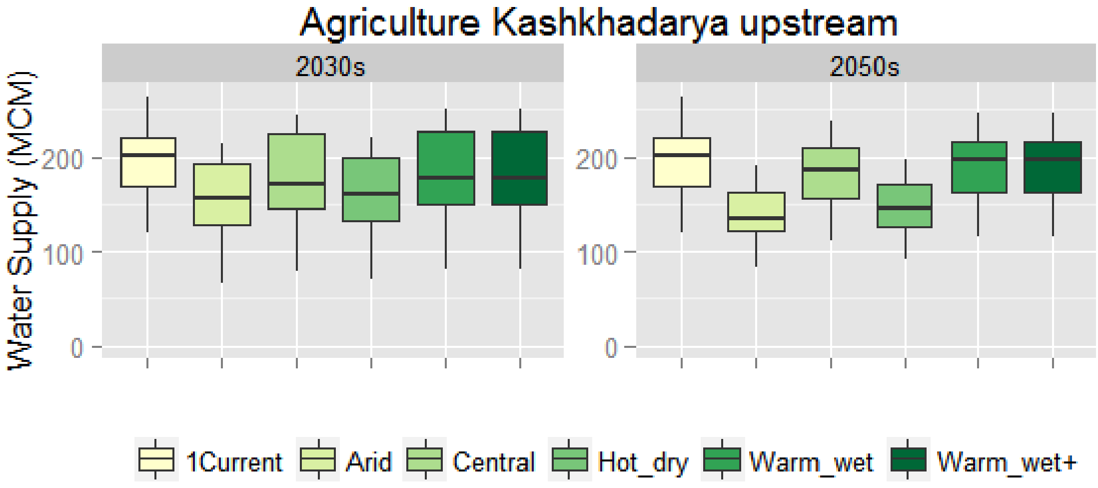
Agriculture Kashkhadarya upstream
2030s
2050s
Water Supply (MCM)
0
100
200
1Current
Arid
Central
Hot_dry
Warm_wet
Warm_wet+

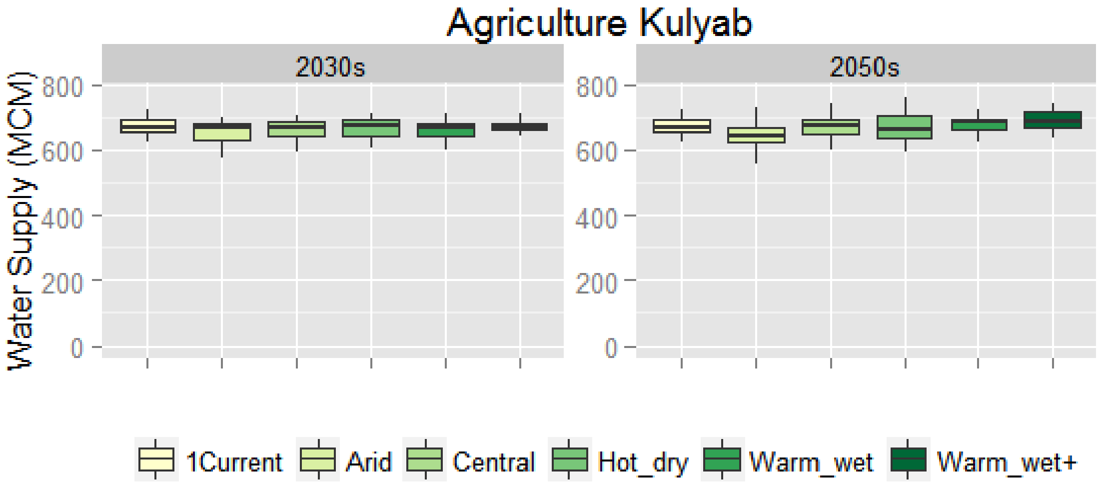
Agriculture Kulyab
2030s
2050s
Water Supply (MCM)
0
200
400
600
800
1Current
Arid
Central
Hot_dry
Warm_wet
Warm_wet+

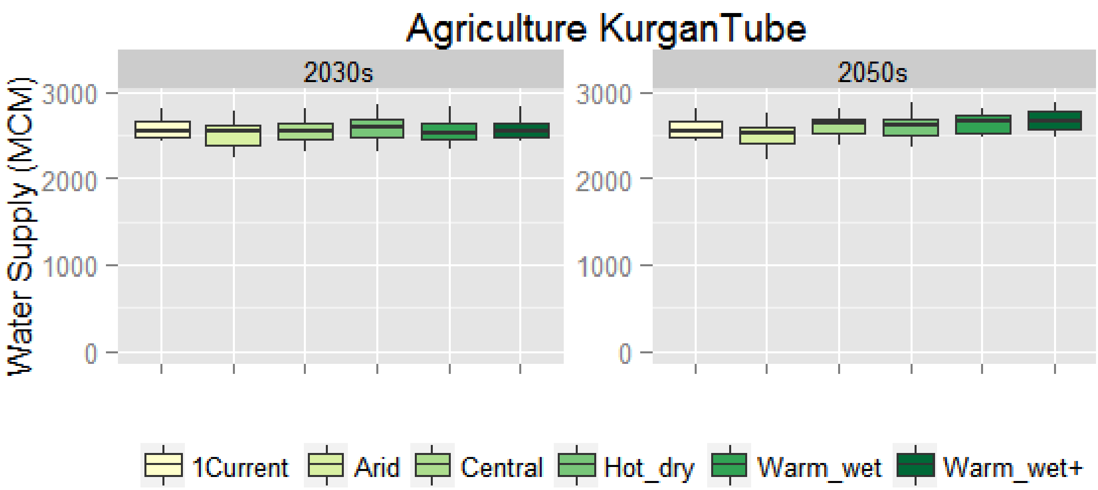
Agriculture KurganTube
2030s
2050s
Water Supply (MCM)
0
1000
2000
3000
1Current
Arid
Central
Hot_dry
Warm_wet
Warm_wet+

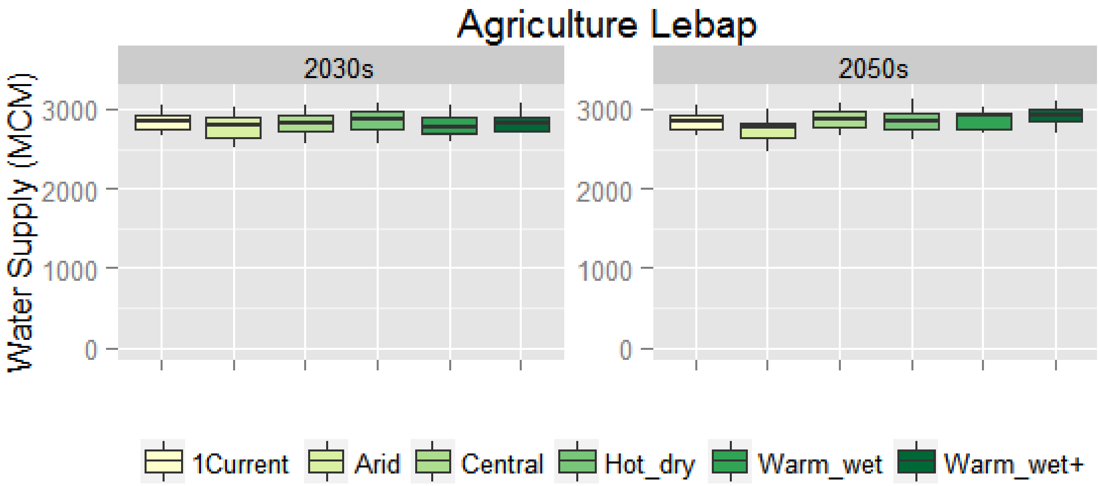
Agriculture Lebap
2030s
2050s
Water Supply (MCM)
3000
2000
1000
0
1Current
Arid
Central
Hot_dry
Warm_wet
Warm_wet+

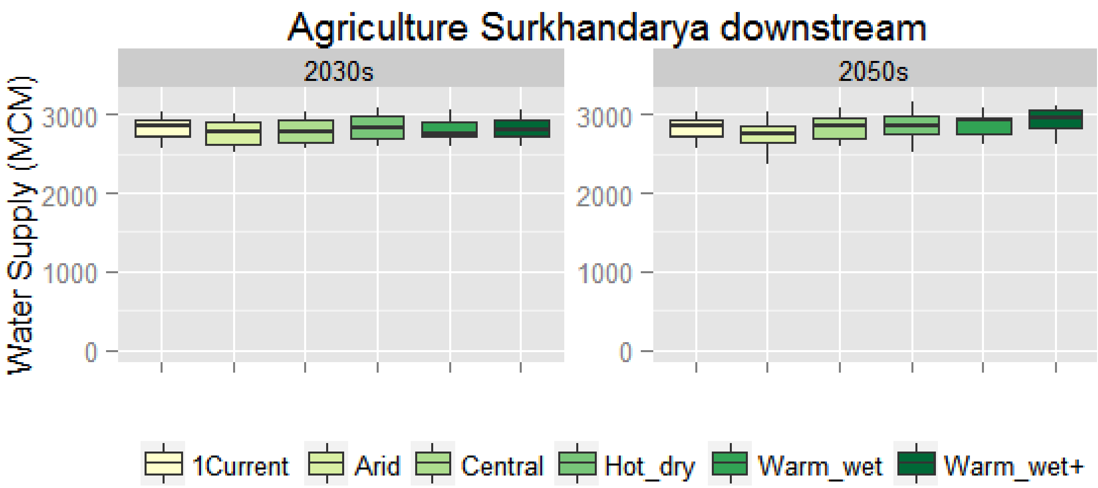
Agriculture Surkhandarya downstream
2030s
2050s
Water Supply (MCM)
3000
2000
1000
0
1Current
Arid
Central
Hot_dry
Warm_wet
Warm_wet+

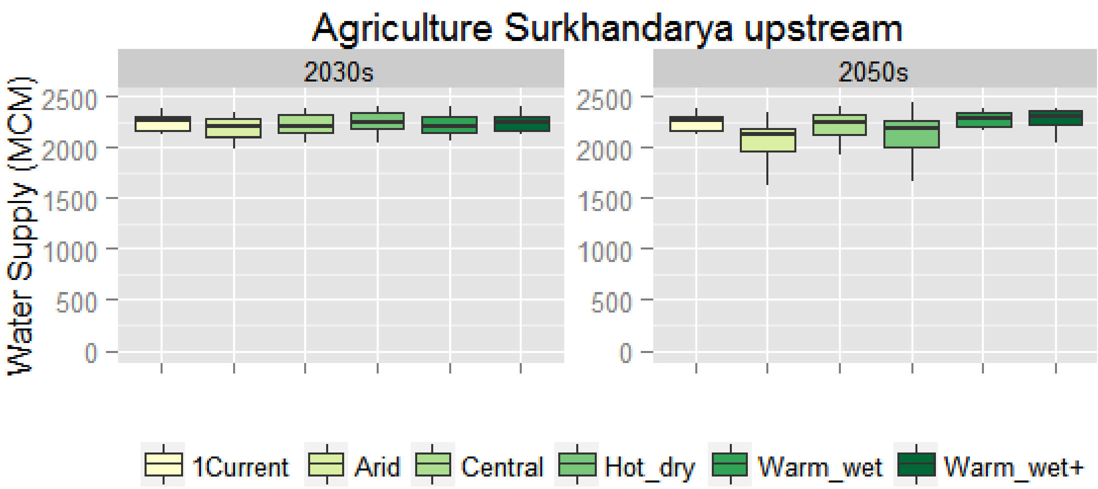
Agriculture Surkhandarya upstream
2030s
2050s
Water Supply (MCM)
2500
2000
1500
1000
500
0
1Current
Arid
Central
Hot_dry
Warm_wet
Warm_wet+

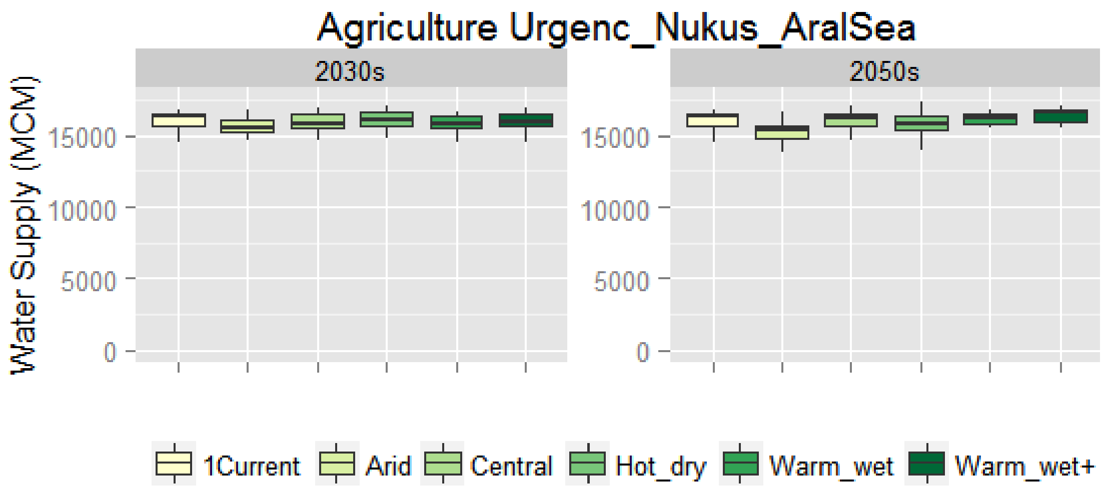
Agriculture Urgenc_Nukus_AralSea
2030s
2050s
Water Supply (MCM)
15000
10000
5000
0
1Current
Arid
Central
Hot_dry
Warm_wet
Warm_wet+

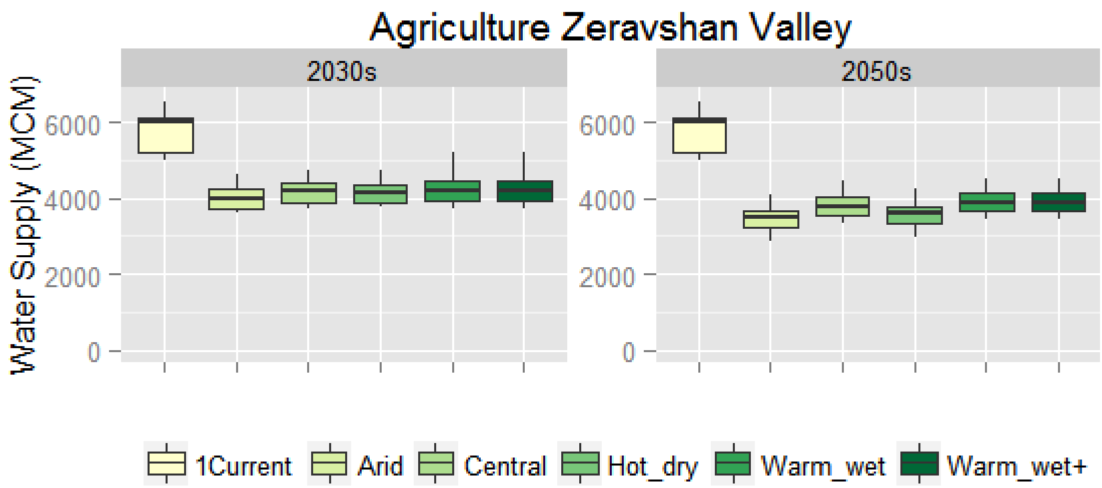
Agriculture Zeravshan Valley
2030s
2050s
Water Supply (MCM)
6000
4000
2000
0
1Current
Arid
Central
Hot_dry
Warm_wet
Warm_wet+